

Clinical introduction of MR-guided radiotherapy for esophageal cancer

Mick Remo Boekhoff

Clinical introduction of MR-guided radiotherapy for esophageal cancer

PhD Thesis, Utrecht University, The Netherlands

© **Mick Remo Boekhoff, Utrecht, 2024**

All rights reserved. No part of this publication may be reproduced or transmitted in any form or by any means without prior permission in writing from the author. The copyright of the papers that have been published has been transferred to the respective journals.

Manuscript

Cover design: Else Wisselink
Lay-out: Mick Remo Boekhoff
Typeset: L^AT_EX 2_ε
Printed by: Gildeprint
ISBN: 978-94-6496-030-3
DOI: 10.33540/2140

Clinical introduction of MR-guided radiotherapy for esophageal cancer

Klinische introductie van MR-gestuurde radiotherapie
voor slokdarmkanker

(met een samenvatting in het Nederlands)

Proefschrift

ter verkrijging van de graad van doctor aan de
Universiteit Utrecht
op gezag van de
rector magnificus, prof. dr. H.R.B.M. Kummeling,
ingevolge het besluit van het college voor promoties
in het openbaar te verdedigen op

dinsdag 27 februari 2024 des middags te 2.15 uur

door

Mick Remo Boekhoff
geboren op 25 september 1992
te Amsterdam

Promotor:

Prof. dr. J.J.W. Lagendijk

Copromotor:

dr. G.J. Meijer

dr. S. Mook

Beoordelingscommissie:

Prof. dr. U.A. van der Heide

Prof. dr. R. van Hillegersberg

Prof. dr. B.W. Raaymakers

dr. P.S.N. van Rossum

Prof. dr. B.L.A.M. Weusten (voorzitter)

Contents

Chapter 1	
General introduction and thesis outline	5
Chapter 2	
Tumor volume regression during neoadjuvant chemoradiotherapy for esophageal cancer: a prospective study with weekly MRI	13
Chapter 3	
CTV-to-PTV margin assessment for esophageal cancer radiotherapy based on an accumulated dose analysis	27
Chapter 4	
3-Dimensional target coverage assessment for MRI guided esophageal cancer radiotherapy	45
Chapter 5	
An in-silico assessment of the dosimetric benefits of MR-guided radiotherapy for esophageal cancer patients	61
Chapter 6	
Clinical implementation and feasibility of long-course fractionated MR-guided chemoradiotherapy for patients with esophageal cancer: an R-IDEAL stage 1b/2a evaluation of technical innovation	77
Chapter 7	
Intrafraction motion analysis in online adaptive radiotherapy for esophageal cancer	97
Summary and general discussion	107
References	121
Appendices	133
Summary in Dutch (Nederlandse Samenvatting)	135
List of publications	143
Dankwoord	149
Curriculum Vitae	153

Chapter 1

General introduction and thesis outline

Introduction

Esophageal cancer

Patients with esophageal cancer have poor survival rates. Worldwide, esophageal cancer is the 8th most common cancer type and the 6th most cancer-related cause of death [1]. In the Netherlands, for patients with locally advanced, resectable esophageal cancer without metastases the current standard of care is neoadjuvant chemoradiotherapy (nCRT) followed by esophagectomy, according to the CROSS regimen [2]. One of the key aims of nCRT is to reduce the primary tumor, which increases the probability of a radical resection [3]. Tumor reduction induces changes in the thoracic anatomy of a patient during nCRT [4]. In addition, variation in tumor shape and position can be observed during neoadjuvant chemoradiation [5–7]. These uncertainties can be compensated for in the radiotherapy plan by expanding the targeted volume, resulting in an increased radiation dose to the surrounding organs at risk and subsequent toxicity and therefore limiting the maximum radiation dose [8–13]. For these reasons, improvement of the radiotherapy treatment is highly sought-after, and it has been hypothesized to bring a positive impact on the treatment outcome of many patients. This thesis focuses on the improvement of the radiotherapy part in the nCRT treatment of esophageal cancer by using Magnetic Resonance Imaging (MRI). With MRI, we aim to define the required target volumes by accurately determining the change of tumor characteristics over the course of treatment.

Esophageal cancer tumor and treatment characteristics

Generally, the location of an esophageal cancer tumor varies along the length

of the esophagus in the thorax. In the Netherlands, the most prevailing tumor type is adenocarcinoma (75%) which is typically located in the distal third esophagus, sometimes extending into and around the gastroesophageal junction (GEJ) [2]. Squamous cell carcinoma is the second most common histological type of esophageal cancer and is generally located more proximally. Patients with locally advanced, non-metastasized resectable esophageal cancer of both histological subtypes receive neoadjuvant chemoradiation followed by esophagectomy. Standard neoadjuvant chemoradiation consists of a radiation dose of 41.4 Gy spread out over 23 daily fractions (4.5 weeks) of 1.8 Gy. Additionally, a concurrent chemotherapy schedule consisting of weekly intravenous administration of carboplatin and paclitaxel is administered. Approximately three months after finishing the nCRT schedule patients undergo a thoraco-laparoscopic esophagectomy independent of nCRT outcome. The pathological response is assessed to determine the indication for adjuvant treatment.

Current treatment of esophageal cancer

Clinical workflow

The preparation of a radiotherapy treatment is often a lengthy process consisting of multiple steps. First, the patient undergoes a planning Computer Tomography (CT) scan, which can be combined with a 18-F-FDG positron emission tomography (PET) scan to capture the patient's anatomy and exact tumor location. Then, the radiation oncologist delineates the visible tumor, the gross tumor volume (GTV), which is expanded using a margin of 0.5 cm in transverse direction (excluding the heart, large vessels, trachea, bronchial tree and lungs), 3 cm in cranial direction and 2 or 3 cm in caudal direction (depending on tumor extension in the stomach) to create the clinical target volume (CTV). The CTV incorporates the GTV and surrounding tissue to include subclinical microscopic malignant disease and pathologic lymph nodes. The organs at risk (OAR), such as the heart and lungs, are delineated by specialized radiation therapy technologists. Targeting of the CTV alone is not sufficient, as the CTV is subject to geometric variations due to inter- and intrafraction motion, which will be discussed in the next section. It is therefore that the CTV requires expansion with a treatment margin of approximately 10mm in all directions, creating the planning target volume (PTV) [5–7]. Using PTV margins results in an acceptable probability of correct dose delivery [14,15]. Finally, a dose plan is created which targets the PTV while OAR such as the heart and lungs are spared as much as possible (Figure 1.1).

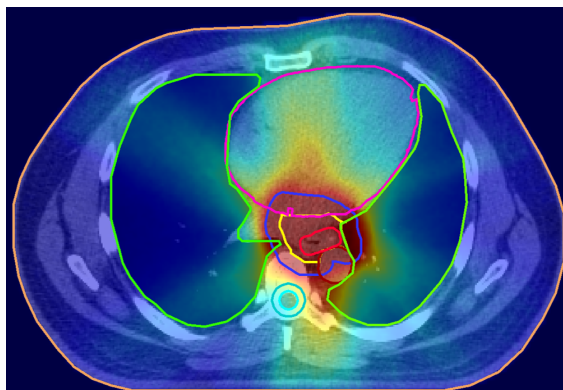


Figure 1.1: Radiotherapy dose plan for the treatment of esophageal cancer. The plan is optimized so that the PTV (blue delineation) is target, while the surrounding organs at risk (heart: pink, lungs: green) are spared as much as possible.

This pretreatment dose plan is used throughout the whole treatment period (23 fractions) without adaptations. During these treatment fractions, it is important that the patient is positioned in such a way that the daily anatomy resembles the anatomy of the planning CT. To achieve this, imaging with cone-beam CT (CBCT) is performed for patient setup verification. Although actual tumor volume-based registration is preferred, this is generally not possible due to the limited soft-tissue contrast in CT and CBCT. Therefore, a rigid registration of the bony anatomy (i.e. vertebrae) as a surrogate of tumor position is currently used [16–18]. After alignment of the anatomy, dose delivery commences, which takes roughly 4–5 minutes per fraction.

Geometric uncertainties and treatment margins

The esophagus is subject to motion, which can lead to tumor movement over time. On a short timescale (intrafraction; during treatment) esophageal motion is mainly caused by breathing motion, while on a longer timescale (interfraction; between treatment fractions) a change in tumor shape, volume or position can be observed, caused by changes of the tumor itself or of the surrounding organs, such as stomach filling [19]. In radiotherapy, it is important to know the location of the tumor so that the radiation dose can be administered to the precise location, while healthy tissue is spared as much as possible. Current state-of-the-art image guided radiotherapy (IGRT) makes use of computed tomography (CT) in combination with cone-beam CT (CBCT) imaging [20]. As previously mentioned, a rigid registration of the bony anatomy is currently used for patient setup verification. As a result, interfractional tumor position variation relative

to bony anatomy is currently a dominant uncertainty that has to be taken into account to ensure adequate target coverage. Irradiation of the last known location of the CTV can result in underdosage if the CTV is subject to motion, deformations and other geometric changes. Various geometric uncertainties are present in the current workflow and require compensation to ensure accurate dose delivery. Uncertainties caused by delineation errors, shape, volume and geometric changes, potential shifts between the tumor and bony anatomy and the influence of breathing motion can lead to an imperfect dose distribution. An error in the dose distribution, that persists throughout treatment, could result in an off-target dose shift, which is undesirable. It is therefore that geometric uncertainties are accounted for with a treatment margin, expanding the CTV to the PTV, to ensure adequate target coverage throughout treatment [5–7, 14]. Multiple studies have reported on the geometric variability of esophageal cancer tumors over the course of treatment. A generous margin of approximately 10mm in all directions is often found to be necessary to allow adequate CTV coverage over the course of treatment. A downside of using large margins is an increased PTV volume, which could lead to a substantial radiation dose to surrounding healthy tissue, often associated with short-term and long-term cardiac and pulmonary complications [8–12]. It has been suggested that the incorporation of MRI into the radiotherapy workflow would bring certainty and quantification of the treatment process as MRI has superior soft-tissue contrast compared to (CB)CT imaging [21, 22]. Improved imaging quality should reduce some geometric uncertainties, leading to a more precise irradiation of the targeted volumes, which allows the use of smaller treatment margins or an increase in radiation dose.

MRI guided Radiotherapy

In the last 15 years, Magnetic Resonance Imaging (MRI) has played an increasing role in radiotherapy. Recently, a combined MRI and linear accelerator (MR-Linac) has been introduced to the clinic [23, 24]. This combination allows for optimal target visualization during treatment and creation of a dose plan of the daily anatomy. With daily imaging, interfraction tumor changes are of no more effect, potentially allowing the use of smaller treatment margins, which in turn could reduce OAR toxicity. This is of interest in the radiation treatment of esophageal cancer tumors, as the heart and lungs are in close proximity of the target volume. These organs have an increased risk of being subject to radiation induced toxicity [25]. Furthermore, the precise shape and location of esophageal cancer tumors can vary between fractions. A change in stomach volume could result in a change of the PTV, which often extends in the stomach, while position changes between fractions could lead to a shift of the esophagus. Due to the increased soft-tissue contrast, these changes are more likely to be noticed with MR-guided

imaging, in comparison to current CBCT-guided imaging (Figure 1.2) and could lead to an improved treatment accuracy. Finally, an increased treatment accuracy might allow for more individualized treatment approaches, such as additional treatment intensification (boosting), which could potentially improve tumor control and treatment outcome.

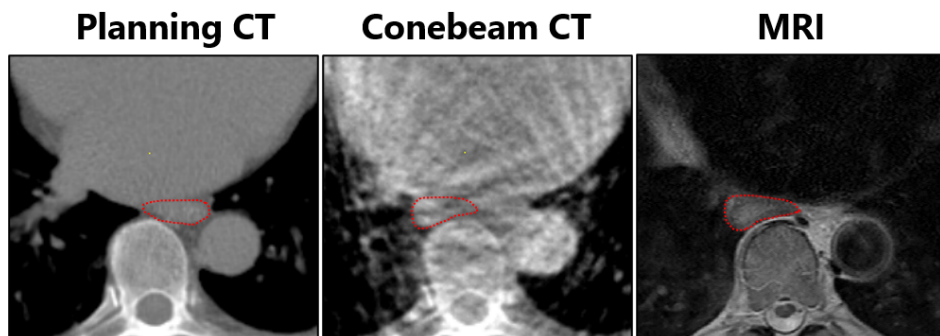


Figure 1.2: Comparison between CT imaging (left), cone-beam CT (middle) and MRI (right). The tumor (red line) is clearly visible on MRI, due to the superior soft-tissue contrast.

Thesis Outline

This thesis focuses on an improvement of the radiotherapy treatment of esophageal cancer by performing accurate CTV-to-PTV treatment margin determination, using the superior soft-tissue contrast of MRI imaging. Hereby, the aim is to ensure sufficient target coverage over the course of treatment, while radiation dose to healthy tissue is as low as possible. Furthermore, this thesis explores the benefits of adaptive MR-guided radiotherapy for patients with esophageal cancer based on the “**RE**peated magnetic resonance imaging in esophageal cancer for **A**daptive radiation treatment planning during neoadjuvant **C**hemoradio**T**herapy” (REACT) trial. Analysis of MRI scans obtained during this trial, in which patients underwent six weeks of MRI treatment simulations, while undergoing conventional neoadjuvant chemoradiotherapy, resulted in chapters 2, 3 4 and 5.

First, the change in tumor volume is evaluated throughout neoadjuvant chemoradiotherapy in **Chapter 2** by comparing weekly delineated MRI scans. The impact of geometric tumor changes is discussed in **Chapter 3**, where a full accumulated dose analysis is performed. Here, we assess the smallest CTV-to-PTV margins for esophageal cancer radiotherapy that yield full dosimetric coverage over the course of treatment, using daily online registration to the bony anatomy. **Chapter 4** covers the quantification of the geometric coverage probability as a function of

a preset margin for online MR-guided and (CB)CT-guided radiotherapy to investigate potential adaptive set-up strategies. The possible dosimetric benefits of using MR-guided RT over conventional CBCT IGRT are explored in **Chapter 5**. In this chapter, the difference in dose to the organs-at-risk is compared for both treatment strategies, while exploring possible boosting strategies for MRgRT without exceeding conventional dose levels to the OAR.

Subsequently, the first esophageal cancer patients were treated on the MR-Linac in the UMC Utrecht, as reported in **Chapter 6**. In this chapter we describe the first experiences with an adaptive MR-guided workflow for patients with esophageal cancer. On top of that, **Chapter 7** discusses the intrafraction motion of the aforementioned patients as captured during dose delivery on the MR-linac.

Finally, a summary of the main results and findings in this thesis followed by a general discussion is presented.

Chapter 2

Tumor volume regression during neoadjuvant chemoradiotherapy for esophageal cancer: a prospective study with weekly MRI

The following chapter is based on:

IL Defize, MR Boekhoff, AS Borggreve, ALHMW van Lier, N Takahashi, N Haj Mohammad, JP Ruurda, R van Hillegersberg, S Mook & GJ Meijer

Acta Oncologica (2020) 59:7

doi:10.1080/0284186X.2020.1759819

Abstract

Background

Neoadjuvant chemoradiotherapy (nCRT) for esophageal cancer causes tumor regression during treatment. Tumor regression can induce changes in the thoracic anatomy, with smaller target volumes and displacement of organs at risk (OARs) surrounding the tumor as a result. Adaptation of the radiotherapy treatment plan according to volumetric changes during treatment might reduce radiation dose to the OARs, while maintaining adequate target coverage. Data on the magnitude of the volumetric changes and its impact on the thoracic anatomy is scarce. The aim of this study was to assess the volumetric changes in the primary tumor during nCRT for esophageal cancer based on weekly MRI scans.

Material and methods

In this prospective study, patients with adeno- or squamous cell carcinoma of the esophagus treated with neoadjuvant chemoradiotherapy according to the CROSS regimen (carboplatin + paclitaxel + 23x1.8Gy) were included. Of each patient, six sequential MRI scans were acquired: one prior to nCRT, and five in each subsequent week during nCRT. Tumor volumes were delineated on the transversal T2 weighted images by two radiation oncologists. Volumetric changes were analyzed using linear mixed effects models.

Results

A total of 170 MRI scans from 29 individual patients were included. The mean (\pm standard deviation (SD)) tumor volume at baseline was 46 cm³ (\pm 23). Tumor volume regression started after the first week of nCRT with a significant decrease in tumor volumes every subsequent week. A decrease to 42cm³ (91% of initial volume), 38cm³ (81%), 35cm³ (77%), and 32cm³ (72%) was observed in the second, third, fourth and fifth week of nCRT, respectively.

Conclusion

Based on weekly MRI scanning during nCRT for esophageal cancer, a considerable decrease in tumor volume was observed during treatment. Volume regression and consequential anatomical changes suggest the possible benefit of adaptive radiotherapy.

Introduction

Neoadjuvant chemoradiotherapy (nCRT) followed by esophagectomy is the standard of care for esophageal cancer patients treated with curative intent [2]. One of the key aims of nCRT is to downsize the primary tumor, which increases the probability of a radical resection [3]. Downsizing – or tumor volume regression – induces changes in the thoracic anatomy of a patient during nCRT [4]. These changes might cause initial radiotherapy plans to become inaccurate, leading to an increased radiation dose to the surrounding organs at risk and subsequent toxicity [13]. To prevent an increase in toxicity caused by changes in anatomical configuration during nCRT, adaptation of the initial radiation plan might be considered [26–28]. Additional imaging and plan adaptation is a costly and time consuming process and its added value in esophageal cancer has not yet been established [29]. Therefore, insight in the magnitude of volumetric changes and the impact on the thoracic anatomy is needed. In addition, knowledge of patient and tumor characteristics (e.g. histopathology) that might influence volumetric changes is essential to identify patients who might benefit from adaptive radiotherapy. Previous studies assessing volumetric changes in esophageal cancer with 4D-computed tomography before nCRT, after 10 fractions and after 20 fractions reported significant tumor regression at both follow-up time points [30,31]. Studies on weekly changes during nCRT for esophageal cancer are lacking, but could provide insight in determining the added value of adaptive radiotherapy. In comparison with CT imaging, magnetic resonance imaging (MRI) provides superior soft tissue contrast which facilitates accurate tumor segmentation without additional exposure to radiation. Therefore, the primary aim of this study was to assess the volumetric changes in the primary tumor during nCRT for esophageal cancer with weekly MRI. In addition, patient and tumor characteristics that might influence tumor regression were explored.

Methods

This single center, prospective cohort study was approved by the institutional review board of the University Medical Center Utrecht (protocol ID 15-340). Informed consent was signed by all participants.

Study population

Patients with histologically confirmed adeno- or squamous cell carcinoma of the esophagus treated with neoadjuvant chemoradiotherapy between December 2015 and April 2018 were eligible for inclusion. Exclusion criteria for enrollment in the

study were age <18 years, previous treatment with thoracic surgery or thoracic radiotherapy, and contraindications for MRI. Routine diagnostic work-up of all patients for clinical staging consisted of an endoscopy with biopsy and a PET-CT scan.

Neoadjuvant Chemoradiotherapy

The nCRT regimen consisted of weekly intravenous administration of carboplatin AUC (area under the curve) 2 and paclitaxel 50 mg/m² for 5 weeks with concurrent radiation therapy (41.4 Gy in 23 fractions of 1.8 Gy) [32]. Volumetric arc therapy based on 3D planning CT was used for treatment planning and delivery. Contouring of the gross tumor volume (GTV) was performed based on the results of the endoscopy and PET-CT imaging. The clinical target volume (CTV) was defined by an extension of 3 cm of the GTV in cranial and caudal direction along the esophageal tract, or by 2 cm in caudal direction in cases where the CTV extended in the stomach, as well as an extension of 0.5 cm in circumferential direction without violation of the anatomical boundaries of the surrounding organs. The planning target volume (PTV) margin was 1 cm isotropically.

Magnetic Resonance Imaging

Six MRI scans were scheduled for all patients. One baseline MRI scan was performed prior to nCRT (mean \pm SD; 5 days \pm 3 days) in addition to the routine diagnostic work-up. Subsequently, 5 additional MRI scans were scheduled during each week of nCRT. Images were acquired on a 1.5T Philips Ingenia (Best, the Netherlands), using anterior/posterior (28 channel) receive coils. Patients were positioned in supine position with both arms next to the body. Respiratory-triggered transversal and sagittal anatomical T2-weighted scans (T2W) were acquired with a multi-slice turbo spin echo sequence in the first 19 patients (TR/TE = 1604/100ms and 1431/100ms, resolution = 0.67x0.67x6.48mm³ and 4.4x0.7x0.7mm³, for transversal and sagittal scans, respectively). From the 20th patient onwards, respiratory-triggered sagittal and transversal anatomical T2W MultiVane XD (MVXD) scans were acquired instead of the previously mentioned scans, as these scans demonstrated improved image quality (TR/TE = 2039/100ms and 2243/100ms, resolution = 0.62x0.62x3.00mm³ and 3.00x0.63x0.63mm³, for transversal and sagittal scans, respectively).

Delineations on MRI

The GTV of the primary tumor was delineated on the transversal T2-weighted images for every MRI scan by a trained radiation oncologist (NT) and reviewed by a dedicated gastro-intestinal radiation oncologist (SM). The initial GTVs were delineated on the first T2 weighted MRI, taking into account information from the

PET-CT and endoscopy acquired in the standard diagnostic work-up. Subsequent GTVs were propagated from the previous scan and adapted based on the tumor volume on the transversal and sagittal T2-weighted images. Any disagreements were solved through discussion. Contouring and subsequent image analyses were performed with in-house developed software (Volumetool) [33].

Statistical analysis

Patient and tumor characteristics were described as counts with percentages, mean with standard deviation, or median with range where appropriate. Volumetric changes over time (i.e. during nCRT) were analyzed using linear mixed models to account for repeated measures. Two models were fitted to analyze the effect of histopathology (i.e. SCC vs. adenocarcinoma) and baseline tumor volume (i.e. smaller vs. larger tumors) on the volumetric changes. To assess the effect of histopathology the following model was fitted; relative tumor volume as a function of scan moment (time variable), histopathology and their interaction whilst correcting for age, sex, N-status, and baseline tumor volume. To analyze the effect of baseline tumor volume the included patients were divided into two groups (1) patients with baseline tumor volumes below the total group median (i.e. smaller tumors) (2) patients with baseline tumor volume above the total group median (i.e. larger tumors). Relative tumor volume was fitted as a function of scan moment (time variable), baseline tumor volume (smaller vs. larger tumors) and their interaction whilst correcting for age, sex, N-status, and histopathology. Since relative tumor volume was used as outcome of the linear mixed effects models, the models were fitted with random slopes only. An autoregressive correlation structure of the first order was used to account for the assumption that repeated measurements of tumor volume at small intervals have a stronger correlation than measurements at larger intervals. Results were presented as mean differences (MD) with 95% confidence intervals. The level of significance was set at $p < 0.05$. All statistical analyses were performed using SPSS Statistics version 23 (IBM Corp., Armonk, NY, USA) and R Core Team (2020) [34].

Characteristics		Full cohort	
		(n=29)	
Age at start of nCRT (range)		65	(46-77)
Sex	Male	26	(87%)
	Female	3	(13%)
Histopathology (based on biopsy) ^a	Squamous cell carcinoma	8	(28%)
	Adenocarcinoma	21	(72%)
Clinical T stage ^b	T2	2	(7%)
	T3	27	(93%)
	N0	9	(31%)
Clinical N stage ^b	N1	14	(48%)
	N2	5	(17%)
	N3	1	(3%)
Tumor location ^c	Middle 1/3	1	(3%)
	Lower 1/3	25	(86%)
	GEJ	3	(10%)
Mean tumor volume at baseline (cm ³)		46	(11-104)
nCRT completed		29	(100%)

^a: Determined in pre-treatment biopsy

^b: Based on the 7th edition of the American Joint Committee in Cancer (AJCC) [35]

^c: Determined with diagnostic endoscopy and PET-CT; nCRT: neoadjuvant chemoradiotherapy.

Table 2.1: Patient and tumor characteristics of the study population.

	Baseline	1st	2nd	3rd	4th	5th
Mean treatment time at scan (days(±))	-5(3)	2 (3)	9(3)	16(2)	23(2)	30(2)
Mean GTV (cm ³ (range))	45.4 (11 – 104)	45.5 (9 – 107)	41.5 (8 – 84)	37.6 (8 – 80)	35.2 (8 – 74)	32.3 (8 – 69)
GTV relative to baseline (%(range))	100	98.9 (70 – 119)	90.8 (74 – 107)*	81.4 (58 – 101)*	76.6 (44 – 106)*	72 (34 – 116)*
Mean time between scans	-	8	7	7	7	7
No. of scans	29	29	29	28	28	27

*p<0.05, statistically significant difference in tumor volume compared to the tumor volume at previous scan; Linear Mixed Effects Model. The minus symbol indicates a time point prior to the start of neoadjuvant chemoradiotherapy. TV; tumor volume.

Table 2.2: Mean absolute and relative tumor volume in each week of neoadjuvant chemoradiotherapy.

Results

Study population

A total of 32 patients with 184 MRI scans were included in the original study population. Three patients were excluded based on primary tumor histology other than adeno- or squamous cell carcinoma, a small tumor volume (<5cm³) at baseline impeding accurate image analysis and not completing the chemotherapy due to patients request. For the final analysis a total of 170 MRI scans of 29 patients were included. Due to patients request, not all patients underwent all six MRI scans resulting in a total of four missing scans in three patients (week 3-5 of nCRT). The final study population had a mean (\pm SD) age of 65 years (\pm 8) and 26 (87%) were men. Most patients (72%) had a histologically proven adenocarcinoma in a cT3 stage (93%) with clinically suspected nodal metastases (69%). The initial GTV had a mean (\pm SD) volume of 45 cm³ (\pm 23) and ranged from 11 to 104 cm³. All included patients completed the neoadjuvant chemoradiotherapy. A complete overview of patient and tumor characteristics is presented in Table 2.1.

Volumetric changes during nCRT

Between the baseline scan and the scan during the first week of nCRT an increase in tumor volume was observed in 16 (55%) patients. Tumor volume started to regress significantly, compared to the previous week, from the second week of nCRT onwards. A decrease to 42cm³ (91% of initial volume), 38cm³ (81%), 35cm³ (77%), and 32cm³ (72%) was observed in the second, third, fourth and fifth week of nCRT, respectively (Table 2.2). A spaghetti plot with the absolute and relative volumetric changes for each patient during nCRT, as well as the group mean, is depicted in Figure 2.1.

Histopathology

Correcting for age, sex, N-stage and baseline tumor volume, no statistical significant difference in tumor volumes between patients with SCC and adenocarcinoma was assessed during nCRT. This suggests that SCCs and adenocarcinomas follow a comparable regression pattern. The largest mean difference was 12% (95% CI; -0.3;24) and was observed in the fourth week of nCRT. A complete overview of the results of this linear mixed effects model is provided in Table 2.3.

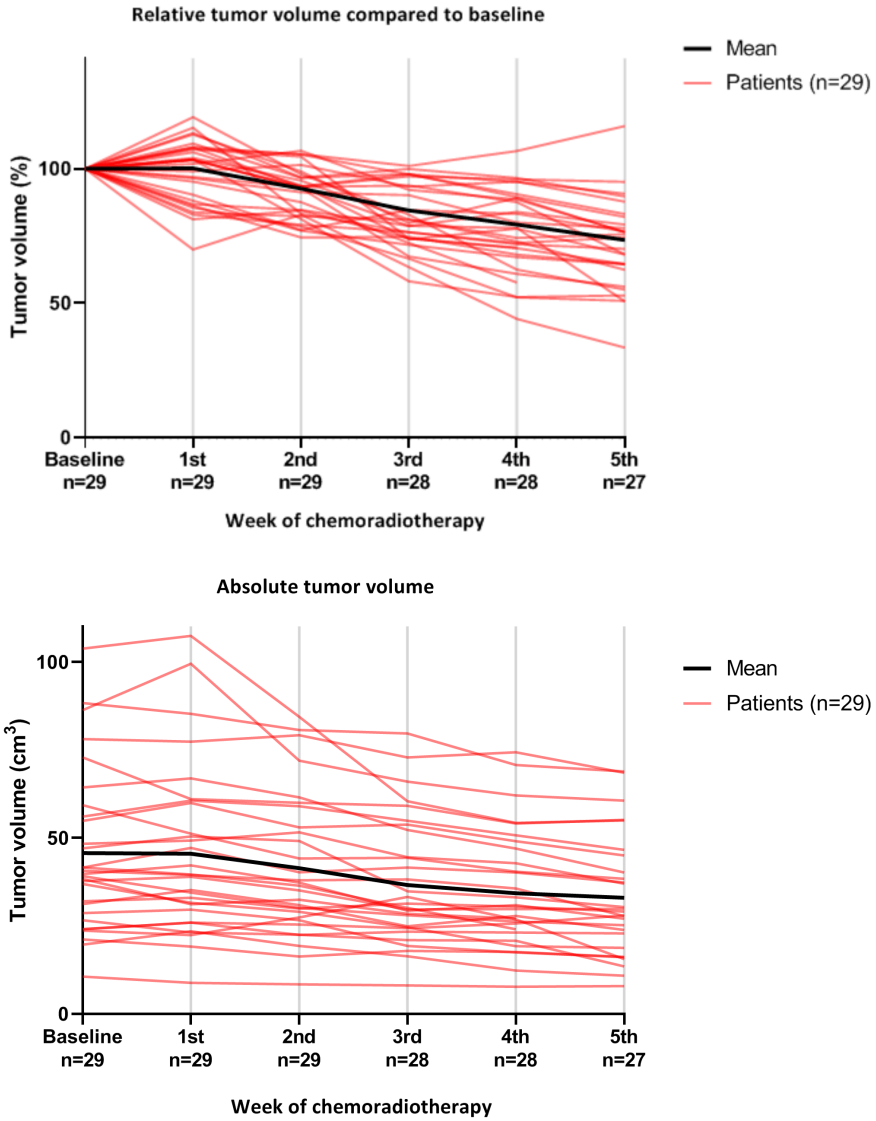


Figure 2.1: Absolute and relative tumor volumes (GTV) over the course of nCRT for each individual patient (red line) as well as the mean (black line). The relative tumor volume at each time point was calculated compared to baseline.

Baseline tumor volume

The largest mean difference of 2.7% (95% CI; -13.8;8.4) in tumor volume between the group with the smaller tumors and the group with the larger tumor was observed in the fourth week of nCRT. Correcting for age, sex, N-stage and histopathology statistical significant differences were not observed. These results indicate that larger and smaller tumors follow a comparable regression pattern during nCRT. A complete overview of the results of this linear mixed effects model is provided in Table 2.3.

Volumetric and anatomical changes on MRI

Tumor volume regression and changes in thoracic anatomy were clearly visible on the MRI scans (Figure 2.2 and Figure 2.3). Tumor volume regression often resulted in movement of the heart dorsally towards the spine and into the initial GTV, which was more prominent in a patient with a tumor of the middle 1/3 of the esophagus located behind the heart (Figure 2.3A). Nevertheless, in a patient with a tumor of the lower 1/3 of the esophagus the heart moved into the baseline GTV as well (Figure 2.3B).

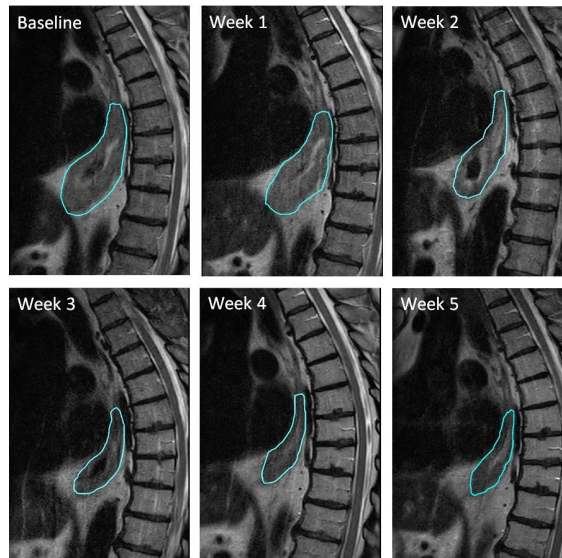


Figure 2.2: Visual representation of tumor volume (light blue contour) regression during 5 weeks of neoadjuvant chemoradiotherapy in a patient with a cT3N2M0 adenocarcinoma of the lower 1/3 of the esophagus (sagittal T2-weighted images).

	Baseline			1st week			2nd week			3rd week			4th week			5th week		
	N	EMM ^a	MD ^b	N	EMM ^a	MD ^b	N	EMM ^a	MD ^b	N	EMM ^a	MD ^b	N	EMM ^a	MD ^b	N	EMM ^a	MD ^b
Model histopathology	8	100	0	8	102.5	Reference group	8	94.2	Reference group	7	77.5	Reference group	7	68.9	Reference group	7	60.3	Reference group
Squamous cell carcinoma	21	100	0	21	97	-5.5	21	88.8	-5.4	21	84.6	-4.1	21	80.8	-3.9	20	72.1	-8.8
Adenocarcinoma	14	100	0	14	98.9	33	14	89.3	1.4	13	81.6	-7.7	13	75.1	-6.5	13	69.5	-5.6
Small tumours (40-70cc)	14	100	0	14	98.9	33	14	89.3	1.4	13	81.6	-7.7	13	75.1	-6.5	13	69.5	-5.6
Small tumours (41-104 cm ³)	14	100	0	14	98.9	33	14	89.3	1.4	13	81.6	-7.7	13	75.1	-6.5	13	69.5	-5.6

Model histopathology: estimated marginal means and mean differences of relative tumor volume between squamous cell carcinomas and adenocarcinomas at the subsequent scan moments during neoadjuvant chemoradiotherapy corrected for age, sex, N-stage and baseline tumor volume.

Model baseline tumor volume: estimated marginal means and mean differences of relative tumor volume between smaller and larger tumors corrected for sex, age, N-stage and histopathology.

N; number of patients
EMM; estimated marginal means
MD; mean difference
95% CI; 95% confidence interval

a; Estimated marginal means of relative tumor volume (%).
b; Mean difference in relative tumor volume (%) compared to the reference group.

Table 2.3: Results of the linear mixed effects models of histopathology and baseline tumor volume.

Discussion

This study aimed at assessing weekly changes in tumor volume during nCRT for esophageal cancer. Our findings demonstrated a tumor volume regression of 28% after five weeks of nCRT, starting after the first week of treatment. Volumetric changes were not statistically significantly influenced by histopathology and tumor volume at baseline during the course of neoadjuvant treatment. . This is the first study that reports volumetric changes during nCRT for esophageal cancer at weekly intervals based on MRI. Previous imaging studies focusing on esophageal tumor volume regression during nCRT on CT reported a volume regression of 10% after 10 fractions and 25% after 20 fractions [30,31]. These results are in line with the results of the current study. Additionally, due the weekly scans and volumetric assessment we were able to accurately assess the rate and pattern of tumor volume regression and its effect on the anatomical configuration. The changes in the anatomical configuration of the thoracic region are substantial during nCRT for esophageal cancer. Due to tumor volume regression, organs at risk (OARs), and especially the heart, could move into the initial GTV. This increases the radiation dose to the heart and thereby the probability of cardiac toxicity. Clinically relevant short- and long-term effects of cardiac toxicity following nCRT for esophageal cancer such as pericardial effusion, ischemic events and heart failure have been reported [36]. More recently, Johnson-Hart et al. demonstrated that image-guided radiotherapy (IGRT) shifts significantly correlate with survival [25]. They found that patients who have a mean residual shift towards the heart have a worse prognosis compared to those who have a mean shift away from the heart. This effect was observed in both esophageal cancer and lung cancer cohorts, underlining the importance of minimizing the radiation dose to the heart. The possible increase in dose to OARs due to tumor regression could be prevented by adapting initial radiation plans during nCRT. In order to contain costs and workload, defining the optimal timing for adaptation of radiation treatment plans is important. The observed regression pattern throughout nCRT in the current study suggests the optimal time point for plan adaptation could well be halfway treatment. At this time point significant tumor volume regression has taken place but also enough time remains for the patient to benefit from the re-optimized plan with better sparing of the heart. Dose reduction to the OARs would be the primary aim of adaptive radiotherapy as it seems that an adequate target coverage is maintained during nCRT. To analyze this hypothesis future dosimetric studies should be performed. In the current study we also investigated whether patient and tumor characteristics had an impact on the volumetric changes observed during nCRT. In our analysis, after correcting for covariates, we found the largest difference (11.9% (95% CI:-0.3;24)) in tumor

volume between SCC and adenocarcinoma in the fourth week of nCRT, however, no statistically significant differences were found. For baseline tumor volume the largest difference (2.7% (95% CI; -13.8;8.4)) between smaller tumors and larger tumor was observed in the fourth week of treatment, again no statistical significant differences were found. These results suggest that the effect of these tumor characteristics on the volumetric changes during nCRT might be marginal. It has to be taken into account that this is possibly due to the limited number of patients in the current analysis. As aforementioned, some limitations apply to the current study. First, due to the small number of patients, both the results of the analysis for histopathology and baseline tumor volume should be interpreted with caution. Due to the homogeneity of our study population in terms of clinical T-stage and tumor location, we were not able to assess the impact of these covariates in our analysis. Studies in larger and more heterogeneous patient groups are warranted to be able to accurately identify patient and tumor characteristics that influence volumetric changes in order to select patients that might benefit from adaptive radiotherapy. Besides the small sample size, the manual delineations on MRI could be considered as a limitation of this study. Literature on the accuracy of delineating on MRI for esophageal cancer is scarce. However, a recent report has shown promising results in terms of the feasibility and interobserver variability in delineation of esophageal cancer on MRI compared to FDG-PET/CT [37]. In conclusion, this study demonstrated a decrease in tumor volume during nCRT for esophageal cancer observed with weekly MRI. Volume regression and consequential anatomical changes were considerable, which suggest the possible benefit of adapting radiation treatment plans during nCRT. This report should act as an incentive to further investigate the added value of adaptive radiotherapy for esophageal cancer.

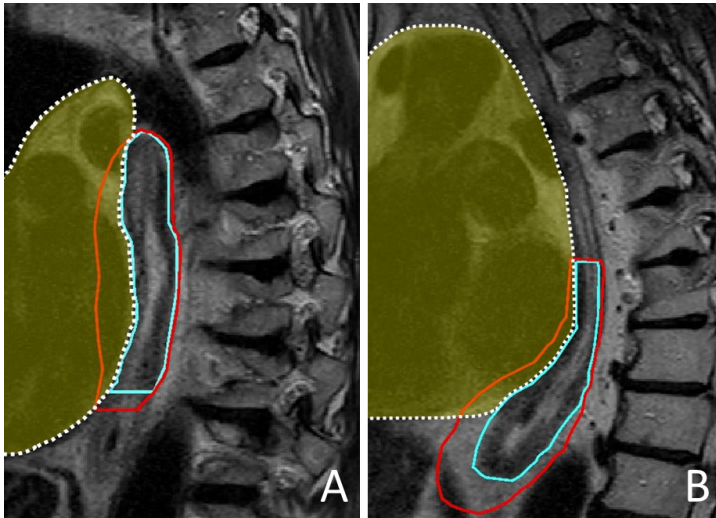


Figure 2.3: Anatomical changes due to volume regression in two patients. A: Patient with a cT3N1M0 squamous cell carcinoma of the middle 1/3 of the esophagus. B: Patient with a cT3N2M0 adenocarcinoma of the lower 1/3 of the esophagus (sagittal T2-weighted images). Red line, tumor volume at baseline; light blue line, tumor volume in the fifth week of nCRT; dotted white line, dorsal border of the heart and pulmonary veins ; yellow area, heart and pulmonary veins.

Chapter 3

CTV-to-PTV margin assessment for esophageal cancer radiotherapy based on an accumulated dose analysis

The following chapter is based on:

MR Boekhoff, IL Defize, AS Borggreve, R van Hillegersberg, ANTJ Kotte, JJW Lagendijk, ALHMW van Lier, JP Ruurda, N Takahashi, S Mook, GJ Meijer

Radiotherapy and Oncology 161 (2021) 16-22

doi:10.1016/j.radonc.2021.05.005

Abstract

Purpose

This study aimed to assess the smallest clinical target volume (CTV) to planned target volume (PTV) margins for esophageal cancer radiotherapy using daily on-line registration to the bony anatomy that yield full dosimetric coverage over the course of treatment.

Methods

29 esophageal cancer patients underwent six T2-weighted MRI scans at weekly intervals. An online bone-match image-guided radiotherapy treatment of five fractions was simulated for each patient. Multiple conformal treatment plans with increasing margins around the CTV were created for each patient. Then, the dose was warped to obtain an accumulated dose per simulated fraction. Full target coverage by 95% of the prescribed dose was assessed as a function of margin expansion in six directions. If target coverage in a single direction was accomplished, then the respective margin remained fixed for the subsequent dose plans. Margins in uncovered directions were increased in a new dose plan until full target coverage was achieved.

Results

The smallest set of CTV-to-PTV margins that yielded full dosimetric CTV coverage was 8mm in posterior and right direction, 9mm in anterior and cranial direction and 10mm in left and caudal direction for 27 out of 29 patients. In two patients the curvature of the esophagus considerably changed between fractions, which required a 17 and 23 mm margin in right direction.

Conclusion

Accumulated dose analysis revealed that CTV-to-PTV treatment margins of 8, 9 and 10 mm in posterior & right, anterior & cranial and left & caudal direction, respectively, are sufficient to account for interfraction tumor variations over the course of treatment when applying a daily online bone match. However, two patients with extreme esophageal interfraction motion were insufficiently covered with these margins and were identified as patients requiring replanning to achieve full target coverage.

Introduction

Esophageal cancer is the eight most prevalent cancer worldwide. Multimodal treatment strategies comprising neoadjuvant chemoradiotherapy plus surgery or definitive chemoradiotherapy have improved survival of patients with locally advanced esophageal cancer [2, 38, 39]. Irradiation of esophageal cancer often comes with large clinical target volumes (CTVs) with complex shapes to secure optimal dose delivery to all tumor cells. Image-guided radiation therapy (IGRT) allows rigid alignment of the bony anatomy on kilo-/megavoltage cone-beam CT (CBCT) or 2D fluoroscopy images with the 3-dimensional (3D) planning computed tomography before radiation dose delivery [16, 40–43]. However, considerable residual geometrical uncertainties due to interfraction tumor position variation and shape changes require the use of treatment margins to establish sufficient coverage of the CTV over the course of treatment. Many studies have investigated these geometrical uncertainties in order to quantify the associated CTV-to-Planning Target Volume (PTV) margins with the use of repetitive CT, CBCT or Magnetic Resonance Imaging (MRI) over the course of treatment [5–7, 40, 42, 44–47]. Of particular interest are the recent studies that reported on the inter- and intrafraction displacement on CBCTs of fiducial markers that were endoscopically placed at some anchor points in the tumor [5–7]. Here, the marker movements were used as a surrogate for the gross tumor volume (GTV) and CTV displacements as generally the 3D anatomy of the CTV cannot be adequately segmented on the CBCT. Based on these displacements, the well-known margin recipe of van Herk et al. was used to derive margins for various set-up strategies [14]. For the most commonly employed set-up strategy, i.e. daily alignment to the bony anatomy (predominantly vertebrae), these studies concluded that large margins are required. Although these studies reported sound and reproducible data on the interfraction motion of the markers, the ensuing CTV-to-PTV margins using the ‘van Herk’-recipe could be biased for a number of reasons. First, the margin recipe assumes rigid movements of the entire CTV, whereas the CTV interfraction variation is often characterized by shape changes. Second, the markers were sampled over the tumor (GTV) and not over the CTV which may lead to different motion characteristics. Thirdly, the margin recipe assumes perfect conformity at every surface element of the PTV surface often in conjunction with steep dose gradients outside the PTV. Aim of the current report was to overcome these aforementioned limitations by doing a full dosimetric assessment in a cohort of esophageal cancer patients and to assess the smallest CTV-to-PTV margins that yield full target coverage in a virtual daily online bone match image-guided treatment series using five weekly acquired MRI scans as treatment samples. By doing so, not only the dosimetric impact of day-to-day translations of the tumor itself is accounted for,

but also the dosimetric effects of all morphologic changes (e.g tumor regression) over the course of treatment are incorporated.

Methods

Patient inclusion

A total of thirty-two patients with histopathologically confirmed esophageal cancer who were scheduled to undergo neoadjuvant chemoradiotherapy according to the CROSS regimen (23 fractions of 1.8 Gy with concurrent carboplatin/paclitaxel³) were included in this single-center prospective cohort study between December 2015 and April 2018. Exclusion criteria for enrollment in the study were age <18 years, previous thoracic surgery or thoracic radiotherapy, and contraindications for MRI. The study was approved by the institutional review board of the University Medical Center Utrecht (protocol ID 15-340). All participants provided written informed consent. In our previous paper, we reported on the isotropic margins required for geometric target coverage for a bone match setup and a rigid tumor registration setup for individual fractions for these patients ¹⁶. In the current work, we assessed the treatment margins in all directions which yielded sufficient target coverage for a whole treatment, based on a full accumulated dosimetric analysis.

Image acquisition

Each patient underwent six times T2-weighted MRI scans, one prior to treatment and five times during neoadjuvant chemoradiotherapy at weekly intervals. Images were acquired on a 1.5T Philips Ingenia (Best, the Netherlands), using anterior/posterior (28 channel) receive coils. Patients were positioned in supine position with both arms next to the body for increased patient comfort during MRI scanning, in contrary to positioning during a conventional treatment session, when arms are positioned above the head. Respiratory-triggered transversal and sagittal anatomical T2-weighted scans (T2W) were acquired with a multi-slice turbo spin echo sequence in the first 19 patients (TR/TE = 1604/100ms and 1431/100ms, resolution = 0.67x0.67x6.48mm³ and 4.4x0.7x0.7mm³, for transversal and sagittal scans, respectively). From the 20th patient onwards, respiratory-triggered sagittal and transversal T2W MultiVane XD (MVXD) scans were acquired instead of the previously mentioned scans, as these scans demonstrated improved image quality (TR/TE = 2039/100ms and 2243/100ms, resolution = 0.62x0.62x3.0mm³ and 3.0x0.63x0.63mm³, for transversal and sagittal scans, respectively).

Delineations

A certified radiation oncologist (N.T.) delineated the GTV on each MRI which was subsequently reviewed by a radiation oncologist specialized in upper gastrointestinal malignancies (S.M.). Any disagreements were solved through a consensus discussion. Next, the CTV was created using a margin of 0.5 cm around the GTV in the left, right, anterior and posterior directions (excluding the heart, large vessels, trachea, bronchial tree and lungs), 3 cm in cranial direction and 2 or 3 cm caudally (2 cm in case of tumor extension in the stomach).

Treatment simulation

An online bone-match IGRT treatment of five fractions was simulated for each patient. The first MRI scan was used as a reference scan and the five follow-up scans were used as individual samples of the patient's anatomy over the course of treatment. The reference MRI was rigidly aligned, based on a bone match, to the clinical planning CT, which was acquired on the same day as the reference MRI scan. Then, the CTV of the reference MRI was projected on the structure set of the planning CT, which consisted of organs at risk. These steps were necessary so that density information of the CT could be used in subsequent treatment planning. For every patient single full arc Volumetric-Modulated Arc (VMAT) plans with varying CTV-to-PTV margins were generated using the autoplanning module of the Pinnacle 16.2 treatment planning system, (Koninklijke Philips NV, Eindhoven, The Netherlands). The reason for using the Pinnacle system instead of the Monaco 5.40.01 treatment planning system (Elekta AB, Stockholm, Sweden) that we clinically use, was that the advanced scripting and autoplanning capabilities required for this study, were not yet available in the Monaco system at the time of this research. The target dose to the PTV was set to 41.4 Gy at 23 fractions (1.8Gy/fraction), whereas the optimization goals in the autoplanning toolkit were set to a mean lung dose <4.2 Gy (high priority) and a mean heart dose <10Gy (medium priority). Additional auxiliary structures were automatically generated to achieve a high 3D-conformity of the 95% isodose surface with respect to the PTV, as loose 95% isodose surfaces could yield an underestimation of the final margins in this study. For each plan, an online IGRT treatment was simulated by rigidly projecting the planned dose distributions on the follow-up scans by a bone-match registration (Figure 3.1). As patient positioning and alignment on the MRI scanner was less thoroughly performed (without laser guidance) than typically at the treatment unit, translational registrations based on the bony anatomy between the follow-up MRI and reference MRI could not directly be used for the treatment simulation, since this would result in an overestimated residual rotation. Therefore a multi-step registration was performed to simulate

patient positioning on a conventional treatment system. First, to adjust for the overestimated residual rotation, follow-up MRI scans were rigidly aligned (translations and rotations allowed) to the reference MRI scan based on grey values in a box around the vertebrae, located over the length of the tumor (typically four or five vertebrae), using the Elastix toolbox [48]. Then, a rotation correction was added to mimic a realistic rotational misalignment. The rotation correction was obtained from the rotational error of the clinical treatment fraction of the corresponding day of MRI acquisition measured with X-ray volume imaging software (Elekta AB, Stockholm, Sweden).

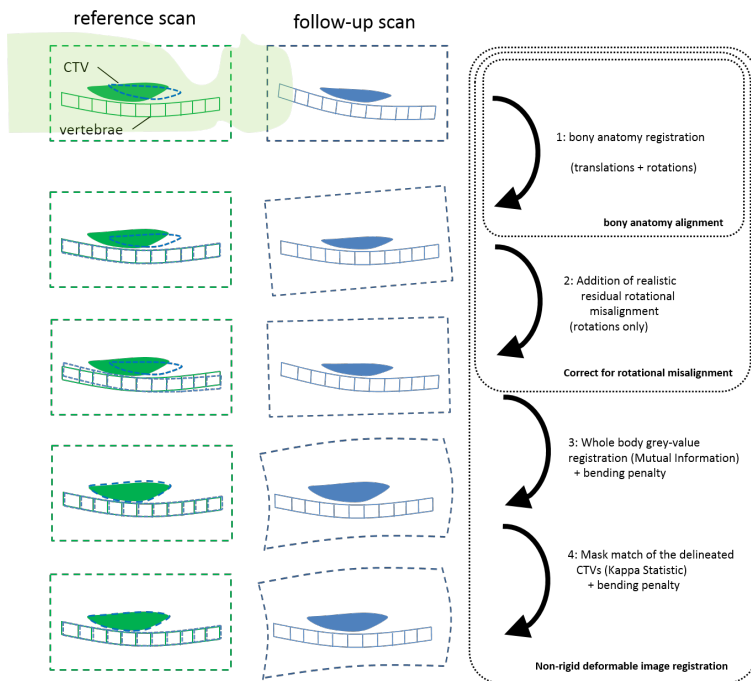


Figure 3.1: Schematic illustration of the registration steps applied to simulate an online IGRT setup procedure based on bony anatomy alignment (Step 1 and 2) followed by a two-step non-rigid deformable image registration used to accurately register the voxels from the follow-up scan to the reference scan in order to obtain an accumulated dose. First, a whole body grey-value registration (mutual information metric) was applied in combination with a bending penalty metric (Step 3). The second step consisted of a mask match of the delineated CTVs were the previous step was used as initial transform (Step 4). The deformation vector field is the combination of both non-rigid deformable image registration steps (Steps 3+4). The blue panels depict the follow-up scan after each registration step. In the green panels a sagittal view of the CTV and vertebrae of the reference scan is depicted. The dashed blue structure in the reference scan refers to the propagated CTV from the follow-up scan.

After the rigid alignment and rotation correction we assumed that the patient's anatomy was representative of positioning on a conventional treatment system. Next, each projected dose distribution on the follow-up scans was non-rigidly warped to the reference scan. For this, a two-step non-rigid B-spline image registration from the Elastix toolbox was used to accurately register the voxels from the follow-up scan to the reference scan for both the transversal and sagittal scans. First, a whole body grey-value registration (mutual information metric) was applied in combination with a bending penalty metric. To ensure correct mapping of the CTV a second registration step was performed. The second registration step consisted of a mask match of the delineated CTVs (kappa statistic metric), which again was also combined with a bending penalty metric. Subsequently, the deformation vector field (DVF) was applied to the projected dose to obtain the 'delivered' dose per fraction (Figure 3.2). All warped dose distributions of the follow-up scans were summed and projected on the reference scan to obtain a surrogate of the total accumulated/delivered dose distribution for each patient. The accuracy of the deformable registration was determined by calculating the dice coefficient between a warped mask of the follow-up CTV and the mask of the reference CTV.

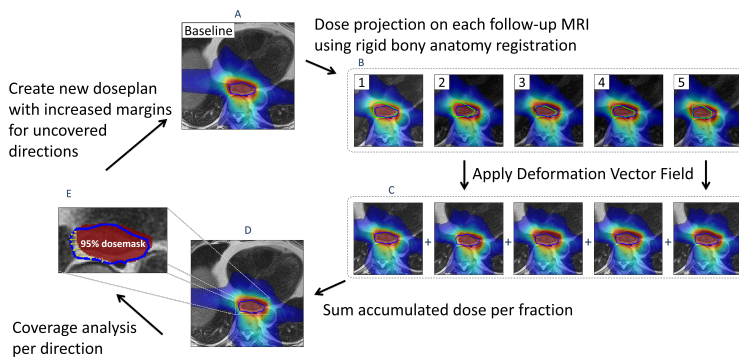


Figure 3.2: Schematic overview of dose warp and coverage analysis of a simulated treatment. First, a dose plan with 0mm CTV-to-PTV margins in all directions was created (A) based on the delineated CTV (blue delineations) in the baseline scan. Then, the dose was rigidly projected on the follow-up fractions (B). Here, the daily CTVs are shown by the green delineations. The deformation vector field, obtained from deformable image registration, was applied on the projected doses and resulted in a warped dose per fraction (C). These warped doses were summed to obtain the total accumulated dose over the course of treatment for a treatment plan with 0mm margins (D). Coverage analysis of the CTV by 95% of the prescribed dose indicated whether a direction was required an additional margin or not (E). Given an uncovered direction, the CTV-to-PTV margin in that direction was increased with +1mm and steps A-E are repeated with a new dose plan.

PTV margin determination

In the search for the smallest set of anisotropic CTV-to-PTV margins that yield full target coverage for all patients an iterative loop was initiated. Starting point was the dosimetric assessment of the accumulated dose of 0-mm plans where the PTV coincides with the CTV for all patients. For each direction the fraction of patients who obtained full coverage in this direction was assessed. In the next iteration the margin for each of the six main directions was increased with 1 millimeter if target coverage was not achieved in the direction in question for at least one patient. If target coverage in a single direction was accomplished for all patients, then the respective margin remained fixed for the subsequent dose plans.

Results

A total of 32 patients with newly diagnosed esophageal cancer were enrolled in this prospective study. Two patients were excluded based on a limited field of view in the cranial caudal direction on the reference scan and one because of withdrawal from study participation. Of the remaining 29 patients, three patients requested cancellation of a follow-up scan and 5 transversal follow-up scans were excluded based on a limited field of view in the cranial-caudal direction and 11 sagittal follow-up scans were excluded based on a limited field of view in the left-right direction. The final study population consisted of 29 patients who underwent a total of 140 transversal and 134 sagittal follow-up scans. Baseline patient and tumor characteristics are presented in Table 3.1. For all treatment plans the autoplanning module yielded very conformal dose distributions. The volume of the 95% isodose surfaces was on average only 14% larger than the PTV volume, which corresponded to an average distance of 1.5 mm between the PTV surface and the 95% isodose surface. This high conformity could generally be achieved without sacrificing any PTV coverage. The median V95 was 99.2% and the 25% and 75% interquartile ranges were 98.5 and 99.8, respectively.

Characteristics	Full cohort (n=32)	
	n	(%)
Age at diagnosis (years), mean (range)	65	(46-77)
Sex		
Male	28	87.5
Female	4	12.5
Tumor Location		
Proximal esophagus	0	0
Middle esophagus	2	6
Distal esophagus	27	84
Gastroesophageal junction (GEJ)	3	10
Clinical T stage*		
cT2	2	6
cT3	30	94
Clinical N stage*		
cN0	9	28
cN1	17	53
cN2	5	16
cN3	1	3
Histology		
Squamous cell carcinoma	9	28
Adenocarcinoma	22	69
Other	1	3

* Clinical and histopathologic T- and N- stage are based on UICC TNM 7th edition.

Table 3.1: Clinical characteristics of the study population.

The average dice coefficient of the warped CTVs was 0.91 ± 0.02 and 0.92 ± 0.02 for transversal and sagittal registrations, respectively. Further visual inspection of all registered images revealed no abnormalities in surrounding tissue (i.e. deformed vertebrae or aorta). As anticipated, at a 0-mm CTV-to-PTV margin underdosing of the CTV occurred in all directions for all patients. The only exception here was patient 2 where the minimum dose of all caudal CTV voxels remained above the 95% prescription dose threshold after the dose warping procedure. Increase of the CTV-to-PTV margin resulted in an increase of target coverage and an isotropic margin of 5 mm yielded full dosimetric CTV coverage for 31% of the patients, whereas an isotropic 8-mm margin resulted in full

coverage for 83% of the patients (Figure 3.3).

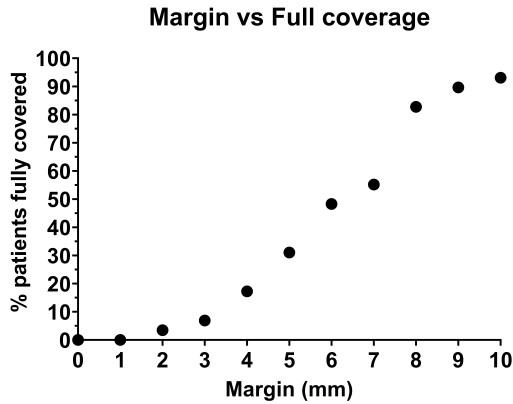


Figure 3.3: Percentage of patients where the CTV is fully covered in all directions on all fractions when an isotropic margin around the CTV is used.

In Table 3.3 the anisotropic margins that would yield full dosimetric CTV coverage are listed for each individual patient. The smallest set of CTV-to-PTV margins that yielded full dosimetric CTV coverage in 27 out of 29 patients was 8 mm in the posterior and right direction, 9 mm in the anterior and cranial direction and 10 mm in the left and caudal direction (Figure 3.4 & 3.5).

In two patients (patients 12 and 15) the curvature of the esophagus considerably changed over the course of treatment. In both patients the esophageal tract at the level of the heart was located left from the midline at the reference scan, however after two weeks of treatment this tract moved entirely over the midline in the right direction. In patient 15 this change was permanent, whereas in patient 12 the tract moved back to its original position in week 4 (Figure 3.6). Subanalysis revealed that for patient 12 a margin of 17 mm in the right direction was required to assure adequate CTV coverage whereas for patient 15 an even larger margin of 23 mm was needed.

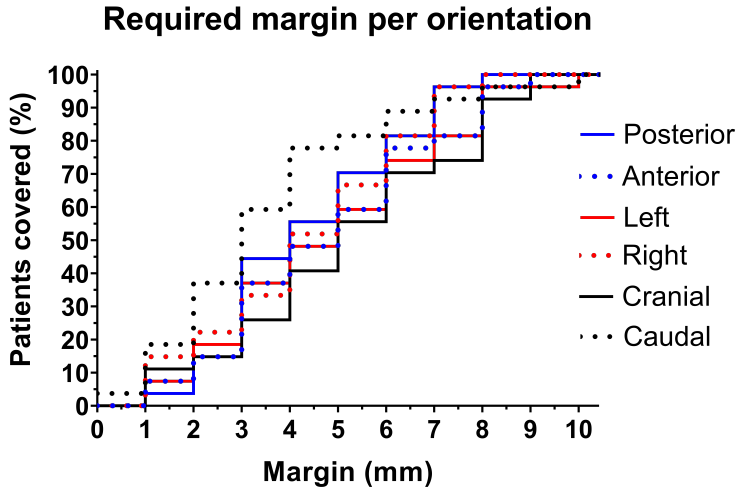


Figure 3.4: CTV covered per CTV-to-PTV margin for each direction. Posterior and right direction require a margin of 8mm, cranial and anterior direction need a 9mm margin and left and caudal direction requires a margin of 10mm for full CTV coverage in 27 out of 29 patients.

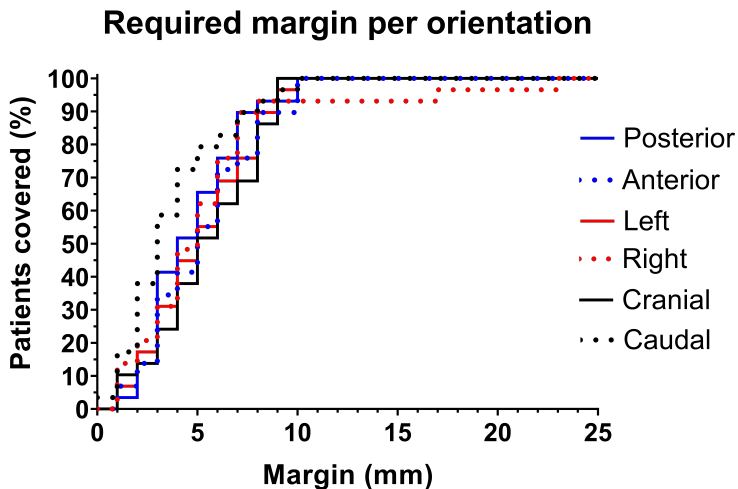


Figure 3.5: Patients covered per CTV-to-PTV margin for each direction. Cranial direction required a 9 mm margin, left, posterior, anterior and caudal directions required a margin of 10 mm and right direction required a margin of 23 mm to achieve full target coverage for all 29 patients.

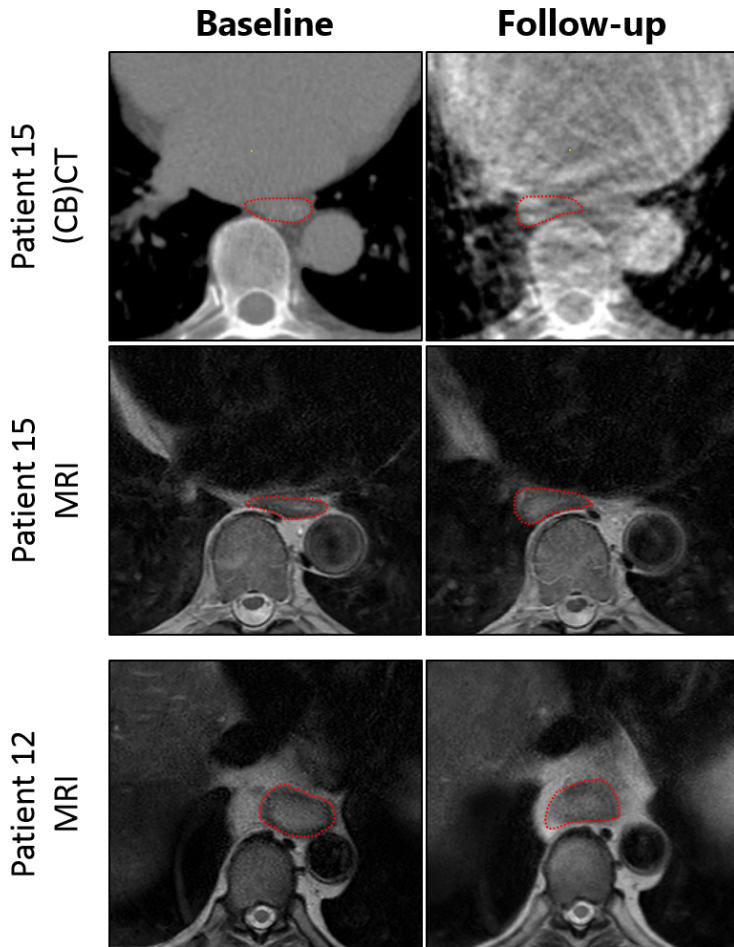


Figure 3.6: Example of a significant change in curvature of the esophageal tract over the course of treatment. This was clinically of concern as these tumor (red) shape changes remained unnoticed during our clinical CBCT procedures (top panels), although very evident on MRI (middle and bottom panels). Here, for patient 12 and 15, the esophageal tract was located left from the midline at the reference scan (left panels) at the level of the heart (patient 15, middle panel), however after two weeks of treatment this tract moved entirely over the midline in the right direction (right panel). The change in curvature occurs above the gastroesophageal junction (patient 12, bottom panel).

Discussion

In this study the dosimetric target coverage was assessed in a cohort of esophageal cancer patients where each patient was virtually treated with a 5-fraction radiotherapy regimen using an online bone match. Accumulated dose analysis via dose warping after MR image registration was used to establish adequate CTV-to-PTV margins. Two patients revealed a very mobile esophagus where part of the esophageal tract crossed the midline of the patient during treatment at the level of the heart, whereas the cardia remained in place. This was quite remarkable as the left-right movement was generally modest in the remaining patients. The movements in these patients were quite substantial and only a local PTV margin in the right direction of 23 mm could dosimetrically absorb this deformation when aligning these patients to the bony anatomy. This was clinically of concern as these shape changes, although very evident on MRI, remained unnoticed during our clinical CBCT procedures (see Figure 3.6) and only fiducial markers might have helped us identifying these patients. If we consider the two patients with the extreme mobile esophagus as outliers then our analysis revealed that CTV-to-PTV margins of 8 mm in posterior and right, 9 mm in anterior and cranial and 10 mm in left and caudal direction are required to ensure adequate target coverage in 27 out of 29 patients. Smallest margins were observed in the posterior and right direction. This could partly be explained by the shape of the CTV and its anatomical orientation with respect to the vertebrae. In most patients, large parts of the CTV posteriorly lie adjacent to the vertebrae and therefore motion in this direction is physically hampered. Largest margins were needed in the left and caudal direction, which was related to typical caudal curvature of the esophagus towards the stomach and variations in stomach filling in this patient cohort. Previously published studies on CTV-to-PTV margins for esophageal cancer - based on the relative motion statistics of implanted gold markers in combination with the 'van Herk'-recipe - reported comparable anisotropic margins for the three main directions. Substantial marker position variability with respect to the bony anatomy has been reported by Voncken et al. yielding PTV margins of 10, 13 and 7 mm in LR, CC and AP direction, respectively [7]. Similarly, Jin et al. reported that a margin of 9 mm in LR direction, 12 mm in CC direction and 7 mm in AP direction should provide sufficient target coverage [5]. Hoffmann et al. reported similar anisotropic margins of 9, 11 and 7 mm in LR, CC and AP directions, respectively [6]. Our findings are to a large extent in agreement with these previously reported margins (Table 3.2).

	Patients	Left (mm)	Right (mm)	Cranial (mm)	Caudal (mm)	Posterior (mm)	Anterior (mm)
This work	27 out of 29	10	8	9	10	8	9
Jin et al. [5]	24	9	9	12	12	7	7
Hoffmann et al. [6]	21	9	9	11	11	7	7
Voncken et al. [7]	56	10	10	13	13	7	7

Table 3.2: Comparison of CTV-to-PTV margins as assessed in our study with other publications.

However, we found smaller CC margins and slightly larger AP margins. A possible explanation for the smaller CC margins could be that the CC motion of the markers (placed in or close to the tumor) could largely be compensated for by AP and LR margins of surrounding CTV tissue, which typically extends in the CC direction due to the shape of the esophagus. In contrast to the marker studies, we were able to independently quantify CTV-to-PTV margins required to compensate for interfraction motion in all 6 main directions by sampling the full CTV surface. As a result, we found larger margins in left, caudal and anterior direction, which are mainly associated with the changes in stomach volume. These variations would remain unseen in marker studies which only give point-based motion measurements. It should be noted that in our patient cohort 30 of 32 patients had a distal esophageal tumor or a tumor at the gastroesophageal junction and as a consequence the CTV includes the proximal stomach in most patients. This means that potentially smaller margins could be applied for patients with proximal tumors where the caudal part of the CTV does not extend beyond the gastro-esophageal junction. Our study has a few weaknesses. First, due to the use of respiratory triggering, imaging is frozen at a near expiration state, while cardiac motion was not or partly (MVXD images) corrected for which leads to slight image blurring. However, this cyclic intrafraction motion leads only to a slight dose blurring and therefore we believe has a minimal effect on the total required margin [6]. Second, because of respiratory-triggered scans, intrafraction motion during dose delivery has not been taken into account. However, we believe that the impact of the intrafraction motion on the CTV-to-PTV margin will be modest. The respiratory motion will generally cause a blurring of the dose in predominantly the CC direction which could only yield a modest increase of the margin of 1.6 mm or less [6]. In addition, we also believe that the impact of tumor/CTV drifts during treatment will only slightly impact the reported margins. This has been shown in a previous study of our group where we reported that not only the mean tumor drift over a 10 minute interval was just 1.5 mm but also that these drifts were generally random, meaning that drifts were different from day to day causing no systematic error, and thus do not substantially add to the required margin [49]. As such, we believe that the impact of respiratory motion and drifts on the total accumulated dose are only marginal and the CTV-to-PTV margins of tumor drifts of individual fractions are of less concern than large day-

to-day interfraction motion. The third weakness of our study is the relatively small sample size of our study population and MRI study simulation. Although we were able to perform a thorough dosimetric analysis on 140 ‘fractions’, the total number of patients eligible for analysis was 29 which is about the lower border for properly assessing a CTV-to-PTV margin. Similarly, the total number of simulated treatment fractions was 5 whereas our clinical regimen consist of 23 fractions. Although we believe that the systematic interfraction changes (sigma) can be properly captured in 5 samples, the tails of these distributions will inherently be undersampled. This means that the impact of an outlier could be overly expressed in the resulting margin, but also reversely, outliers in the real distribution that would have contributed to an increment in the margin could have been missed due to the coarse sampling rate. Fourthly, in our study we assumed the dose distribution to be invariant to density changes between treatment fractions. This means that density changes due to interfractional shifts of the diaphragm are not accounted in the dose analysis, although occasionally these changes could influence the CTV coverage at the level of the diaphragm when lateral fluences are involved, which is the case for our VMAT plans [50]. Therefore, the margins listed in this work do not warrant sufficient dose coverage in case of large base line shifts of the diaphragm. Fifthly, although the deformable image registration yielded high dice coefficients (0.91 ± 0.02 and 0.92 ± 0.02 for transversal and sagittal registrations, respectively), small registration errors did still exist which could have had an impact on the accumulated dose distributions and therefore our listed margins. However, we believe that the impact of these inaccuracies on the final margins are modest, as each accumulated dose distribution comes from the deformation vector fields of five registrations with each a separate error. An increase in registration accuracy could potentially be achieved with improved out of plane image resolutions. Finally, in this simulation study the MRI-scans were acquired in supine position with both arms next to the body whereas in daily clinic patients are typically treated with arms upwards. We believe that this difference in patient positioning did not impact the overall results as the arms-down anatomy was maintained in both the planning and simulation phase. Furthermore an in-house study with volunteers demonstrated that the anatomy of the esophageal tract in relation to the vertebrae was not sensitive to the position of the arms (no data shown). This work again demonstrates that in the absence of proper online target visualization (and adaptation) large margins are required to ensure proper adequate CTV coverage when applying daily online set-up based on bony anatomy. With the advent of MR Linacs, daily MR imaging could be used to correct online for the interfraction variability leaving only a CTV-to-PTV margin for the residual intrafraction motion and delineation uncertainty [22,24,47,51,52]. Online segmentation and replanning would not only reduce the dose to the or-

gans at risk (e.g. heart and lungs) but would also be of particular benefit for the few patients who exhibit extreme deformations that are not absorbed by the current suggested margins and are unlikely to be recognized on CBCT images. In conclusion, in this study we have analyzed and assessed the direction-specific CTV-to-PTV margins based on an extensive dose warping analysis in 29 patients. These margins vary between 8 mm for posterior and right direction up to 10 mm for the left and caudal direction. Adequate target coverage in the vast majority (27 out of 29) of patients was demonstrated when patients are daily aligned to the bony anatomy. However, we have to acknowledge that even at these rather generous margins outlying patients still do exist who may be underdosed and need special attention.

	Anterior	Posterior	Left	Right	Cranial	Caudal	Tumor location
Patient 1	3	1	2	1	4	1	Distal esophagus
Patient 2	3	3	4	1	1	0	Distal esophagus
Patient 3	6	6	6	6	3	3	Distal esophagus
Patient 4	8	7	8	5	9	3	GEJ
Patient 5	Withdrawal from study participation						Distal esophagus
Patient 6	1	5	1	6	1	4	Middle esophagus
Patient 7	Field of view limitations						Distal esophagus
Patient 8	5	5	6	3	5	2	Distal esophagus
Patient 9	2	3	3	2	3	1	Distal esophagus
Patient 10	6	4	1	6	4	4	Distal esophagus
Patient 11	2	3	3	2	5	2	Distal esophagus
Patient 12	10	10	9	17	9	1	Distal esophagus
Patient 13	3	3	3	1	8	1	Distal esophagus
Patient 14	8	3	8	7	6	6	Distal esophagus
Patient 15	10	10	9	23	9	9	Distal esophagus
Patient 16	4	4	4	4	3	4	Distal esophagus
Patient 17	3	3	4	3	6	3	Middle esophagus
Patient 18	8	6	8	6	6	4	Distal esophagus
Patient 19	6	7	6	7	7	7	Distal esophagus
Patient 20	3	5	5	5	4	3	Distal esophagus
Patient 21	4	4	3	4	5	5	Distal esophagus
Patient 22	8	8	8	8	8	2	Distal esophagus
Patient 23	9	6	10	5	7	10	Distal esophagus
Patient 24	5	5	2	7	4	5	GEJ
Patient 25	3	3	4	4	8	3	Distal esophagus
Patient 26	6	3	6	4	8	7	Distal esophagus
Patient 27	5	2	5	4	5	3	Distal esophagus
Patient 28	5	7	7	3	8	2	GEJ
Patient 29	1	2	2	1	1	2	Distal esophagus
Patient 30	Field of view limitations						Distal esophagus
Patient 31	7	7	7	7	9	1	Distal esophagus
Patient 32	6	2	5	5	2	8	Distal esophagus

Table 3.3: Required margin per direction for full dosimetric CTV coverage.

Chapter 4

3-Dimensional target coverage assessment for MRI guided esophageal cancer radiotherapy

The following chapter is based on:

MR Boekhoff, IL Defize, AS Borggreve, N Takahashi, ALHMW van Lier, JP Ruurda, R van Hillegersberg, JJW Lagendijk, S Mook, GJ Meijer

Radiotherapy and Oncology 147 (2020) 1-7

doi:10.1016/j.radonc.2020.03.007

Abstract

Purpose

This study aimed to quantify the coverage probability for esophageal cancer radiotherapy as a function of a preset margin for online MR-guided and (CB)CT-guided radiotherapy.

Methods

Thirty esophageal cancer patients underwent 6 T2-weighted MRI scans, 1 prior to treatment and 5 during neoadjuvant chemoradiotherapy at weekly intervals. Gross tumor volume (GTV) and clinical target volume (CTV) were delineated on each individual scan. Follow-up scans were rigidly aligned to the bony anatomy and to the clinical target volume itself, mimicking two online set-up correction strategies: a conventional CBCT-guided set-up and a MR-guided set-up, respectively. Geometric coverage probability of the propagated CTVs was assessed for both set-up strategies by expanding the reference CTV with an isotropic margin varying from 0 mm to 15 mm with an increment of 1 mm.

Results

A margin of 10 mm could resolve the interfractional changes for 118 out of the 132 (89%) analyzed fractions when applying a bone-match registration, whereas the CTV was adequately covered in 123 (93%) fractions when the registration was directly performed at the CTV itself (soft-tissue registration). Closer analyses revealed that target coverage violation predominantly occurred for distal tumors near the junction and into the cardia.

Conclusion

Online MR-guided soft-tissue registration protocols exhibited modest improvements of the geometric target coverage probability as compared to online CBCT-guided bone match protocols. Therefore, highly conformal target irradiation using online MR-guidance can only be achieved by implementing on-table adaptive workflows where new treatment plans are daily generated based on the anatomy of the day.

Introduction

Radiation therapy is an integral part of the treatment of esophageal cancer in all stages of the disease. Due to the risk of subclinical spread along the esophagus and the involvement of regional lymph nodes, large volumes with often complex shapes are targeted [5, 30, 31, 40, 44, 53]. In image-guided radiation therapy (IGRT) for esophageal cancer, it is currently common practice to rigidly register the bony anatomy on kilo-/megavoltage (kV/MV) cone-beam CT (CBCT) or 2D fluoroscopy images with the 3-dimensional (3D) planning computed tomography (pCT) for patient setup verification [16, 40–43]. Although actual tumor volume-based registration is preferred, this is generally not possible due to the limited soft-tissue contrast in CT and CBCT, especially in the region of the diaphragm. As a result, interfractional tumor position variation relative to bony anatomy is currently a dominant uncertainty that has to be taken into account to ensure adequate target coverage. Many groups have investigated interfractional esophageal tumor motion relative to the bony anatomy using repetitive CT, CBCT or Magnetic Resonance Imaging (MRI) scans [30, 40, 44–46]. Of particular interest are the studies that analyzed the interfraction displacement of fiducial markers over the course of treatment [5, 6, 42]. All studies concluded that, particularly for distal tumors, large margins ($>1\text{cm}$) are required, resulting in bulky planning target volumes (PTVs) and a high irradiation burden to surrounding organs at risk. The advent of MRI linacs with onboard MRI guidance has enabled online visualization of both the tumor and organs at risk and thereby provided the opportunity of soft tissue set-up correction [22–24, 54, 55]. Furthermore, the incorporation of more detailed information regarding a patient's anatomy creates the opportunity of online target definition and online replanning, allowing high precision treatments with a possible reduction of treatment margins. Two online adaptive regimens can typically be applied. The first and most elementary regimen is equivalent to the widely applied online CBCT regimen, where patient set-up is adapted online to daily variations. However, instead of aligning the patient to the bony anatomy, the soft-tissue contrast of the MR images allows for direct alignment to the target anatomy. This procedure is also referred to as adapt-to-position [56, 57] or (virtual) couch shift [58, 59] and translates the pre-treatment dose distribution (without new contour regeneration) to compensate for the positional changes in a patient's anatomy. This is a fast and simple procedure that can be easily implemented in daily clinic, as all operations involved are matched with the current staffing levels and responsibilities of the radiation therapy technologist. The downside is that residual errors due to rotations and anatomical changes are not corrected. In the second strategy, this weakness is subdued by propagating and adapting all delineations to the current anatomy. This results in an on-table adap-

tive workflow where a new plan for the anatomy of the day is generated. This procedure, also referred to as adapt-to-shape [56,60] or SMART [61–63], might only yield minimal residual errors, originating from respiratory movements and other intrafraction motion. Here, accurate target definition is key and therefore the presence of a well-trained radiation oncologist is required at every treatment fraction. Besides recontouring, daily replanning makes this procedure also more time consuming than the straightforward adapt-to-position strategy. Aim of this study was to quantify the coverage probability as function of a preset margin when performing soft tissue registrations (i.e. adapt-to-position regimen) in a series of esophageal cancer patients that were weekly imaged with MRI. In addition, the target coverage probability was also assessed when applying bony-anatomy registrations to evaluate the benefit of soft-tissue registrations over bony-anatomy registrations.

Methods

Patient inclusion

Thirty-two patients with histopathologically confirmed esophageal cancer who were scheduled to undergo neoadjuvant chemoradiotherapy (23 fractions of 1.8 Gy with concurrent carboplatin/paclitaxel [2]) followed by esophagectomy, were included in this single center, prospective cohort study between December 2015 and April 2018. Exclusion criteria for enrollment in the study were age <18 years, previous treatment with thoracic surgery or thoracic radiotherapy, and contraindications for MRI. The study was approved by the institutional review board of the University Medical Center Utrecht (protocol ID 15-340). All participants provided written informed consent.

Image acquisition

All patients underwent 6 T2-weighted MRI scans, 1 prior to treatment and 5 during neoadjuvant chemoradiotherapy at weekly intervals. Images were acquired on a 1.5T Philips Ingenia (Best, the Netherlands), using anterior/posterior (28 channel) receive coils. Patients were positioned in supine position with both arms next to the body. Respiratory-triggered transverse anatomical T2-weighted scans (tT2W) were acquired with a multi-slice turbo spin echo sequence in the first 19 patients (TR/TE = 1604/100ms, resolution = 0.67x0.67x6.48mm³, FOV = 336x336x28 voxels). From the 20th patient onwards, respiratory-triggered transverse anatomical T2W MultiVane XD (MVXD) scans were acquired instead of the previously mentioned tT2W scans, as these scans demonstrated improved resolution (TR/TE = 2039/100ms, resolution = 0.62x0.62x3mm³, FOV = 672x672x60

voxels). Respiratory-triggering was performed with a 1-D navigator on the liver-lung boundary and triggered on the expiration.

Delineations

The GTV was delineated on each individual MRI by a certified radiation oncologist (N.T.) and subsequently reviewed by a radiation oncologist specialized in upper gastrointestinal malignancies (S.M.). Any disagreements were solved through a consensus discussion. Next, the CTV was created using a margin 0.5 cm around the GTV in the transverse direction (excluding the heart, large vessels, trachea, bronchial tree and lungs), 3 cm in cranial direction and 2 or 3 cm caudally (2 cm in case of tumor extension in the stomach) [64].

Treatment simulation

A 5-fraction radiation treatment with MRI was simulated for each patient individually. The first MRI scan was used as reference scan and the 5 follow-up scans were used as individual samples of the patient's anatomy over the course of treatment. Two online patient set-up scenarios were mimicked. In the first scenario, a CBCT correction strategy was simulated where set-up corrections were based on bony anatomies. In the second scenario, a soft-tissue online set-up correction strategy was mimicked where the CTV on the follow-up scan was rigidly aligned with the CTV on the reference scan. As patient positioning and alignment on the MR scanner was less thoroughly performed than at the treatment unit, the translational MR-to-MR registrations could not directly be used for the treatment simulation, since this would result in an overestimated residual rotation. Therefore, the sampling of the individual simulated treatment fractions was performed in a multistep process. In Figure 4.1 each of these following steps is schematically depicted. First, all follow-up scans were rigidly registered (translations and rotations allowed) to the reference scan based on grey values in a mask around the vertebrae using Elastix [48]. Second, a rotation was added to mimic a realistic rotational misalignment. Here the rotational error of the clinical treatment fraction of corresponding to the day of MR acquisition measured with our X-ray volume imaging (XVI) software (Elekta AB, Stockholm, Sweden) was propagated, as we assume that the residual rotational positioning errors using the laser system are similar for MRI linacs and regular linacs. In the third and final step, a soft tissue match of the CTV was simulated by maximizing the dice-coefficient of the reference CTV mask with the CTV mask in the follow-up scan by applying translations only. Here, a direct mask match was chosen as a grey-value registration in a deforming anatomy typically yielded unsatisfactory match results. After both the bony anatomy and soft tissue alignments, the CTV delineations in the follow-up scans were propagated to the reference scan for analysis, with the transformations

resulting from both set-up simulation scenarios. In the final step the geometric coverage probability of the propagated CTV with an expanded margin around the reference CTV was assessed. Here, the reference scan was resampled to a high resolution grid with a slice thickness of 1mm and the CTV of the reference scan was expanded to a new structure with an isotropic margin varying from 0 mm to 15 mm with an increment of 1 mm. In-house developed software was used for coverage analysis [65]. Follow-up fractions were marked as covered if more than 99% of the propagated CTV was covered by the expanded reference CTV.

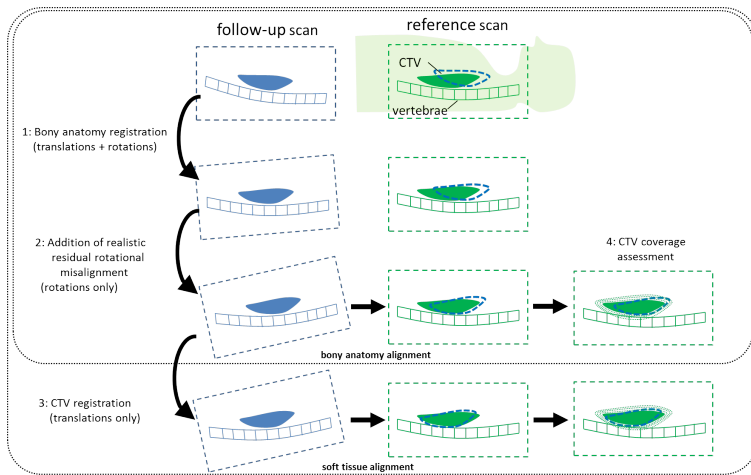


Figure 4.1: Schematic illustration of the registration steps applied to mimic a CBCT bony anatomy set-up procedure (Step 1 and 2) and a set-up procedure where the CTVs are aligned using soft-tissue MR contrast (Step 1, 2 and 3). The blue panels depict the follow-up scan after each registration step. In the right green panels a sagittal view of the CTV and vertebrae of the reference scan is depicted. The dashed blue structure in the reference scan refers to the propagated CTV from the follow-up scan. In step 4 the geometric target coverage of the expanded CTV is assessed for both setup regimens.

Results

A total of 32 patients with newly diagnosed esophageal cancer were enrolled in this prospective study. One patient was excluded based on a limited field of view in the cranial caudal direction on the reference scan and one because of withdrawal from study participation. Furthermore, of the remaining 30 patients, 3 appointments for follow-up scans were cancelled upon patient request and 8 follow-up scans were excluded based on a limited field of view in the cranial caudal direction. The final study population consisted of 30 patients who underwent a total of 139 follow-up scans. Baseline patient and tumor characteristics are presented in

Table 4.1. Visual inspection of the results of the patient set-up scenario revealed that the image registration of the follow-up scans to the bony anatomy and to the tumor of the reference scan was feasible for all scans, without the need for manual corrections. Considerable day-to-day shape changes of the CTV regularly occurred over the course of treatment of esophageal cancer patients and could not be compensated for by translational shifts based on soft-tissue registration. An isotropic margin of 5 mm around the CTV could only resolve the effect of shape changes in 79% of the fractions if the CTV of the follow-up scan was rigidly aligned to the CTV of the reference scan (i.e. adapt-to-position strategy) (Figure 4.2, solid black line). In addition, in 6% of the fractions the anatomical deformations of the CTV could not be compensated by a 10-mm margin. These deformations came from lateral tumor displacement in the middle and distal esophagus and from changes in stomach filling. The target coverage probability decreased when bone match registrations were applied instead of soft-tissue matching. An isotropic margin of 5 mm around the CTV resolved the combined misalignment and shape deformations in 61% of the evaluated fractions and even a margin of 12 mm could not prevent a geometrical miss of the target in 9% of the fractions (Figure 4.2, dashed blue line).

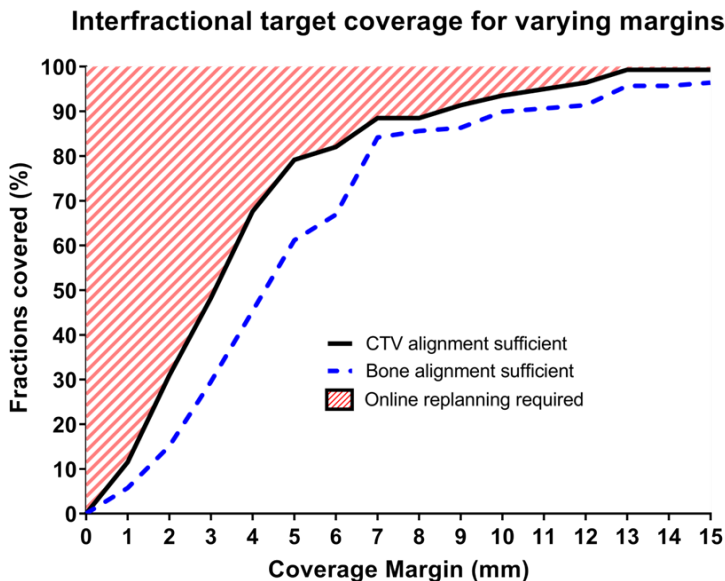


Figure 4.2: Percentage of fractions fully covered (139 fractions, 30 patients) for varying coverage margins shown for alignment to the bony structure (dashed blue line) and the soft-tissue strategy with direct alignment to the CTV (solid black line). Fractions without adequate target coverage for these coverage margins require online replanning (red striped area).

Characteristics	Full cohort (n=30)	
	n	(%)
Age at diagnosis (years), mean (range)	65	(46-77)
Sex		
Male	26	87
Female	4	13
Tumor Location		
Proximal esophagus	0	0
Middle esophagus	2	7
Distal esophagus	25	83
Gastroesophageal junction	3	10
Clinical T stage*		
cT2	2	7
cT3	28	93
Clinical N stage*		
cN0	9	30
cN1	15	50
cN2	5	17
cN3	1	3
Pathology biopsy*		
Squamous cell carcinoma	9	30
Adenocarcinoma	20	67
Undefined	1	3

* Clinical and histopathologic T- and N- stage are based on UICC TNM 7th edition.

Table 4.1: Clinical characteristics of the study population.

A paired samples t-test showed a significant higher target coverage when comparing CTV alignment to bone alignment ($p < 0.001$). Furthermore, it turned out that if the target coverage was compromised, this mostly occurred at the distal part of the CTV, near the gastroesophageal junction and into the cardia (Figure 4.3 and 4.4). Occasionally, large changes in the esophageal tract occurred at more proximal levels. This is illustrated in Figure 4.5, which shows MRI scans of 2 fractions of the same patient where at a proximal level large lateral deformations were observed (5a and 5b) while the distal part of the esophagus remained in place (5c and 5d). Subanalysis revealed that the target coverage could only marginally be restored if couch rotations were allowed. In a separate exercise, we mimicked a 6-D couch by omitting the addition of the clinical residual rotational error and allowing full rotational degrees of freedom in the mask match. The resulting CTV coverage probability curves showed large agreement with the original curves (Figure 4.6), underlining that interfractional shape changes of the CTV are the dominant source of geometrical uncertainties in contemporary radiotherapy of the esophagus.

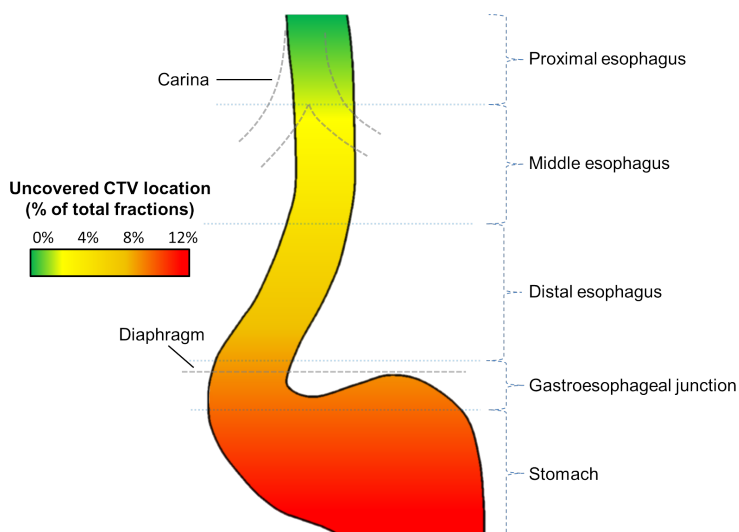


Figure 4.3: Schematic overview of the areas in the esophagus where target coverage is compromised when an isotropic margin of 5mm around the CTV is used. A total of 29 fractions out of the analyzed 139 fractions were not fully covered of which the most fractions had an uncovered CTV in the distal part of the esophagus near the junction (8 fractions) and into the upper part of the stomach (16 fractions).

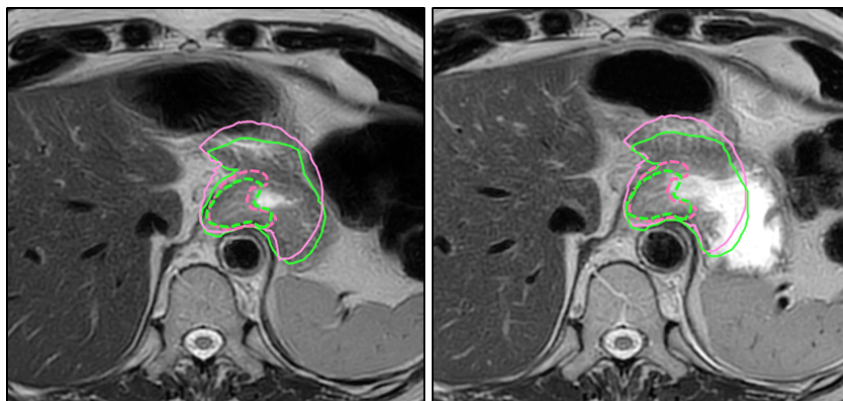


Figure 4.4: Example of interfractional changes in the shape of the stomach which resulted in large variations in the gross tumor volume (dashed lines) and clinical target volume (solid lines) between the reference scan (left, green delineation) and a follow-up fraction (right, pink delineation) on MVXD images.

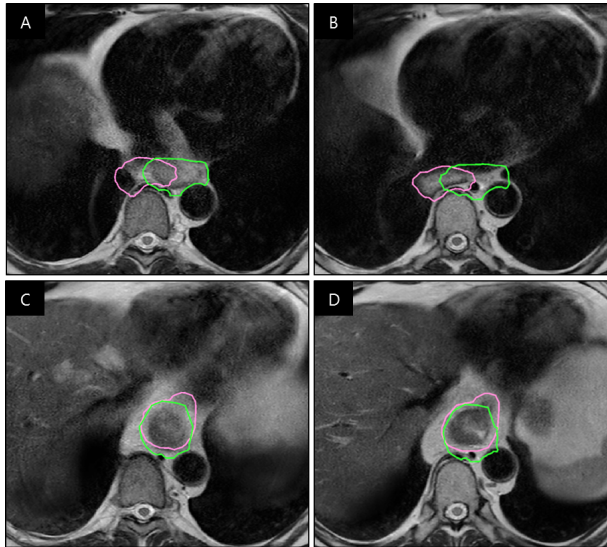


Figure 4.5: Example of interfraction tumor displacement depicted on the reference tT2W scan (A and C, green delineation) versus the second follow-up tT2W scan (B and D, pink delineation). The proximal part of the tumor demonstrated large lateral displacement (A-B), whereas the distal part of the tumor remained at the same position (C-D).

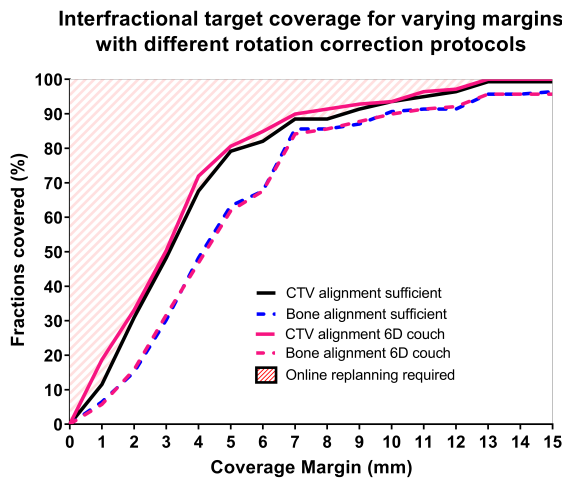


Figure 4.6: Difference between target coverage for different rotational alignment protocols. A 6D couch set-up correcting for all residual rotations (solid pink line) shows large agreement with the original curve (solid black line). Similar coverage is achieved when only bony anatomy rotations are corrected (dashed pink line vs dashed blue line).

Discussion

MRI-guided radiation (adaptive) therapy (MRgRT) is a novel treatment method that not only allows for superior soft-tissue contrast at imaging prior to dose delivery, but also allows for inter-fractional plan re-optimization or adaptation [22–24, 54–56, 61]. Due to these unique features, MRgRT is increasingly and successfully used for the treatment of various tumor sites [60, 61, 66, 67]. To our knowledge this is the first study that investigates the potential benefit of online MR guidance within the radiotherapy treatment of esophageal cancer patients. The esophagus is an appealing treatment site in this context, as the primary tumor, involved nodes and the CTV consisting of the peri-esophageal fat along the esophagus often can be hardly discriminated on CBCT. This is particularly true for tumors located in the distal esophagus, which are most common in the Western world, where the GTV and CTV often involve the proximal part of the stomach. Hence, set-up corrections are typically performed by registering the bony anatomy visible on CBCT. Many researchers have assessed the interfractional tumor position variation relative to bony anatomy by analyzing the relative shifts of fiducial markers in the GTV in relation to the bony anatomy in esophageal cancer [5, 6, 42, 68–70]. The studies of Jin et al. [5] and Hoffmann et al. [6] both demonstrated systematic shifts of the markers in relation to the bony anatomy of approximately 3–4 mm. Due to the systematic character of the shifts, both groups reported these errors to have a profound impact on the CTV-to-PTV margins in contemporary radiotherapy. An important asset of (in-room) MRgRT is that changes in target size and shape are not only assessed at some anchor points (i.e. marker locations) but that the entire 3D geometry of the GTV and CTV can be evaluated and plan adaptations can be made accordingly. This asset will prompt the team involved in the daily execution of the treatment to secure target coverage on a fraction-by-fraction basis. In this in-silico study we investigated what isotropic margins around a pre-treatment CTV are required to resolve interfractional anatomy changes that occur on a day-to-day basis after rigid alignment to the original CTV (i.e. MR-guided soft tissue set-up). In addition, we also investigated the coverage probability as function of the applied margin when the repeated scans were registered to the bony anatomy, thereby mimicking the clinically widely applied CBCT setup scenario. An important finding of this study was that interfraction changes of the CTV (and GTV) are not characterized by translations only, but that interfractional anatomy changes of the CTV are a prominent cause of geometric uncertainties in conventional radiotherapy. This means that small margins can only be safely implemented using an on-table adaptive workflow where new plans are daily regenerated based on the anatomy of the day. A few weaknesses are associated to the current study. The first weakness

is that all MRI scans were acquired using respiratory triggering, meaning that respiratory motion effects have not been taken into account in the margin assessments and the reported margins should be regarded as a lower-limit. This can be of concern, although for most patients the peak-to-peak amplitude is less than 10 mm [6,49,71,72] and only a modest blurring of the intended dose will occur once the mid-position of the target volume has been properly identified [73,74]. In the study of Hoffmann et al. the margin increment as a result of this blurring in the aggregated data was estimated 1.7 mm or less [6]. Another weakness is the coarse trough plane image resolution of the MRI scans in this study. The slice thickness for the first 19 patients was 6.48 mm and for the last 12 patients the slice thickness was reduced to 3 mm. This discretization could well have impacted the individual coverage assessment of a single fraction. However, we believe that the overall effect in the aggregated data is limited as there are no systematic errors expected. In addition, the expanded CTV structures were defined in a high resolution grid (0.67 mm x 0.67 mm x 1 mm) and target coverage was assessed in 3D. This is also illustrated in Figure 4.7 where both cohorts showed comparable target coverage probabilities, despite the small sample sizes in the separate cohorts.

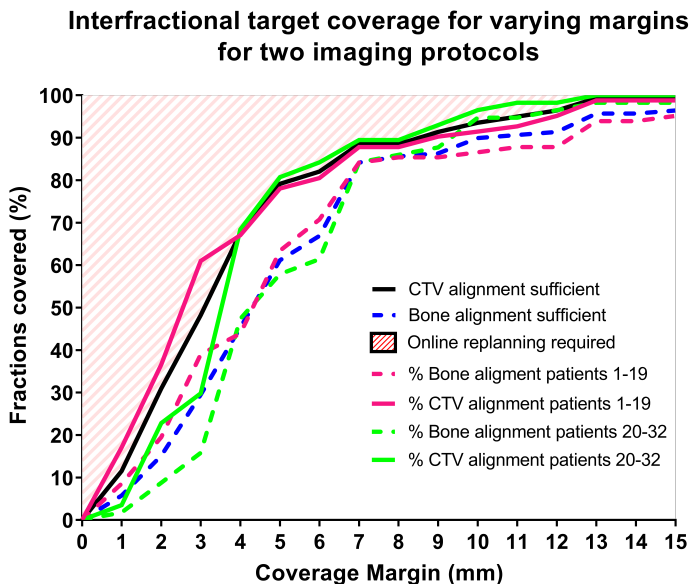


Figure 4.7: Difference between target coverage for fractions scanned with the two imaging protocols: tT2W scans for patients 1-19 (pink lines) and higher resolution MVXD scans for patients 20-32 (green lines). Percentage of fractions fully covered (139 fractions, 30 patients) for varying coverage margins shown for alignment to the bony structure (dashed lines) and the soft-tissue strategy with direct alignment to the CTV (solid lines).

Lastly, the primary focus of this study was put on geometric coverage and not on dosimetric coverage. However, geometric coverage does not always imply dosimetric coverage and vice versa as the 95% isodose level does not always perfectly coincide with the PTV surface. To obtain a general estimate of the concordance of the geometric and dosimetric coverage, VMAT plans with a 5-mm CTV-to-PTV margin were created for all patients. After registration, the dosimetric coverage of the CTV in each of the follow-up scans was analyzed and compared to the geometric coverage (Figure 4.8). As expected, the average V95% and D98% were high for the covered fractions (99.5% and 97.5% respectively) but dropped severely in the fractions where the CTV was not covered (95% and 85%). This again demonstrates that a 5-mm margin could not prevent severe underdosage at some fractions even after soft-tissue registrations, which can only be circumvented by either (further) increasing the margins or using an on-table adaptive workflow. The on-table adaptive workflow has the extra advantage that all anatomic changes including density changes are intrinsically incorporated in the daily (re)planning of the dose. This is of importance as Nyeng et al. reported that severe inter-fractional elevations of the average diaphragm position could occasionally cause a decrease of target coverage even if geometric coverage is accomplished [50]. Despite these limitations, this study clearly demonstrates that CTV shape changes require on-table adaptive workflows when pursuing highly conformal target irradiations. At this point, it is unclear yet what the lower limit is of a margin that can safely be applied to ensure full target coverage on a daily basis. As pointed out earlier, dose blurring as a result of respiratory movements can occasionally be of concern as is the time interval between MRI acquisition and the end of radiation delivery, which could easily take up to 15 minutes. Heethuis et al. demonstrated that the mean tumor drift during a 10 min interval was generally modest (1.5mm), but that larger drifts (>5mm) could be incidentally observed [49]. This advocates workflows that integrate online monitoring of tumor drifts during treatment, together with appropriate action levels. Finally, as margins decrease, accurate and precise target definition becomes more critical, especially in the pre-treatment phase where the reference structures are delineated. We believe that MRI can facilitate accurate and precise definition of the GTV and CTV in esophageal cancer. However, we acknowledge that the data to substantiate this is still scarce. A recent study by Vollenbrock et al. demonstrated that the interobserver variability in GTV delineations on MRI were only similar to those on FDG-PET/CT, but considerable variations in the cranial and caudal extension of the GTV were observed [37]. The authors suggest that the inclusion of diffusion weighted MRI (DW-MRI) imaging could improve the precise demarcation of the caudal border when the gastroesophageal junction is involved. Alternatively, there is recent evidence emerging that fiducial markers carefully implanted during an endoscopic

ultrasound (EUS) procedure could also improve the definition of the cranial and caudal border of the GTV in the pre-treatment phase [75]. Once an accurate reference GTV at the pre-treatment (planning) MRI scan is established, deformable registration techniques will propagate the GTV to the anatomy of the day. These propagated GTVs will be a good starting point for the recontouring of the actual GTV and CTV. However, we acknowledge that training and experience is important here, especially if the redefinition of the target has to be done under a certain time pressure with the patient in treatment position. In conclusion, direct CTV (or GTV) registration methods using in-room MRI only yielded a moderate increase in target coverage compared to the current clinical (bone match) CBCT-IGRT protocols. Therefore, on-table adaptive workflows requiring on-site full staffing levels are essential when pursuing highly conformal target irradiations for every treatment fraction.

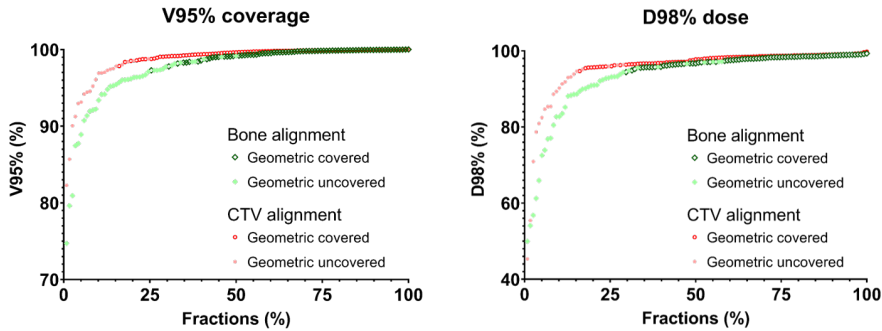


Figure 4.8: VMAT plans with a 5-mm CTV-to-PTV margin were created for all patients. The V95's (top) and D98's (bottom) of all CTVs in the follow-up scans were ranked and compared to the geometric coverage. Geometrically covered fractions are depicted with open symbols, whereas uncovered fractions are depicted with solid symbols.

Chapter 5

An in-silico assessment of the dosimetric benefits of MR-guided radiotherapy for esophageal cancer patients

The following chapter is based on:

MR Boekhoff, IL Defize, AS Borggreve, R van Hillegersberg, ANTJ Kotte, JJW Lagendijk, ALHMW van Lier, JP Ruurda, N Takahashi, S Mook, GJ Meijer

Radiotherapy and Oncology 162 (2021) 76-84

doi:10.1016/j.radonc.2021.06.038

Abstract

Purpose

To assess the dosimetric benefits of online MR-guided radiotherapy (MRgRT) for esophageal cancer patients and to assess how these benefits could be translated into a local boosting strategy to improve future outcomes.

Methods

29 patients were in-silico treated with both a MRgRT regimen and a conventional image guided radiotherapy (IGRT) regimen using dose warping techniques. Here, the inter and intrafractional changes that occur over the course of treatment (as derived from 5 MRI scans that were acquired weekly during treatment) were incorporated to assess the total accumulated dose for each regimen.

Results

A significant reduction in dose to the organs-at-risk (OARs) was observed for all dose-volume-histogram (DVH) parameters for the MRgRT regimen without concessions to target coverage compared to the IGRT regimen. The mean lung dose was reduced by 28%, from 7.9 to 5.7 Gy respectively and V20Gy of the lungs was reduced by 55% (6.3 % to 2.8 %). A reduction of 24% was seen in mean heart dose (14.8 to 11.2 Gy), while the V25Gy of the heart was decreased by 53% (14.3% to 6.7%) and the V40Gy of the heart was decreased by 69% (3.9 to 1.2 %). In addition, MRgRT dose escalation regimens with a boost up to 66% of the prescription dose to the primary tumor yielded approximately the same dose levels to the OARs as from the conventional IGRT regimen.

Conclusion

This study revealed that MRgRT for esophageal cancer has the potential to significantly reduce the dose to heart and lungs. In addition, online high precision targeting of the primary tumor opens new perspectives for local boosting strategies to improve outcome of the local management of this disease.

Introduction

Neoadjuvant chemoradiotherapy followed by esophagectomy is the standard of care for locally advanced, resectable esophageal cancer (EC) [2, 32]. Typically large clinical target volumes (CTVs) are irradiated to treat the possible subclinical/microscopic spread along the esophagus and involvement of regional lymph nodes [6, 7, 76]. In conventional image-guided radiation therapy (IGRT) for esophageal cancer the bony anatomy of the 3-dimensional cone-beam computed tomography (CBCT) is typically rigidly registered to the bony anatomy of the planning computed tomography [5, 7, 16–18, 25, 46, 77] as direct registration to the CTV is often challenging due to the poor soft tissue contrast of the CBCTs.

To account for geometric uncertainties such as the daily variability of the CTV in relation to the bony anatomy and breathing motion, the CTV is expanded to a planning target volume (PTV). Recent studies have suggested an expansion of 7–12 mm in different directions, resulting in PTVs that are approximately three times the volume of CTVs [6, 7, 76, 78]. These large PTVs inherently result in large high and intermediate dose levels at nearby organs-at-risk (OARs) such as the lungs and heart. Radiation dose to the lung and heart is associated with a decrease in survival due to severe pulmonary and cardiac complications [8–12]. Furthermore, inter- and intrafractional changes in diaphragm motion could lead to dose distribution changes, potentially increasing the dose to OARs and decreasing the dose to the tumor [50, 77, 79]. The risk of increasing toxicity has also been of concern when evaluating strategies for dose escalation to the primary tumor. Dose escalation, especially in a definitive setting, could be of clinical benefit as over 80% of recurrences occur at the primary treatment site [80, 81]. However, one of the first studies that evaluated the effectiveness of dose-escalation for esophageal tumors showed that sequential dose escalation to 64.8 Gy did not improve overall survival or locoregional control [82]. In addition, there were multiple deaths in the high dose arm and as such the trial was prematurely closed. More recently, the phase III ART DECO study could also not demonstrate an increase in local control in patients who received an integrated boost dose to the tumor [83]. However, it could be argued that a total dose of 61.6 Gy is too low to establish an increase in local control and that the OAR dose is a limiting factor in further dose escalation. Recently, multiple online adaptive treatment platforms have been released by various vendors which allow for online replanning and thereby potentially bypassing all interfractional anatomy geometry variations. These platforms could either be based on X-ray imaging [84, 85] or MR imaging [21, 24, 56] and could have onboard imaging capabilities that allow for online intrafraction monitoring to allow gating [61, 66] and tracking [86] to mitigate effects from intrafraction

motion. Within the framework of esophageal cancer radiotherapy, online adaptive MR-guided radiotherapy (MRgRT) could be beneficial due the superior soft tissue contrast of MRI in the mediastinum and upper abdomen. In contrast, the image quality of contemporary CBCT imaging is often still considered too poor for online GTV and CTV definition, which has prompted some clinics to explore the use of fiducial markers in this context [5–7, 43]. Daily changes in the anatomy of the target and OARs could be visualized immediately prior to treatment allowing online plan adaptation. Secondly, cine-MRI during dose delivery allows for online monitoring of all intrafraction motion including respiratory motion and will secure accurate dose delivery. Additionally, treatment could be interrupted if the intrafraction motion exceeds certain thresholds and replanning is deemed necessary. Theoretically, both features enable precise targeting with smaller PTV margins which reduces the radiation dose to the organs at risk.

The study aim has been divided into two parts. The first and main goal of this study is to assess whether dosimetric benefits to lungs and heart exist for a MRgRT treatment compared to a conventional CBCT-guided treatment by assessing the 3D accumulated dose distributions in a cohort of EC patients. The second goal of this study is to explore the potential of MRgRT to trade this organ-at-risk sparing for a treatment intensification (boost dose) of the primary tumor.

For reasons of readability we will address online adaptive free breathing (without active motion management) MR-guided radiotherapy simply as MRgRT from here onwards. Similarly, we will refer to conventional free breathing (CBCT) image guided RT with alignment to the bony anatomy without (daily) plan adaptations as IGRT.

Methods

Patient population

Patients with histologically confirmed esophageal cancer treated with neoadjuvant chemoradiotherapy between December 2015 and April 2018 were eligible for inclusion. All patients gave written informed consent and the study was approved by the institutional review board of the University Medical Center Utrecht (protocol ID 15-340). Exclusion criteria for enrollment in the study were age <18 years, previous treatment with thoracic surgery or thoracic radiotherapy, and contraindications for MRI.

Image acquisition

Patients underwent six sequential MRI scans, 1 prior to treatment followed by 5 weekly scans during neoadjuvant chemoradiotherapy. Images were acquired on a 1.5T Philips Ingenia (Best, the Netherlands), using anterior/posterior (28 channel) receive coils. Patients were positioned in supine position with arms next to the body. During each scan session patients underwent a respiratory-triggered transverse and sagittal T2-weighted (T2W) MRI scan. The scans were acquired with a multi-slice turbo spin echo sequence (TR/TE = 1604/100ms and 1431/100ms, resolution = $0.67 \times 0.67 \times 6.48 \text{mm}^3$ and $4.4 \times 0.7 \times 0.7 \text{mm}^3$, for transversal and sagittal scans, respectively). From the 20th patient onwards, respiratory-triggered sagittal and transversal anatomical T2W MultiVane XD scans were acquired instead of the previously mentioned T2W scans, as these scans demonstrated improved image quality (TR/TE = 2039/100ms and 2243/100ms, resolution = $0.62 \times 0.62 \times 3.0 \text{mm}^3$ and $3.0 \times 0.63 \times 0.63 \text{mm}^3$, for transversal and sagittal scans, respectively). After the T2W scans, patients underwent two sagittal and coronal cine-MRI series of each 45 seconds at 1.6 Hz. For the cine-MRI series the scanning plane was positioned through the center of the tumor, which was identified using the transverse T2-weighted scan. The images were both acquired with a resolution of $2.01 \times 2.01 \text{mm}^2$ and 5 mm slice thickness [49]. The time interval between the two cine-MRI series was 10 minutes which was used for additional DWI imaging for response assessment purposes [87].

Delineations

The gross tumor volume (GTV) was delineated on each MRI by a certified radiation oncologist (N.T.), which was subsequently reviewed by a radiation oncologist specialized in upper gastrointestinal malignancies (S.M.). Any disagreements were solved through a consensus discussion. Next, the CTV was created using a margin of 0.5 cm around the GTV in the transverse direction, taking the anatomical border into account, 3 cm in cranial direction and 2 or 3 cm caudally (2 cm in case of tumor extension in the stomach).

Motion characterization

An optical flow algorithm (RealTITracker) was used to quantify tumor motion per fraction during free breathing on the cine-MRI series [88, 89]. Here, the first frame of the first cine-MRI series was used as a reference frame for both cine-MRI series of each 45 s that were separated by a 10 minute interval, to capture both short term motion (periodic respiratory motion) and long term motion (drifts) [49]. Motion vector fields within delineated CTVs were calculated for each frame with respect to the reference frame and analyzed to obtain intrafraction motion

over the course of one treatment fraction. Left-right and cranio-caudal motion trajectories were obtained from the transversal scan, while analysis of the sagittal scan provided the motion tract in the anterior posterior direction. The motion trajectories were normalized using the mean motion of the first three breathing cycles. Finally, the obtained motion fields were applied on the projected doses to simulate intrafraction motion during dose delivery.

Treatment Planning

Each MRI scan was rigidly aligned to the (clinical) planning CT based on the bony anatomy and each CTV (as delineated on the MRI) was propagated to the planning CT. Overlapping voxels with (clinical) organs at risk, if any, were assigned to the CTV. For each patient two sets of treatment plans were generated. For the IGRT regimen, a single plan was generated with a CTV-to-PTV margin of 7 mm in the anterior-posterior directions, 9 mm in the left-right directions and 12 mm in cranio-caudal directions as per the guidelines/recommendations for bone match procedures 3–5. For the MRgRT regimen, 5 plans were generated in which each plan was associated to a follow-up scan representing the single tumor anatomy for a 5-fraction treatment. Here, CTV-to-PTV margins of 2 mm in the axial direction and 5 mm in the cranio-caudal direction were used as the online planning procedure resolves the interfraction fraction variation and only leaves the intrafraction motion (breathing and drifts) as an intrinsic uncertainty. For each regimen multiple VMAT plans were generated using the autoplanning toolkit of the Pinnacle 16.2 treatment planning system (Koninklijke Philips NV, Eindhoven, The Netherlands). The PTV target dose was set to 41.4 Gy, whereas the optimization goals in the autoplanning toolkit were set to a mean lung dose <4.2 Gy (high priority) and a mean heart dose <10 Gy (medium priority) [32]. For the creation of simultaneously integrated boost plans, a separate boost PTVGTV was defined with similar margins as the PTVCTV (i.e. GTV-to-PTV margins of 2-mm in the axial direction and 5-mm cranio-caudally), for each reference anatomy. For each patient a series of six boost plans was generated with the same autoplanning objectives as described in the previous section, with the addition of an extra target dose for PTVGTV. The extra target boost dose was initially set to 17% (1/6th) of the prescription dose and was subsequently incremented with 17% of the prescription dose until a boost of 100% was effectuated.

Treatment Simulation

For both regimens a 5-fraction treatment was simulated, where the pretreatment reference anatomy was linked to the pretreatment MRI and each of the follow-up MRIs represented a sample of the anatomy of a single fraction. In case of missing scans treatment was only simulated for the available scans. The accumulated

or total ‘delivered’ 3D dose distribution was calculated in multiple steps, illustrated in Figure 5.1. First, the 3D intrafraction motion trajectories, captured from the cine-MRIs, were used to convolve the static fractional dose into the fractional ‘delivered’ doses. In this step, all dose voxels were sampled over the motion trajectories. The fractional ‘delivered’ dose distributions were then warped and accumulated to the pretreatment reference anatomy. Here, a two-step non-rigid B-spline image registration with the Elastix toolbox was used to assess the inter-fractional changes between each follow-up scan and the reference scan [48]. First, the follow-up scans were rigidly aligned to the reference scan. Then, a whole body grey-value registration (mutual information metric) was applied in combination with a bending penalty metric, which was used to prevent extreme unreal deformations. To ensure correct mapping of the CTV, a second registration step was performed. This final registration step consisted of a mask match of the delineated CTVs (kappa statistic metric), which again was also combined with a bending penalty metric [78].

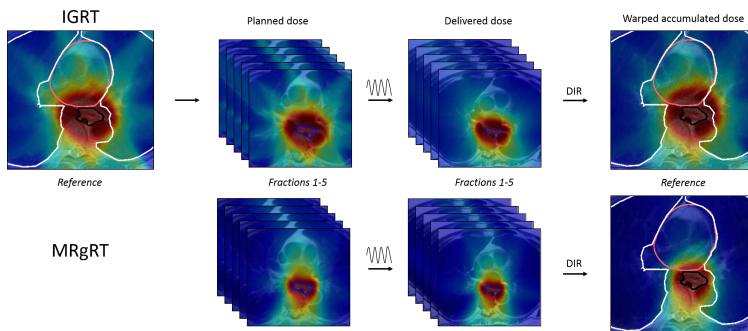


Figure 5.1: Schematic overview of the treatment simulation workflows. The IGRT treatment simulation (top row) consisted of a doseplan created on the reference scan with 7, 9 and 12 mm margins around the reference CTV (black delineation) which was subsequently projected on follow-up MRIs to simulate daily planned dose. MRgRT treatment simulation (bottom row) consisted of daily treatment plans with 2 mm axial and 5 mm CC margins around adapted CTVs (blue delineation) used to create the daily planned doses. Breathing motion was applied to obtain the actual daily delivered dose. Finally, the daily doses were warped to the reference scan via the vector fields, obtained from deformable image registration (DIR), and summed. This resulted in the warped accumulated dose for each patient.

Statistics

All PTVs and relevant dose volume histogram (DVH) parameters of the IGRT and MRgRT regimen were assessed using a paired t-test in SPSS (IBM Corp., Armonk, NY). $p < 0.05$ was considered statistically significant.

Results

A total of 32 patients with esophageal cancer were enrolled in this study before the start of neoadjuvant chemoradiotherapy. One patient withdrew from study participation and two patients were excluded based on a limited field of view in the cranial caudal direction on the reference scan. Of the remaining 29 patients, three follow-up scans were cancelled upon patient request and five transverse follow-up scans were excluded based on a limited field of view in the cranial caudal direction. The final study population consisted of 29 patients who underwent a total of 140 transverse follow-up scans, together with 2 cine-MRI scans per transverse follow-up scan. The average PTV volume for IGRT plans was 375 cm^3 whereas the average PTV volume for MRgRT plans was 194 cm^3 (Figure 5.2). For all automatically generated plans 99% of the PTV was covered with at least 95% of the prescribed dose. Furthermore, all plans were highly conformal; i.e. the 95% isodose volumes were on average 18% and 13% larger than the PTV for the MRgRT and IGRT regimen, respectively (Figure 5.3). This small discrepancy is explained by the difference in size of the PTVs for both regimens.

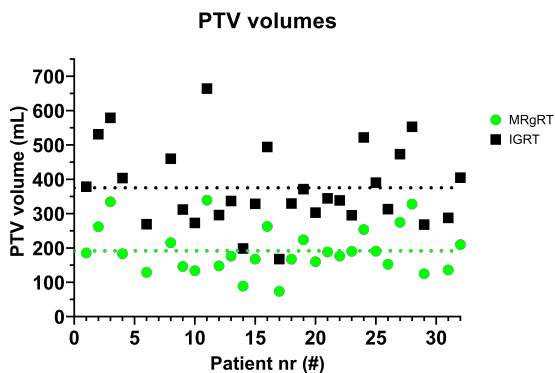


Figure 5.2: PTV volumes of IGRT plans (black squares) vs MRgRT plans (green circles). Average PTV volume for IGRT plans with CTV-to-PTV margins of 7, 9 and 12mm in AP, LR and CC direction, respectively, was 375 cm^3 (black dashed line) and for MRgRT plans with 2mm axial and 5mm CC CTV-to-PTV margins the average PTV volume was 194 cm^3 (green dashed line).

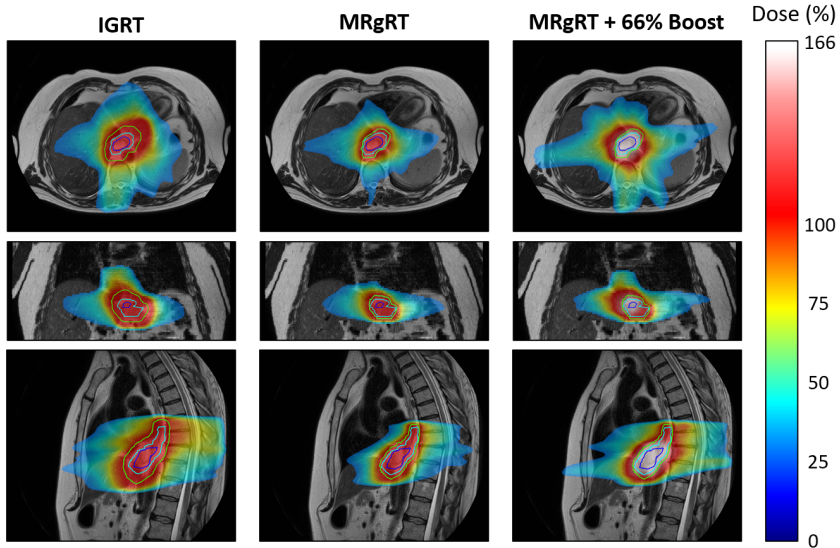


Figure 5.3: Dose plans for each treatment regimen. For the IGRT treatment (left) the dose is planned to a PTV (green delineation), created with margins of 7, 9 and 12 mm around the CTV (cyan delineation). For the MRgRT treatment (middle) the dose is planned to a PTV with margins of 2 mm in axial direction and 5 mm in CC direction. These two PTVs are covered with 100% of the prescribed dose (red colormap), while the dose in the boost plan (right) shows higher dose levels (white colormap) than prescribed to the GTV (blue delineation).

The CTV coverage of the total accumulated dose was $D_{99} > 39.33\text{Gy}$ for 27 (93%) patients indicating adequate CTV coverage (Figure 5.4). Underdosing was observed in two patients during the IGRT regimen and was due to interfraction changes in the curvature of the esophagus in the right lateral direction, exceeding the 9 mm PTV margin. In one patient this change was permanent, and in one patient the esophagus returned to its original position in week 4. For the MRgRT regimen, underdosing of the CTV occurred for patient 24 and 25 in three fractions and one fraction, respectively, due to large and irregular breathing motions (Figure 5.5). Patient 24 repeatedly exhibited an unusually large peak-to-peak breathing amplitude of almost 3 cm, this amplitude was present in 3 of the 5 follow-up scans. Similarly, patient 25 revealed a rather atypical motion pattern, especially on the 4th MRI where a 10-mm drift occurred in the time interval between the acquisition of the cine-MRIs, which caused an underdosing at the caudal part of the CTV (Figure 5.6).

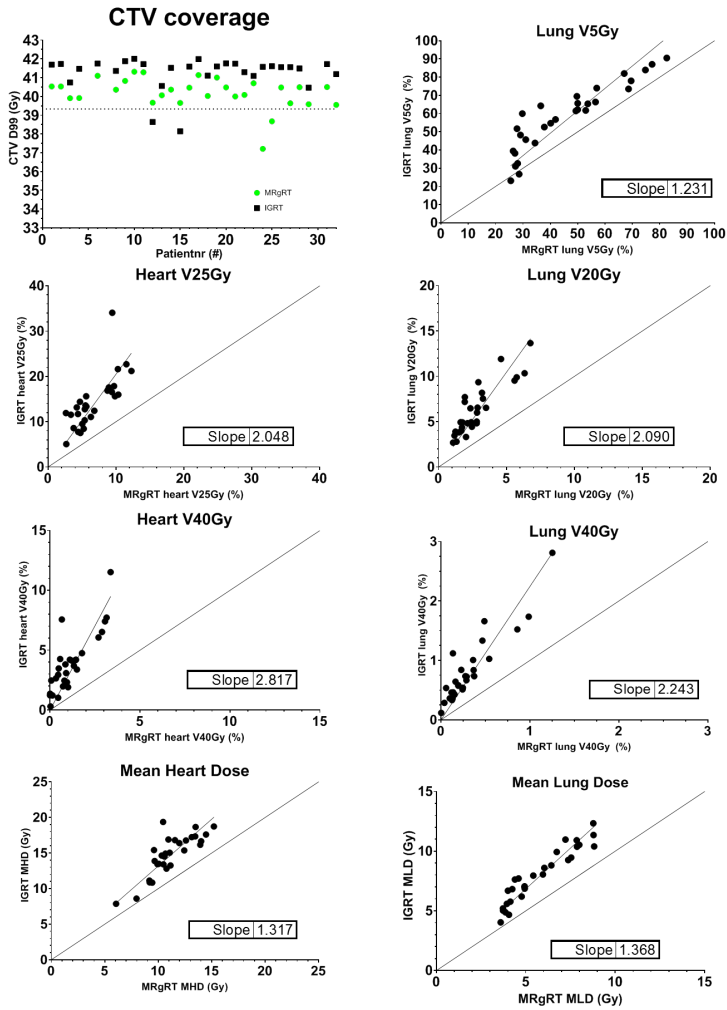


Figure 5.4: Comparisons of various DVH parameters. The D98 of the accumulated doses of the CTV is displayed in the top left panel for each patient. Scatter plots of lung and heart DVH parameters are shown in the remaining panels, where the DVH value of the IGRT treatment plans (y-axis) is plotted vs the DVH value of the MRgRT treatment plans (x-axis).

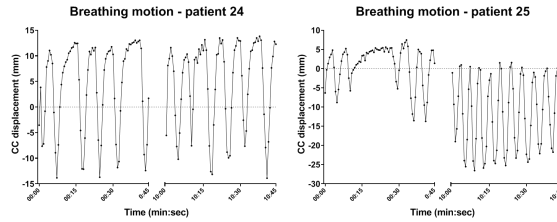


Figure 5.5: Extreme crano-caudal displacement as a result of different breathing patterns. Large peak-to-peak motion for patient 24 (left) and tumor drift in fraction 4 for patient 25 (right) resulted in insufficient target coverage for these two patients.

A significant reduction in OAR dose was observed for all DVH parameters for the MRgRT regimen (Table 5.1, Figure 5.4). Mean lung dose was reduced by 28%, from 7.9 to 5.7 Gy respectively, and lung V20Gy was reduced by 55% (from 6.3% to 2.8% respectively). A reduction of 24% was seen in mean heart dose (14.8 to 11.2 Gy), while heart V25Gy decreased by 53% (14.3% to 6.7%) and heart V40Gy decreased by 69% (3.9 to 1.2 %). For each patient a set of simultaneously integrated boost MRgRT plans were generated with increasing boost levels. The integrated boost regimens revealed an increasing dose to OARs with each increment of the boost dose to the GTV (Figure 5.7). However, this dose increase was generally modest. It turned out that for most patients the mean lung dose, $V_{\text{lung}20\text{Gy}}$, mean heart dose and $V_{\text{heart}40\text{Gy}}$, for the boost plans were still below the reference values of the IGRT plan at a boost level of 66% of the prescription dose (boost of 27 Gy).

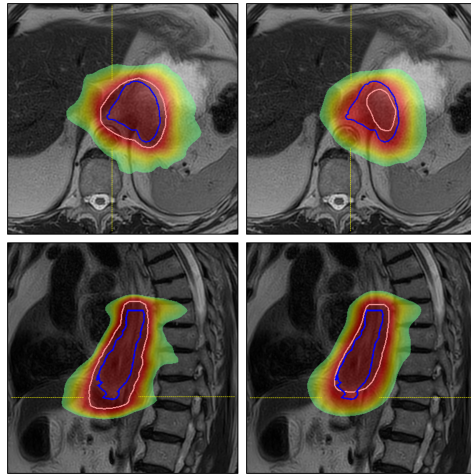


Figure 5.6: Caudal underdosing in fraction 4 of patient 25 as a result of caudal tumor drift transversal (top) and sagittal (bottom) plane. At least 95% of the prescribed dose (pink) is achieved in the CTV (blue delineation) in the MRgRT treatment plan (left), while the accumulated dose (right) is reduced as a result of intrafraction motion (see also Figure 5.5).

DVH parameter	IGRT Mean \pm SD	MRgRT Mean \pm SD	Reduction (%)	p
PTV				
Volume (mL)	375 \pm 117	194 \pm 68	48.3	<0.001
Lungs				
Dmean (Gy)	7.9 \pm 2.3	5.7 \pm 1.8	27.8	<0.001
V5Gy (%)	58.3 \pm 18.2	45.8 \pm 17.6	21.4	<0.001
V10Gy (%)	31.1 \pm 14.0	17.6 \pm 8.9	43.4	<0.001
V20Gy (%)	6.3 \pm 2.8	2.8 \pm 1.6	55.6	<0.001
V30Gy (%)	2.2 \pm 1.2	1.0 \pm 0.7	54.5	<0.001
V40Gy (%)	0.8 \pm 0.6	0.3 \pm 0.3	62.5	<0.001
Heart				
Dmean (Gy)	14.8 \pm 2.9	11.2 \pm 2.1	24.3	<0.001
V5Gy (%)	90.3 \pm 14.3	83.4 \pm 14.7	7.6	<0.001
V10Gy (%)	62.6 \pm 16.3	44.2 \pm 12.3	29.4	<0.001
V20Gy (%)	21.8 \pm 7.7	11.2 \pm 3.9	48.6	<0.001
V25Gy (%)	14.3 \pm 5.8	6.7 \pm 2.8	53.1	<0.001
V30Gy (%)	10.0 \pm 4.4	4.3 \pm 2.1	57.0	<0.001
V40Gy (%)	3.9 \pm 2.5	1.2 \pm 1.0	69.2	<0.001

Table 5.1: PTVs and DVH parameters for both the IGRT and MRgRT regimen; overview of results in 29 patients.

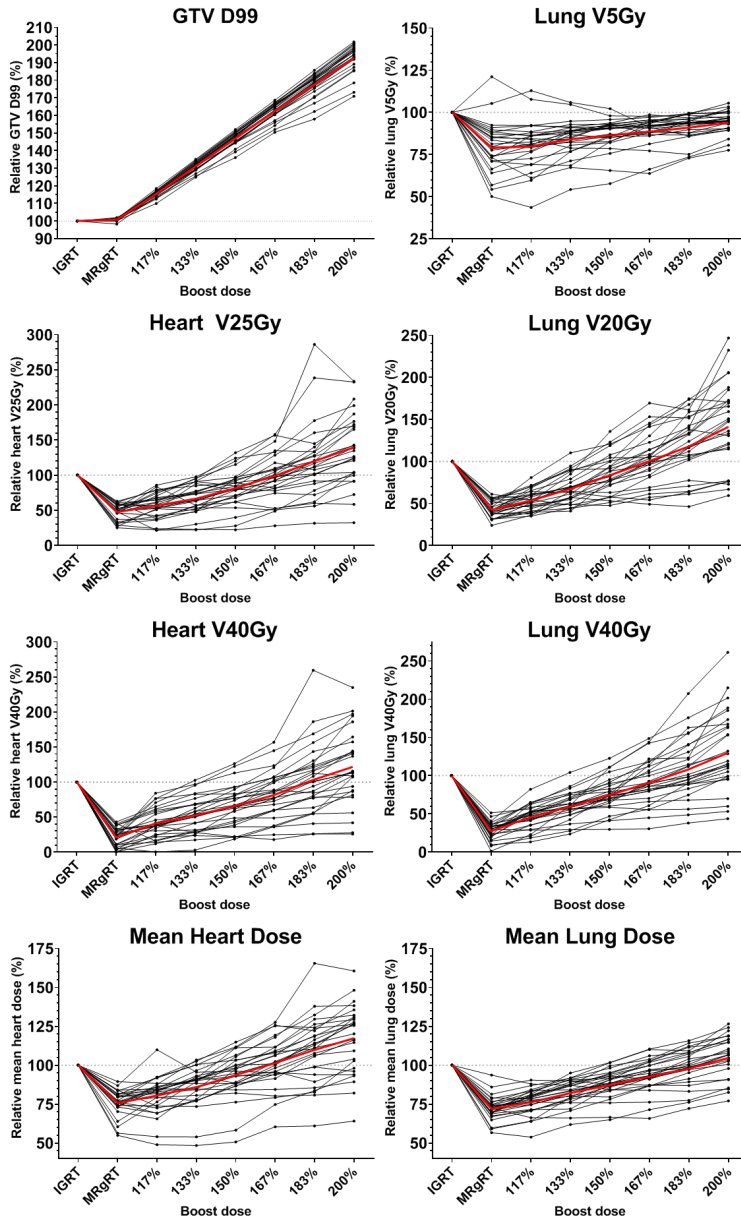


Figure 5.7: Relative dosimetric differences between integrated boost plans with a boostdose up to 200% of the prescribed dose compared to the IGRT treatment plan. Each black line represents the relative DVH value of an individual patient for different boost levels, while the average of all patients is displayed with a red line.

Discussion

In this study we demonstrated the dosimetric benefits of an online adaptive (free breathing) MR-guided radiotherapy regimen for esophageal cancer patients. Our results demonstrate that the dose to the organs at risk can significantly be reduced when online plan adaptation with MR guidance is used. In particular, the high dose regions receiving a dose of 40 Gy or higher were reduced by 65% for both the lungs and heart. A reduction of 25% was seen for both the mean lung dose and mean heart dose. Subsequently, 53 to 55 percent less heart and lung tissue was subjected to 25 Gy and 20 Gy, respectively. This resulted from a 50% PTV volume reduction for the MRgRT regimen in comparison the IGRT regimen, while similar target coverage was achieved. Furthermore, dose escalation strategies were explored demonstrating the administration of an additional 66% of the conventional dose to the primary tumor without increasing the dose to the OARs in comparison to conventional IGRT treatment. Additionally, we have shown that the IGRT regimen with large anisotropic CTV-to-PTV margins of 7, 9 and 12 mm was insufficient to correct for interfraction variation and failed to preserve target coverage in 2 out of 29 (7%) patients. In these 2 patients underdosing of the CTV occurred due to a large lateral displacement of the esophageal tract in relation to the vertebrae at multiple fractions. Online plan adaptation resolves this issue and only requires CTV-to-PTV margins to correct for the residual intrafraction motion. In this study we have demonstrated that a CTV-to-PTV margin of 2 mm in axial and 5 mm in cranial-caudal direction was large enough to absorb the residual intrafraction motion. There were only two patients where the CTV coverage was compromised because of either a large drift that occurred during one of fractions or because of repeatedly large breathing amplitudes. These findings illustrate that active surveillance on intrafraction motion during treatment is advised, however, for the vast majority of patients no active motion management is required even at these tight margins. However, gating or tracking strategies as offered by some vendors could potentially further reduce cranio-caudal treatment margins, resulting in a possibly larger decrease of OAR toxicity than reported in this work [61, 66, 90]. It should also be noted that recent innovations in cone-beam IGRT have improved the image quality in modern machines potentially allowing full adaptive radiotherapy for esophageal cancer patients at dedicated X-ray based systems [84, 85]. Previous studies on radiation-induced toxicity after chemoradiation for esophageal cancer showed multiple correlations between an increase in lung and heart dose and pulmonary and cardiac complications and mortality. This emphasizes the need for strategies, such as MRgRT, to reduce these doses. Thomas et al. recently published a normal tissue complication probability (NTCP) model for postoperative pulmonary complications and one-year mortal-

ity after trimodality treatment in esophageal cancer. In their NTCP model, mean lung dose was the only dosimetric parameter associated with pulmonary complications [11]. Kanski et al. showed that high V20, V30 and V40 of the heart were associated with symptomatic cardiac toxicity [10]. Other studies found similar correlations between dosimetric parameters to be strongly associated with the incidence of post-treatment pulmonary, cardiac and other complications [91–96]. These dosimetric parameters were all reduced in the MRgRT treatment regimen in our study. In addition, the gained dose reduction with online adaptive MRgRT could also be employed to increase the dose to the primary tumor while preserving the dose levels to the OARs from the conventional non-adaptive IGRT. In this study we have demonstrated that with online MR-guidance we could potentially simultaneously increase the dose to the primary tumor with an extra 66%, without exceeding the dose levels that we administer to the lungs and heart in our current clinical protocols. For definitive chemoradiation with a standard dose of 50.4 Gy this would mean that the dose to the primary tumor could be simultaneously escalated isotoxic to 84 Gy, which is higher than the dose levels we currently apply to other tumor sites such as lung, larynx, pharynx, prostate, anus and bladder that have proven to accomplish high local control rates. Whether such high dose to the tumor is necessary to achieve good local control remains the question. Moreover, besides lung and heart toxicity, radiation-induced toxicity to the esophagus itself such as fistula, might be the dose limiting toxicity in dose escalation schedules. There are a few limitations in the present work that should be acknowledged. First, the number of follow-up MRI scans used in the study is lower than the number of fractions that is typically given in a neoadjuvant (or definitive) scheme (6 versus 23–28 respectively). We believe that the impact of this undersampling won't affect the general conclusions when it comes to the reporting of the dose to organs at risk. However, the limited sample size might have impacted the reported data on the target coverage for both the IGRT and MRgRT regimen as an outlying result in the sampling data might be overrepresented in the final dose accumulation thereby underestimating the target coverage. On the other hand, due to the sparse sampling outlying results might also have been missed causing a too optimistic target coverage. Secondly, only 2 times 45 seconds of motion data is available, so respiratory intrafraction motion is only partially captured. However, the time interval between the scans was approximately 10 minutes meaning that one-directional drifts over this period were properly incorporated in the dosimetric assessments. Thirdly, the electron density distribution derived from the planning CT is assumed to be static over all fractions for both the IGRT and MRgRT workflow. This could potentially lead to inaccuracies of the accumulated 3D dose distributions. However, the d99 of the CTV will primarily be determined by the interfractional and intrafractional CTV motion and

the impact on the DVH parameters of the OARs will be negligible. Fourthly, small registration errors could have impacted the accumulated dose distribution. However, the accuracy of the image registration was high (dice coefficient of 0.91 ± 0.02) and therefore we believe that the impact of the uncertainty on the results is modest, as the dose distribution for each patient is calculated from the accumulated dose of five registrations, each with a separate error [78]. Furthermore, with the addition of a bending penalty metric the deformation vector field in the organs at risk is distributed more evenly and less subject to unexpected deformations. Fifthly, all simulations were done in an in-silico environment assuming no residual errors originating from mechanical instabilities, misalignment of imaging and irradiation isocenter and imperfections in geometric fidelity of the MR images. Earlier studies have shown that at least for the ring-based 1.5T MR-linac systems these errors turn out to be very small. Tijssen et al. reported the geometric displacements within a sphere of 15cm of the isocenter (typically the region of esophagus) to be 0.7mm or less [97]. Similarly, Raaymakers et al. have demonstrated that MRI based targeting on a 1.5T MR-linac system was better than 0.5 mm [98]. Nevertheless, although we have shown that a 2-mm radial margin was able to absorb most of the (radial) intrafraction motion, in a clinical setting these margins might still be perceived too tight in conjunction with the above listed uncertainties. Lastly, all autoplanning was done for a conventional accelerator, whereas the combination of a MRI with a linear accelerator with the MRI component placed within the gantry brings about relevant technical differences with possible implications for treatment plan quality. The most important differences that may influence treatment plan quality are a larger source to isocenter distance, the interaction of secondary electrons with the magnetic field and limited possibilities for patient positioning in the MRI bore [21, 99, 100]. However, a planning study of Nachbar et al. revealed that at least for the Elekta high-field MRI-linac (Elekta AB, Stockholm, Sweden) the MRgRT plans for esophageal cancer patients are very much comparable to plans for a conventional linear accelerator [101]. In conclusion, a considerable dose reduction to the OARs was observed, which has the potential to reduce toxicity and subsequent complications, when MR-guided daily adapted treatment plans were used. MRgRT plans with axial margins of 2 mm and CC margins of 5 mm around the CTV yielded similar CTV coverage as conventional IGRT treatment when motion is taken into account. It was shown that the reduced OAR dose could potentially be traded in for dose escalation in a simulated integrated boost setting.

Chapter 6

Clinical implementation and feasibility of long-course fractionated MR-guided chemoradiotherapy for patients with esophageal cancer: an R-IDEAL stage 1b/2a evaluation of technical innovation

The following chapter is based on:

MR Boekhoff, R Bouwmans, PAH Doornaert, MPW Intven, JJW Lagendijk, ALHMW van Lier, MJA Rasing, S van de Ven, GJ Meijer, S Mook

Clinical and Translational Radiation Oncology (2022) 34:82-89
[10.1016/j.ctro.2022.03.008](https://doi.org/10.1016/j.ctro.2022.03.008)

Abstract

Purpose

This R-Ideal stage 1b/2a study describes the workflow and feasibility of long-course fractionated online adaptive MR-guided chemoradiotherapy with reduced CTV-to-PTV margins on the 1.5T MR-Linac for patients with esophageal cancer.

Methods

Patients with esophageal cancer scheduled to undergo chemoradiation were treated on a 1.5T MR-Linac. Daily MR-images were acquired for online contour adaptation and replanning. Contours were manually adapted to match the daily anatomy and an isotropic CTV-to-PTV margin of 6 mm was applied. Time was recorded for all individual steps in the workflow. Feasibility and patient tolerability were defined as on-table time of ≤ 60 minutes and completion of $>95\%$ of the fractions on the MR-Linac, respectively. Positioning verification and post-treatment MRIs were retrospectively analyzed and dosimetric parameters were compared to standard non-adaptive conventional treatment plans.

Results

Nine patients with esophageal cancer were treated with chemoradiation; eight patients received 41.4 Gy in 23 fractions and one received 50.4 Gy in 28 fractions. Four patients received all planned fractions on the MR-Linac, whereas for two patients $>5\%$ of fractions were rescheduled to a conventional linac for reasons of discomfort. A total of 183 (86%) of 212 scheduled fractions were successfully delivered on the MR-Linac. Three fractions ended prematurely due to technical issues and 26 fractions were rescheduled on a conventional linac due to MR-Linac downtime (n=10), logistical reasons (n=3) or discomfort (n=13). The median time per fraction was 53 minutes (IQR=3min). Daily adapted MR-Linac plans had similar target coverage, whereas dose to the organs-at-risk was significantly reduced compared to conventional treatment (26% and 12% reduction in mean lung and heart dose, respectively).

Conclusion

Daily online adaptive fractionated chemoradiotherapy with reduced PTV margins is moderately feasible for esophageal cancer and results in better sparing of heart and lungs. Future studies should focus on further optimization and acceleration of the current workflow.

Introduction

Magnetic Resonance Imaging (MRI) is an imaging modality which provides excellent soft tissue contrast allowing clear visualization of both the esophageal tumor and surrounding organs at risk. Integrated MR-guided radiotherapy (MRgRT) systems such as the Elekta Unity 1.5T MR-Linac (Elekta AB, Stockholm, Sweden) allow for an adaptive workflow with online contour adaptation and replanning [22, 24, 54]. Moreover, MRgRT provides real-time imaging to characterize and eventually track intrafraction motion to ensure even more precise and accurate dose delivery. On the downside, online MRgRT will substantially increase the treatment time per fraction. Therefore, most clinical experience with MRgRT with online plan adaptation has been achieved for confined target volumes that are treated with hypofractionated regimens such as lymph nodes, prostate, pancreas and lung lesions [51, 60, 61, 63, 102]. For patients with esophageal cancer the role of MRgRT is relatively unexplored, although MRgRT has some potential benefits over contemporary cone-beam CT (CBCT) guided radiotherapy [103]. Firstly, the clinical target volume (CTV), which contains the esophageal tract and sometimes the proximal stomach, is subject to large interfraction variations [47]. Due to the limited soft-tissue contrast of CBCT imaging, these variations are often unnoted. Moreover, because of limited soft tissue contrast patients are typically aligned on the bony anatomy (e.g. vertebrae) during treatment. To account for these patient positioning and other inaccuracies the CTV is expanded to a relatively large planning target volume (PTV). Recent studies have suggested margins varying between 7 mm and 12 mm for different directions, resulting in PTVs that are about three times the volume of the CTV [6, 7, 76, 78]. Online MRI provides excellent soft tissue contrast, thereby enabling accurate target definition for each fraction and with online plan adaptation, interfractional variations (including potential tumor shrinkage) can be corrected for [104]. Secondly, respiratory motion and changes in respiratory patterns together with patient movements and relaxation could lead to intrafractional tumor changes [49, 71, 72]. Online cine-MR can capture these intrafraction changes and thereby potentially allows for gating and tracking strategies. In addition, during free breathing treatment dose delivery treatment can be interrupted in case intrafraction motion exceeds a preset threshold [59]. These motion management strategies will increase treatment accuracy. Thirdly, the onboard MRI also allows for online functional diffusion-weighted imaging (DWI). Multiple studies have shown that the change in DWI signal is a biomarker for treatment response [87, 105, 106]. It could be hypothesized that functional imaging potentially allows for dose painting and smart dose escalation strategies based on the residual disease demarcated by the DWI signal, which might increase treatment efficacy. However, MRgRT presents some disad-

vantages as well. Online imaging, replanning and verification procedures generally take more time and might be more demanding from a patient perspective. In addition, at this moment treatment costs of MRgRT will be higher compared to conventional CBCT guided radiotherapy. Therefore, systematic evaluation of MRgRT in esophageal cancer according to the R-Ideal framework is of utmost importance for evidence-based implementation [107]. As a first step to gain experience in the treatment of esophageal cancer on an MR-Linac and to explore the feasibility of MRgRT, we started an R-Ideal stage 1b/2a study, treating patients with esophageal cancer with fractionated chemoradiotherapy on the 1.5 T MR-Linac (Unity) with reduced PTV margins, at our institute, from July 2019 onwards. In this study we describe the workflow of MRgRT on a 1.5 T MR-Linac and report on our first clinical experiences in terms of treatment times, patient compliance and dose reduction to normal tissue.

Methods

Patients

Patients referred for chemoradiotherapy in accordance with the Dutch guidelines, with a good performance status and limited nodal disease, were eligible for treatment on a 1.5T MR-Linac (Elekta Unity, Elekta AB, Stockholm, Sweden). The chemoradiotherapy regimen consisted of 5 weeks or 6 weeks radiotherapy of 41.4 Gy in 23 fractions or 50.4 Gy in 28 fractions, with concurrent weekly intravenous administration of carboplatin and paclitaxel. Exclusion criteria were general contraindications for 1.5T MRI, an inability to tolerate a one-hour treatment as judged by the radiation oncologist, and an expected cranio-caudal length of the clinical target volume (CTV) of >18 cm because of limitations in maximum field size on the MR-Linac. All patients consented to the MOMENTUM study (NCT04075305), which has been approved by the Medical Research Ethics Committee of the University Medical Centre Utrecht in the Netherlands [108].

Clinical workflow

All steps of the workflow are depicted in Figure 6.1 and described in detail below.

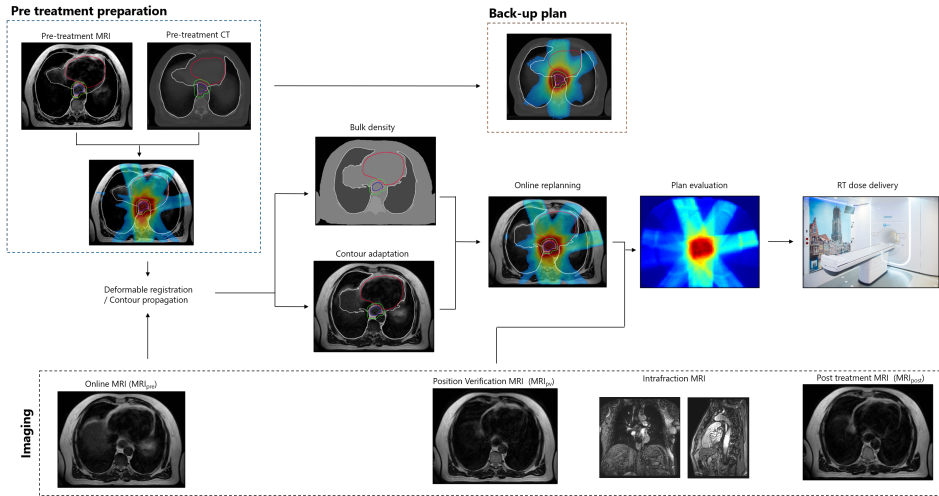


Figure 6.1: Clinical workflow for online adaptive radiotherapy on the MR-Linac for patients with esophageal cancer.

Pre-treatment imaging

Pre-treatment imaging consisted of an MRI scan and a planning (18F-FDG PET)-4DCT. MR imaging was acquired on a 1.5 T Philips Ingenia MRI scanner (Philips Medical Systems, Best, NL). Patients were scanned in free breathing conditions in head-first, supine treatment position with arms down for patient comfort, on a flat table top. The patient set-up was indexed to a special table overlay as described by Werensteijn-Honing et al. (2019) [60] and an anatomical 3D-T2-weighted scan (0.59x0.59x0.2 mm³, TE=87.5, TR=1300ms, scan time = 6 minutes) was acquired.

Delineations

Target volumes were delineated on the anatomy of the pre-treatment MR images. As this 3D-scan was acquired under free breathing conditions over 5-6 minutes, the time averaged anatomy was reconstructed over multiple breathing cycles with Cartesian k-space sampling [109]. First, the GTV was delineated on the 3D T2 weighted MR scan by a radiation oncologist subspecialized in esophageal cancer, where fused PET and CT images were used as extra guidance. Subsequently, the

CTV was defined as the gross tumor volume (GTV) of the primary tumor with a 3-cm cranio-caudal extension along the gastroesophageal tract (2 cm in caudal direction in cases where the CTV extended in the stomach) and radially with a 5-mm margin excluding anatomical structures such as heart, lungs, large vessels, trachea and main bronchi and vertebrae. Pathologic lymph nodes were also included in the CTV with a 5-mm margin where the previously listed anatomical structures were excluded. As the CTV was confined by both geometrical and anatomical borders that varied on a day-to-day basis, a multi-step delineation procedure was initiated involving three aiding structures (Figure 6.2). The first aiding structure (AID1) was defined as the GTV with a 0-cm cranial margin and a 3-cm margin (or 2 cm in case of tumor extension in the stomach) in all other directions. This structure was used to indicate the ultimate geometric limits of the caudal part of the CTV in the stomach region. The second aiding structure (AID2) was constructed by adding a 3-cm cranial margin to AID1. This structure was used to mark the upper transversal slice to be included in CTV definition. A third aiding structure (AID3) was defined as the GTV with an isotropic margin of 5 mm to mark the radial extensions of the CTV around the GTV. In an earlier in-silico study we demonstrated that a CTV-to-PTV margin of 2 mm in axial and 5 mm in cranial-caudal direction was large enough to absorb the residual intrafraction motion in the vast majority of patients [103]. However, in this clinical pilot study the PTV was conservatively created by an isotropic expansion of the CTV with 6 mm. OARs were delineated by a specialized radiation therapy technologist and checked and - if necessary - adapted by a radiation oncologist.

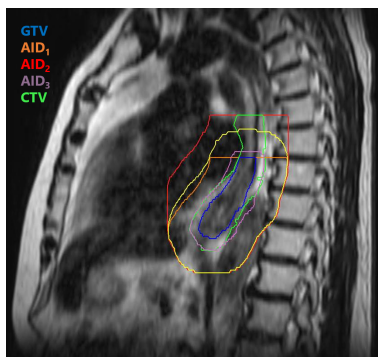


Figure 6.2: Aiding structures for fast reproducible online CTV definition. The first aiding structure (AID1) was defined as the online manually adapted GTV with a 0-cm cranial margin and a 3-cm margin (or 2 cm in case of tumor extension in the stomach) in all other directions. The second aiding structure (AID2) was constructed by adding a 3 cm cranial margin to AID1. A third aiding structure (AID3) was defined as the online manually adapted GTV with an isotropic margin of 5 mm. The propagated CTV was automatically confined by AID2 and subsequently adapted manually according to anatomy visible on the MRI. AID3 was used to facilitate manual adaptation of the CTV.

Pre-treatment planning

A pre-treatment step-and-shoot intensity-modulated radiotherapy (IMRT) plan was created in Monaco, to serve as a patient-specific template for online treatment planning. Here a dose of 41.4 Gy in 23 fractions (or 50.4 Gy in 28 fractions) was prescribed to 95% of the PTV, while minimizing the dose to the lungs, heart and spinal cord (Table 6.1). The calculation grid size for the Monte-Carlo dose engine was 4 mm and the relative electron densities for lungs, trachea, main bronchi and bony tissue were adapted from the planning CT, while the density of the remaining body tissue was set to 1.01 g/cm³. The 1.5 T magnetic field along the direction of the scanner bore was taken into account for all dose calculations. Seven non-uniformly spaced beam angles were used, avoiding the couch at beam angles of 115°-135° and 225°-245° the cryostat connection pipe at 8°-18° and avoiding patients' arms at beam incidence. Furthermore, a back-up plan was generated in case the patient needed to be rescheduled to a conventional linear accelerator. Therefore, a VMAT plan was generated with a 10-mm isotropic CTV-to-PTV margin based on the anatomy of the phase-averaged 4D planning CT.

Organ	Dosimetric parameter	Objective
PTV	V107%	<2 cm ³
	V95%	>98 %
	V90%	>99 %
Lungs	V20Gy	<30 %
	V5Gy	<75 %
Heart	V40Gy	<30 %
Spleen	Dmean	<20 Gy
CTV	V95%	>99 %

Table 6.1: Dosimetric parameters and objectives for online replanning. V107%, V95% and V90% represent the volume which receive at least 107, 95 and 90 of the prescribed dose, respectively. V5Gy, V20Gy and V40Gy represent the volume which receives 5, 20 and 40 Gy, respectively. Dmean represents the mean dose to the corresponding organ.

Online workflow

Online patient setup

Patients were in supine position with arms down on the MR-Linac couch using specific couch index points, which were intended to ensure that the position of the patient along the length of the couch was known and reproducible between the pre-treatment planning scans and each treatment session. In addition, an institutionally added in-room laser system was used for patient positioning on the MR-Linac.

Online contour adaptation and replanning

After patient alignment, a 3D T2 MRI scan (MRI_{pre}) was acquired using the same parameters as for the pre-treatment scan. Contours were propagated from the pre-treatment MRI using first a rigid and then a deformable registration in Monaco, version 5.40.01 (Elekta AB, Stockholm, Sweden). Next, the propagated GTVs were adapted by a specialized radiation oncologist. Then, the aiding structures AID1, AID2 and AID3 were regenerated and the propagated CTV was automatically confined by AID2 and subsequently adapted manually according to anatomy visible on the MRI. AID3 was used to facilitate manual adaptation of the CTV. Finally, a PTV of 6 mm in all directions was generated for the adapted CTV and, if deemed necessary, the contours of the propagated OARs were partially adapted. Once all contours were adapted to the anatomy of the day, online replanning was started using the objectives of the pretreatment IMRT plan, which is also referred to as the ‘adapt to shape’ workflow [56,60].

Plan evaluation, motion management and dose delivery

The new treatment plan was evaluated by the radiation oncologist. During plan optimization, a position verification (PV) MRI scan (MRI_{pv}) was acquired, with the same parameters as the online planning MRI scan. Visual inspection of an overlay of adapted contours from MRI_{pre} , especially the CTV, on the PV scan was used to observe the presence of significant target motion that possibly occurred during the recontouring and recalculation phase. If target shifts were judged to be inappropriate the plan could be readjusted in two manners. If the difference in the CTV anatomy was characterized by a shift, then the MRI_{pre} was rigidly registered to the MRI_{pv} . The corresponding translations were used to virtually shift the isocenter and the leaf positions of the multi-leaf-collimator, effectuating a virtual couch correction. Furthermore, the beam weights of the adapted segments were optimized to mimic the dose distribution of the earlier generated IMRT dose distribution. This procedure is also referred to as the adapt-to-position (ATP)

procedure and is fast (typically 1 minute) [110]. However, if the anatomical changes between MRI_{pre} and MRI_{pv} could not be captured by a rigid translation, the contours were adapted to the new anatomy and the entire replanning procedure was restarted, including a new position verification scan and plan evaluation. Meanwhile, an in-house made dose-check assessed the complexity of the treatment plan by comparing the total number of monitor units, number of segments, beam irregularity, and beam modulation to the pre-treatment plan. Furthermore, an independent 3D dose check was performed (Oncentra, Elekta AB, Stockholm, Sweden) 28. This independent dose calculation was based on a collapsed cone dose algorithm, therefore no magnetic field effect was taken into account.

Treatment delivery

After approval of the plan and independent dose check, radiotherapy delivery was initiated using 7 MV FFF IMRT. Over the entire delivery time, interleaved sagittal and coronal cine-MRIs were acquired at 1.6 Hz to visually inspect unexpected patient motion during treatment. Immediately after treatment, a 3D T2 MRI scan (MRI_{post}) was acquired for offline assessment of intrafraction shifts. No gating strategies were used as this was not supported by the system.

Outcomes

In order to assess the feasibility and the patient tolerability of the treatment, the percentage of treatment fractions delivered on the MR-Linac and the percentage of patients who received all treatment fractions on the MR-Linac were determined. In addition, total on-table time per fraction, as well as the duration of all steps of the workflow were recorded and for each step the median duration was calculated over all delivered MR-Linac treatment fractions. The treatment was arbitrarily scored as feasible when the on-table time interval was ≤ 60 minutes for $> 75\%$ of the treatment fractions and completion of $> 95\%$ of fractions on the MR-Linac, reflecting patient tolerability. Wilcoxon signed rank testing was performed to compare the target coverage, heart dose and lung dose between adaptive MRgRT plans and the back-up plan. Data were analyzed using SPSS version 25.0 (IBM Corp., Armonk, NY).

Intrafraction drifts

Intrafraction target drifts during treatment were assessed by registering the MRI_{post} to the MRI_{pv} . Here a rigid registration was performed with the Elastix toolbox using only the grey values within the CTV mask [48].

Results

Nine patients with esophageal cancer were scheduled to undergo chemoradiation on the MR-Linac between July 2019 and January 2021. Patient and tumor characteristics are summarized in Table 6.2. Most patients had a good WHO score and limited nodal disease. Eight patients were scheduled for 23 treatment fractions and one patient for 28 treatment fractions. Out of 212 scheduled treatment fractions, a total of 186 fractions were initiated on the MR-Linac, of which 183 were completed successfully. Two of the three unsuccessfully delivered treatment fractions were prematurely ended due to technical issues (at 89% and 63% of the delivered dose, respectively) and for one fraction it was decided to switch to the conventional back-up plan because of a cranial-caudal misalignment of the patient, which was only detected in the planning phase and inhibited the PTV expansion (Figure 6.3).

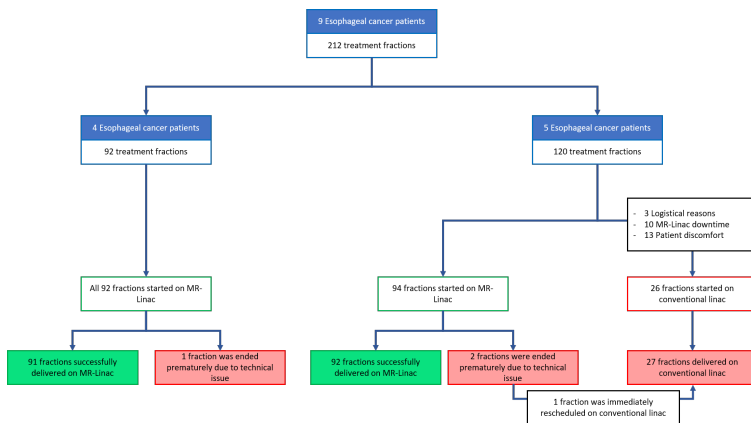


Figure 6.3: Flowchart of planned and delivered fractions on MR-Linac for nine patients with esophageal cancer.

	Median (range)	N (%)
Age (yrs)	59 (51-73)	
WHO performance		
0		1 (11 %)
1		7 (78 %)
2		1 (11 %)
Histopathology		
Adenocarcinoma		5 (56 %)
Squamous cell carcinoma		4 (44 %)
Tumor location		
Mid		2 (22 %)
Distal		5 (56 %)
GE Junction		2 (22 %)
T stage		
2		1 (11 %)
3		7 (78 %)
4b		1 (11 %)
N stage		
0		6 (67 %)
1		3 (33 %)

Table 6.2: Patient baseline characteristics.

Twenty-six fractions were rescheduled on a conventional linac prior to start of the treatment fraction due to MR-Linac downtime (n=10), logistical reasons (n=3) or reasons of discomfort associated with the long on-table times (n=13). For two patients (patient 5 and 6) > 5% of fractions were rescheduled to a conventional system for reasons of discomfort (after fraction 16 and 18 respectively), to reduce the burden of the long on-table times. For one patient (patient 8) this was only for a single fraction when the patient was suffering from a tickling cough. Lastly, in four patients all treatment fractions were delivered on the MR-Linac as planned. The median total time per fraction was 53 minutes (IQR 3 minutes), of which 19 minutes (36%) consisted of GTV, CTV and OAR delineation adjustments (Figure 6.4, Table 6.3). The median time between the start of the first MRI and the end of treatment was 49 minutes (IQR 10 minutes). The median planning time was 5 minutes and could take up to 12 minutes when ATP (3x) or full replanning (5x) procedures were performed after the initial online planning.

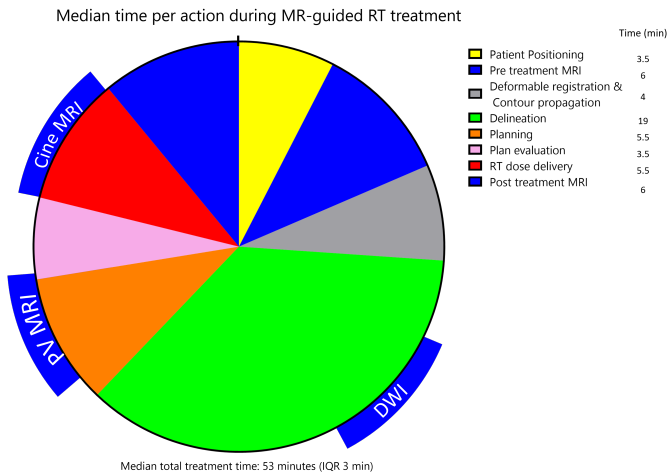


Figure 6.4: Overview of timings per action of the online workflow of MR-guided radiotherapy for patients with esophageal cancer.

Patient	Median (IQR) time per action in minutes				
	Delineation	Replanning	Plan evaluation	Dose delivery	1st MR – end treatment
PT 1	16 (30)	4 (1)	2 (1)	5 (1)	42 (4)
PT 2	24 (10)	4 (1)	2 (2)	4 (1)	51 (8)
PT 3	20 (7)	6 (3)	4 (4)	5 (2)	51 (8)
PT 4	17 (4)	4 (1)	4 (1)	5 (1)	45 (3)
PT 5	19 (3)	6 (1)	4 (1)	7 (0)	49 (4)
PT 6	21 (5)	6 (1)	4 (4)	7 (2)	55 (8)
PT 7	20 (10)	6 (1)	4 (1)	5 (0)	51 (10)
PT 8	19 (10)	6 (2)	3 (1)	7 (0)	52 (10)
PT 9	19 (7)	6 (1)	4 (2)	6 (0)	48 (10)
All	19 (7)	5 (2)	3 (2)	5 (2)	49 (10)

Table 6.3: Overview of timing per action of the online workflow for all patients. Abbreviation: IQR (interquartile range).

Comparison between the daily adapted MR-Linac plans and the back-up plan showed similar PTV coverages ($p=0.91$) (Figure 6.5). In an incidental case (10 out of 186 fractions) PTV coverage was below $< 97\%$, however CTV coverage was $> 99\%$ in all treatment fractions and therefore this was deemed acceptable. However, the dose to the OARs was significantly reduced with daily adaptive MRgRT. The average mean lung dose reduced by 26 % ($p<0.001$) and the average mean heart dose by 12% ($p<0.001$) compared to the VMAT back-up plan. Furthermore, a reduction in high dose to the heart (V40Gy), and dose to the lungs (V5Gy and V20Gy) was observed for most adapted plans in comparison to the back-up plans ($p<0.001$).

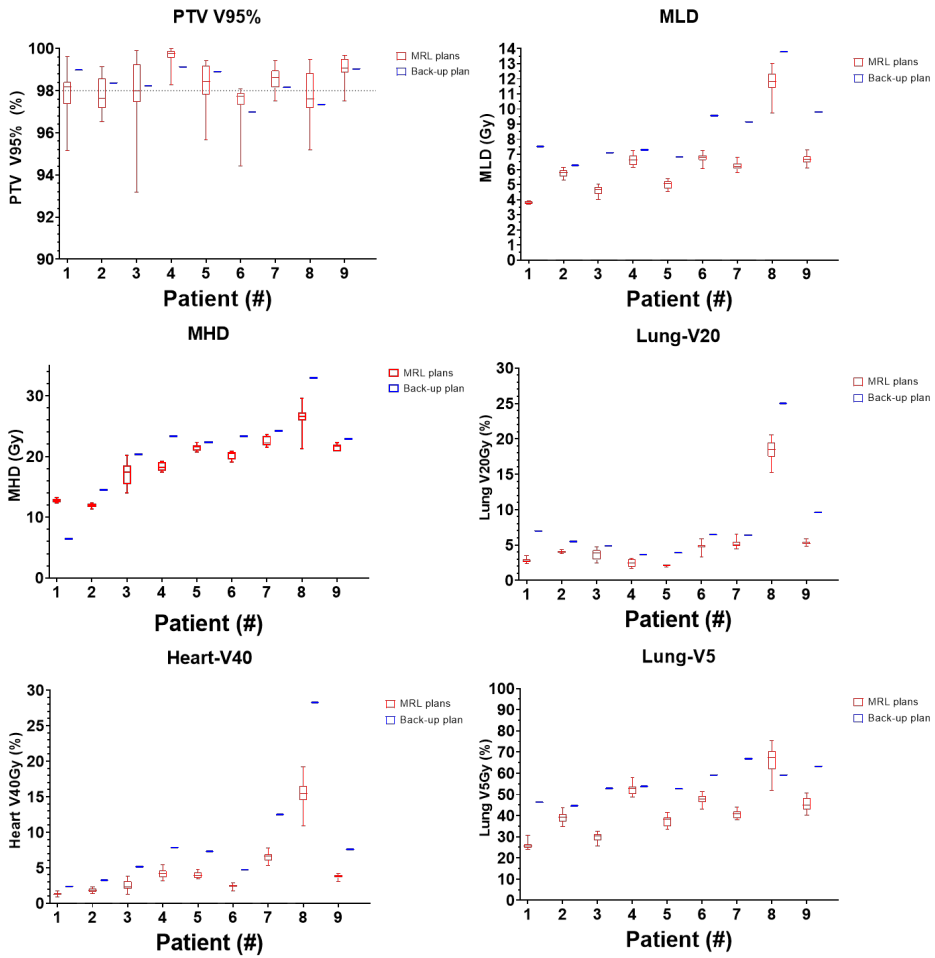


Figure 6.5: Comparison of target coverage and dose to the organs at risk between daily adapted MR-Linac plans (red) and the back-up plan (blue). The boxes show the 25th to 75th percentiles, where the median is displayed by a line inside the box.

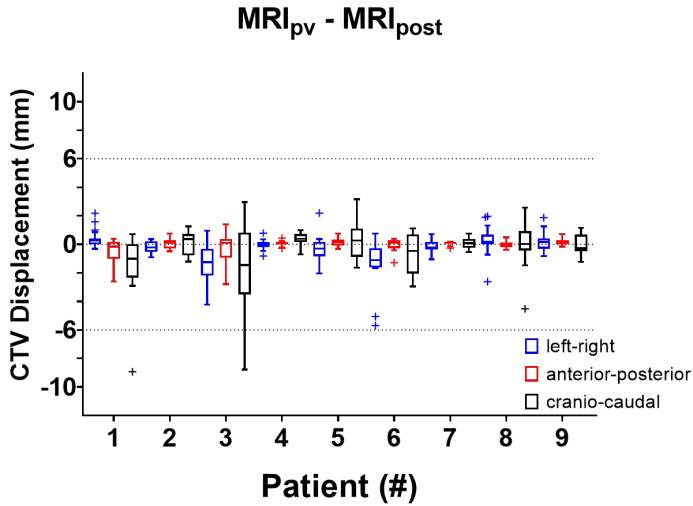


Figure 6.6: Box plot of the intrafraction drift of the CTV during beam-on time. for left-right (blue), anterior-posterior (red) and cranio-caudal (black) directions for all patients. Negative values represent a shift in right, anterior and caudal direction.

The median intrafraction motion during beam on time (between MRI_{pv} and MRI_{post}) was 0.9mm (IQR 1.0 mm) (Figure 6.6). Subanalysis revealed that the intrafraction motion was smallest in the left-right (average -0.2 mm, SD 1.0 mm) and anterior-posterior (average 0 mm, SD 0.6 mm) directions. Some fractions displayed larger motion in cranio-caudal direction (average -0.4 mm, SD 1.7 mm). Furthermore, it was observed that tumor volumes were smaller in the second half of the treatment course, compared to first half, which also was reflected in the volume of the CTVs and PTVs (Figure 6.7).

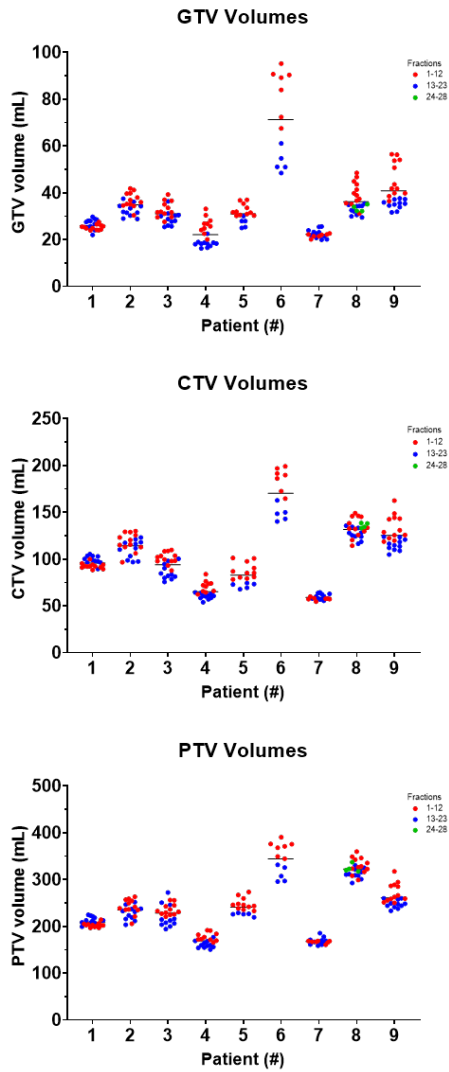


Figure 6.7: Change in GTV, CTV and PTV volume over the course of treatment. Difference between first half of the fractions and final half of the fractions is visible for most patients.

Discussion

To our knowledge, this is the first report on the clinical implementation of online MRgRT for patients with esophageal cancer, with an on-table re-imaging and replanning workflow. The presented workflow was feasible with a median time per fraction of 53 minutes (IQR 3 minutes). In addition, 2 out of 9 patients required treatment on a conventional linac for reasons of discomfort for more than 5% of fractions, therefore long-course fractionated chemoradiation on the 1.5T MR-Linac with the current workflow is moderately tolerable in selected patients with esophageal cancer. The use of daily plan adaptation allowed for an initial experience with smaller treatment margins, resulting in reduced dose to heart and lungs in comparison to the back-up treatment plan, while similar target coverage was achieved. The presented workflow for the on-table adaptive MRgRT for esophageal cancer was associated with some complexities, which are often unfamiliar to other treatment sites treated with online adaptive MRgRT. First, the size of the target volume for chemoradiation of esophageal cancers is large, which requires more extensive delineation of both target volume and adjacent organs at risk. Second, the online definition of the target volume involves recontouring of the GTV as well as a regeneration and adaptation of the CTV, instead of the generally applied GTV-to-PTV concept in stereotactic adaptive MRgRT. Therefore, the workflow for online adaptive MRgRT for esophageal cancer is more labor intensive and did require the onsite presence of a radiation oncologist. Third, the total treatment consisted of 23 or 28 fractions, which is at least uncommon, if not unprecedented, within the general framework of online adaptive MRgRT. These elements made the online adaptive MR-guided radiotherapy workflow for chemoradiation in esophageal cancer not only more demanding for patients and staff, but also required extensive logistic planning. These tumor specific complexities and challenges require a well-structured optimization and evaluation of the workflow, to facilitate timely and evidence-based implementation of MRgRT in esophageal cancer. According to the R-Ideal framework, we therefore conducted this phase 1b/2a study to provide the first experience of fractionated long-course chemoradiotherapy on the MR-Linac [107]. For this feasibility study we aimed to enroll 10 patients, however, due to the COVID pandemic only 9 patients could be enrolled within a reasonable timeframe. Nevertheless, still 186 treatment fractions on the MR-Linac were available for analyses. For most patients the long on-table procedure was tolerated well. However, the long overall treatment time (23 or 28 fractions) in combination with concurrent chemotherapy induced toxicity during the course of treatment negatively influenced the patients' compliance. For 2 out of 9 patients the physical condition gradually worsened over time making the long on-table workflows difficult to tolerate. It was therefore decided to

divert to a regular CBCT-guided workflow at the cost of an approximate 40% increase in mean lung dose for the remaining fractions (Figure 6.5). The moderate tolerability emphasizes the need for shorter on-table times. In the current procedures a large proportion of the preparation time (19 minutes) was spent on contour adaptation and regeneration of the CTV. Daily redefinition was necessary as the anatomy of the GTV and CTV changed from fraction to fraction for example due to changes in stomach filling and also due to tumor shrinkage (Figure 6.7) [47, 111]. Enhanced deformable registration procedures together with improved contour propagation techniques could potentially fully automate the online target and OAR definition process and thereby drastically reducing the pre-beam process. This would then allow on-table workflows of 20 minutes – 25 minutes which we believe would substantially increase patient compliance. In this feasibility study an isotropic CTV-to-PTV margin of 6 mm was pragmatically and conservatively chosen, which already yielded a considerable dose reduction to the lungs and heart compared to our regular CBCT-guided RT plans while maintaining target coverage in line with findings of Nachbar et al. [101]. In only 3 out of 186 fractions an interfractional drift was observed that exceeded the 6-mm margin, most likely as result of a change in breathing pattern (Figure 6.8).

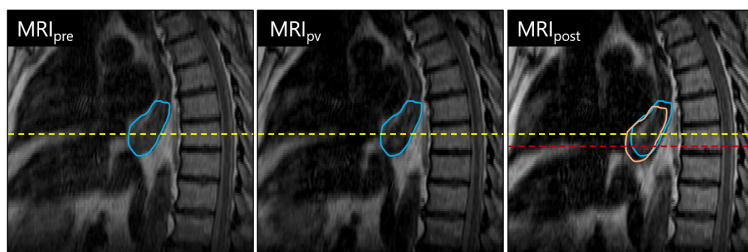


Figure 6.8: Example of a (rare) large caudal intrafraction shift between the pre-treatment (left) and position verification (middle) MRIs and the post-treatment MRI (right) for patient 3. No baseline shift was observed between MRI_{pre} and MRI_{pv} , while substantial lowering of diaphragm position (yellow and red dashed lines) was observed in the post-treatment scan which was partially propagated to the GTV (blue and orange contour).

Further dose reduction could be obtained by prospectively adapting patients' individual margins based on the measured intrafraction motion. In a previous in-silico study we have demonstrated that an axial margin of 2 mm in combination with a 5-mm cranial caudal margin could well absorb the intrafraction motion in almost all patients [103]. This work substantiates the earlier findings, as we showed that the lateral and anterior-posterior components of the intrafraction motion were small and random of nature, allowing smaller margins to be applied in these directions, thereby further reducing the dose to lungs and heart. On a

different note, treatment on an MR-Linac opens up the possibility of functional MR imaging. In particular, for patients with esophageal cancer changes in the diffusion-weighted imaging (DWI) signal have been shown to correlate to treatment response [87,105,106,112]. MR-Linac treatments potentially allow for daily quantification of these signal changes over the entire treatment without an increase in treatment time, as these 2-minute DWI scans can be acquired during the recontouring phase (Figure 6.4). Although beyond the scope of this work, an example of the changes of the b500 signal over the course of treatment are depicted in Figure 6.9.

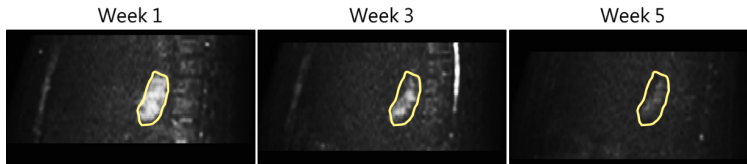


Figure 6.9: Example of reduction of the DWI b500 signal during chemoradiotherapy in a patient with esophageal cancer.

In conclusion, an online adaptive workflow with full replanning to the daily anatomy for esophageal cancer radiotherapy on a 1.5T MR-Linac results in a reduced dose to the organs-at-risk without compromising target coverage compared to our conventional CBCT treatment. However, due to the long treatment times MRgRT was only moderately feasible in a selected patient group. Future studies should be focused on further optimization and acceleration of the current workflow and on employing the full potential of daily MR-guided radiotherapy for the development of new treatment strategies, such as biology-driven dose escalation.

Chapter 7

Intrafraction motion analysis in online adaptive radiotherapy for esophageal cancer

The following chapter is based on:

MR Boekhoff, JJW Lagendijk, ALHMW van Lier, S Mook, GJ Meijer

Physics and Imaging in Radiation Oncology (2023) 26, 100432

10.1016/j.phro.2023.100432

Abstract

Intrafraction motion during magnetic resonance (MR)-guided dose delivery of esophageal cancer tumors was retrospectively analyzed. Deformable image registration of cine-MR series resulted in gross tumor volume motion profiles in all directions, which were subsequently filtered to isolate respiratory and drift motion. A large variability in intrafraction motion patterns was observed between patients. Median 95% peak-to-peak motion was 7.7 (3.7 – 18.3) mm, 2.1 (0.7 – 5.7) mm and 2.4 (0.5 – 5.6) mm in cranio-caudal, left-right and anterior-posterior directions, relatively. Furthermore, intrafraction drift was generally modest (<5mm). A patient specific approach could lead to very small margins (<3mm) for most patients.

Introduction

Radiation therapy has become an integral part in the neoadjuvant treatment of locally advanced esophageal cancer [2,32]. Optimal radiotherapy delivery accounts for day-to-day changes in target volumes. The introduction of magnetic resonance (MR) guided radiotherapy (MRgRT) has allowed for online plan adaptation of the treatment plan based on MRI visualization of the daily anatomy [22,24,113]. In a recent study we have demonstrated in a cohort of patients with esophageal cancer that MRgRT reduces the dose to organs at risk (OAR) when daily plan adaptation is applied in combination with the use of smaller treatment margins [103,113]. Daily plan adaptation compensates for set-up inaccuracies and interfraction tumor changes, leaving only intrafraction motion (e.g. breathing motion and tumor drifts) as residual errors. The aim of the current work was to retrospectively assess the intrafraction motion in this patient cohort.

Materials & Methods

Nine esophageal cancer patients received neoadjuvant chemoradiotherapy treatment on a 1.5T MR-Linac (Elekta Unity, Elekta AB, Stockholm, Sweden) between July 2019 and March 2021, as previously reported by our group [113]. All patients consented to the MOMENTUM study (NCT04075305), which has been approved by the Medical Research Ethics Committee of the University Medical Centre Utrecht in the Netherlands [108]. In this cohort, the tumor location varied from the mid- (2) to distal-esophagus (5) and around the gastroesophageal junction (2). Clinical T and N stage were distributed as follows: cT2 (1), cT3 (7) and cT4b (1), N0 (6) and N1 (3).

All patients underwent a T2 weighted anatomical MR scan at the start of each treatment fraction. After registration to a reference scan, the gross tumor volume (GTV) and clinical target volume (CTV) contours were propagated and subsequently adapted by a radiation oncologist. An isotropic treatment margin of 6 mm was used to expand the CTV to create the planning target volume (PTV). Next, a treatment plan was created. In the meantime a second MR scan was acquired and treatment was started if the intrafraction motion between the scans was deemed appropriate (i.e. small) otherwise the plan was readapted. Cine-MR series were recorded for the full duration of dose delivery during each treatment on the MR-Linac. The series consisted of interleaved scans in the coronal and sagittal plane with an in-plane resolution of $1.2 \times 1.2 \text{ mm}^2$ with a frequency of 3 Hz.

The delineated GTV was rigidly propagated to the reference frames of both the coronal and sagittal cine-MR series, which were chosen based on representation of the anatomy of the planning MRI (Figure 7.1). Cine images were registered to the reference frame with a Matlab (Mathworks Inc., Natick, MA, USA) GPU implementation of Evolution [114]. The motion fields following from registration of the cine slices were applied on a binary mask of the GTV and for every cine instance the motion trajectory of the center of mass of the GTV-mask was calculated. Analysis of the coronal slices resulted in the motion trajectory in cranio-caudal and left-right directions, while the anterior-posterior and again the cranio-caudal directions were obtained from analysis of the sagittal slices.

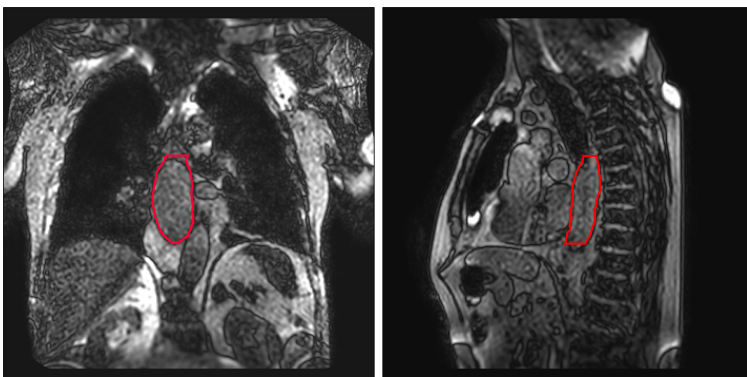


Figure 7.1: Coronal (left) and sagittal (right) cine slices. Tumor motion is tracked within the daily adapted GTV (red).

Two filters were used to separate the drifts from the periodic breathing motion. A high-pass filter of 0.05 Hz was used to extract the drift motion, while a low-pass average filter (50 frames, 20 seconds) was used to isolate the respiratory motion. Furthermore, for each direction the difference between the maximum and minimum (peak-to-peak) value of the respiratory motion was calculated, excluding the top and bottom 5 percentiles to reduce sensitivity to outliers. Similarly, the minimum and maximum values of the filtered drift motion were determined to obtain the largest drift in each direction.

In order to calculate the impact of the intrafraction motion on the CTV-to-PTV margin, the motion trajectories were used to assess the standard deviation of the motion of the GTV throughout all fractions (σ_m). The difference between the blurred and non-blurred 95%-isodose level could then be estimated by:

$$M_{\text{intrafraction}} = 1.64\sqrt{[\sigma_m]^2 + [\sigma_p]^2} - 1.64[\sigma_p]$$

where the parameter σ_p , describing the width of the penumbra modeled by a cumulative Gaussian which was set to 3 mm [6, 14, 15].

In total 183 fractions were successfully completed on the MR-Linac, yielding 183 sets of coronal and sagittal cine-MR series.

Results

The median (range) 95% peak-to-peak motion obtained from the coronal scans was 7.7 (3.7 – 18.3) mm in cranio-caudal direction and 2.1 (0.7 – 5.7) mm in left-right direction (Figure 7.2). Analysis of sagittal scans showed a median of 6.1 (2.3 – 15.5) and 2.4 (0.5 – 5.6) mm peak-to-peak motion in cranio-caudal and anterior-posterior directions, respectively. The largest peak-to-peak motion was observed in patients 1 and 3. For these patients a peak-to-peak respiratory amplitude of more than 1 cm in cranio-caudal direction was observed for all fractions.

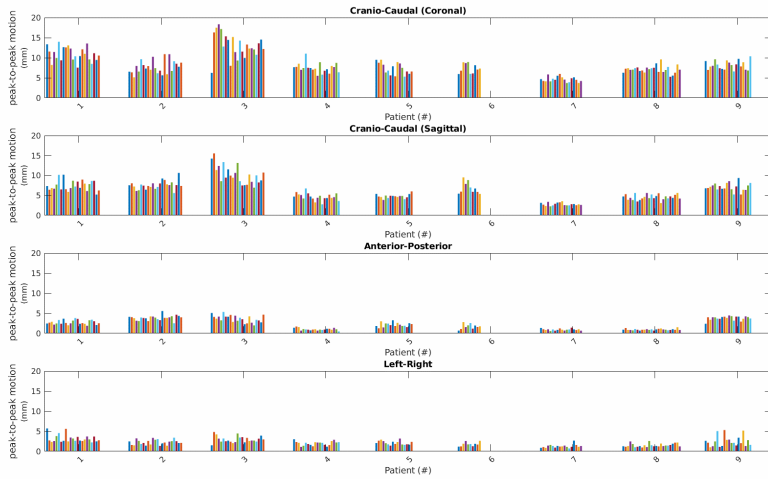


Figure 7.2: 95% Peak-to-peak breathing motion for all patients

The median (range) drift was largest in cranio-caudal direction, in particular as measured on the coronal scans: 2.7 (0.6 – 14.7) mm, while the cranio-caudal drift measured on the sagittal scans was 2.1 (0.5 – 9.9) mm. The median drift in AP and LR directions was 1.0 (0.1 – 5.2) mm and 1.0 (0.2 – 4.7) mm, respectively (Figure 7.3). The largest systematic cranio-caudal drift was 10 mm for two patients. However, when averaged over all fractions no systematic drifts >1mm were observed in any direction for any patient indicating that drifts could be systematic within a fraction, but were random over the entire treatment course.

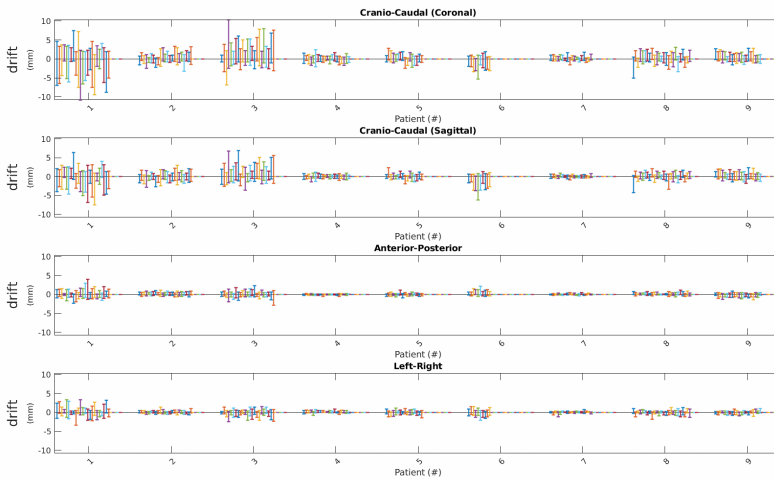


Figure 7.3: Min-max drift motion per fraction for each direction for all patients.

In Table 7.1, the standard deviation of the motion of the GTV throughout all fractions (σ_m) for each patient is listed together with associated intra-fraction motion.

Patient	σ_m (mm)				$M_{\text{intrafraction}}$ (mm)			
	CCc	CCs	AP	LR	CCc	CCs	AP	LR
1	4.7	3.2	1.2	1.5	4.2	2.3	0.4	0.6
2	2.7	2.6	1.3	0.8	1.7	1.6	0.4	0.2
3	4.9	3.6	1.3	1.2	4.6	2.8	0.4	0.4
4	2.5	1.6	0.4	0.6	1.5	0.6	0.0	0.1
5	2.6	1.7	0.7	0.8	1.5	0.7	0.1	0.2
6	2.7	2.6	0.8	0.9	1.7	1.6	0.2	0.2
7	1.6	0.9	0.3	0.5	0.6	0.2	0.0	0.1
8	2.6	1.7	0.4	0.7	1.6	0.7	0.0	0.1
9	2.8	2.4	1.3	0.9	1.8	1.4	0.4	0.2

Table 7.1: Required margin $M_{\text{intrafraction}}$ in mm per patient to deliver at least 95% of the prescribed dose to the GTV in 90% of the beam-on time. Here, σ_m is the standard deviation of the motion of the GTV throughout all fractions.

Discussion

This study provided an analysis of esophageal tumor motion during online MR-guided radiotherapy. A large variability in intrafraction motion patterns was observed between patients. Two patients displayed a systematic cranio-caudal drift of 10 mm, while three patients did not show an intrafraction cranio-caudal drift larger than 5 mm in any of their fractions. This indicated that small treatment margins (<5mm) would have been sufficient for these patients to ensure sufficient target coverage for each fraction. Furthermore, some patients displayed a large variability of breathing patterns during dose delivery, which was observed as changes in amplitude or periods of breath-hold as shown in Figure 7.4.

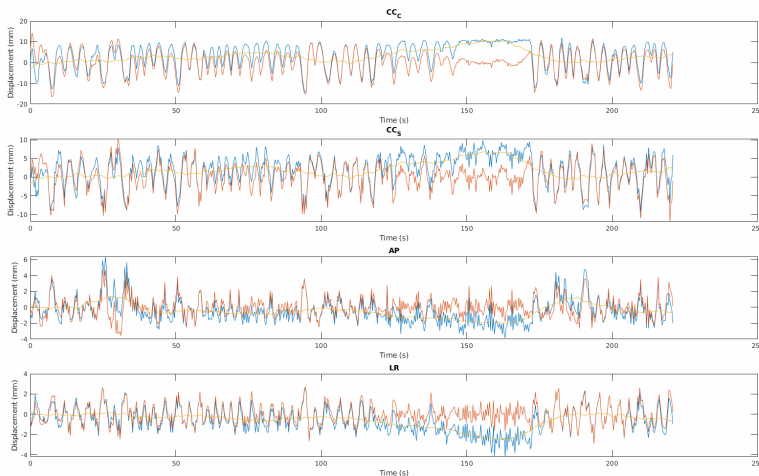


Figure 7.4: Irregular motion pattern for patient 3 during dose delivery. The total motion (blue) is split in a (low-frequency) drift motion (orange) and a (high-frequency) respiratory motion (red).

The peak-to-peak motion caused by breathing was largest in cranio-caudal direction and typically 5-10 mm, while the motion in anterior-posterior and left-right directions was generally modest (<5 mm). In general, similar peak-to-peak distances were observed for each patient throughout all fractions, although small variations in breathing amplitude were observed between fractions.

We observed a difference of 0.1 – 3.5 mm in measured cranio-caudal motion between the coronal and sagittal cine scans. The largest cranio-caudal motion was measured on the coronal scans which is consistent with the findings of Lever et al. [71]. This difference could be explained by the difference in center of mass of

the GTV-mask between the cine planes. Delineations projected on the coronal plane included a larger part of the stomach than those in the sagittal plane. This could result in a different location of the center of mass, which could be more subject to intrafraction changes of the stomach. Patient two displayed almost no difference between the scans for all fractions, while patient one, who had more tumor extension into the stomach, showed an average difference of 3.5 mm between cranio-caudal motion obtained from coronal and sagittal scans.

Previous studies on intrafraction motion patterns for esophageal cancer reported a similar spread of cranio-caudal respiratory motion between patients [5–7, 49, 70, 115, 116]. As all interfraction variations are inherently corrected in the online adaptive workflow, the CTV-to-PTV margins stem from the interfraction motion as listed in Table 1. Most margins were small (≤ 2 mm) and only patient 1 and 3 would have needed margins of 4 mm and 5mm for the cranio-caudal direction. All margins were below the 6-mm CTV-to-PTV margin that were clinically applied in this study, but based on these results smaller margins could be safely applied in future studies, allowing a further dose reduction to the OARs. As the interfraction variation of the motion patterns within each patient were small, an adaptive strategy could be envisioned where the margin is adapted based in the observed motion patterns in the first fractions. Also gating and tracking strategies could be employed for patients with breathing amplitudes of 12 mm or more [59, 117]. The use of MRgRT allows for potential treatment intensification of the tumor (boost dose) [103]. In this scenario it is crucial that target movement is anticipated for to prevent increased toxicity to the surrounding OAR and to ensure that the dose is correctly administered to the target volume [82, 83]. Sub-analysis of GTV coverage revealed that margins < 5 mm would have been sufficient in this patient group to deliver at least 95% of the prescribed dose to the GTV in 90% of the fractions (Table 7.1). These relatively small margins might allow incorporation of dose escalation in the current workflow.

There were a few limitations in our study that need to be acknowledged. First, the relative small sample size of nine patients, with mostly distal tumors, could have influenced the results as distal tumors are more subject to large position variations [47]. Furthermore, a larger sample size might have concluded that it could be possible to adjust treatment margins based on intrafraction motion patterns after the first week(s) of treatment, as the interfraction variability of individual patients appeared to be low in this study, as no outliers were observed in Figure 7.2 & 7.3.

Secondly, the high-pass filter of 0.05 Hz was chosen to be low enough to contain all frequency components of the respiration motion, while allowing some variation in motion patterns. The breathing amplitude of patients who breathed at a very

low rate could have been filtered out. This could have led to an underestimation of the respiratory amplitudes. We believe this would not have a large impact on our findings, as we had long recordings of multiple fractions for each patient.

Thirdly, the motion trajectories were determined from 2D cine-MR images, without adaptation of the GTV-mask. Deformations of the GTV-mask were not taken into account, which could have influenced the position of the center of mass. Furthermore, out-of-plane motion could have potentially resulted in inaccuracies in the determined motion patterns. Especially patients with a caudal tumor extension into the stomach might have been more vulnerable for out-of-plane motion. A solution could be to use deformable image registration to adapt the GTV contours to follow-up frames. However, this would have significantly increased the complexity and could have introduced an increase in sensitivity to registration errors, while the change in tumor shape was generally modest. Another possibility to capture out-of-plane motion could be to explore 3D cine imaging, which might decrease temporal resolution leading to an underestimation of the respiratory motion.

In conclusion, intrafraction drift was generally modest ($<5\text{mm}$), but showed a high interpatient variability. The calculated treatment margin indicated that a patient specific approach could lead to very small margins ($<3\text{mm}$) for most patients.

Summary and general discussion

Overview

In the Netherlands, for patients with locally advanced, resectable esophageal cancer without metastases the current standard of care is neoadjuvant chemoradiotherapy (nCRT) followed by esophagectomy. nCRT is administered according to the CROSS regimen and consists of 23 fractions of 1.8Gy with weekly carboplatin and paclitaxel [2]. One of the main goals of nCRT is to downsize the primary tumor and thereby increase the chance of a radical resection. This tumor shrinkage during treatment can result in target deformation. In addition, tumor position can vary substantially over the course of treatment. Moreover, intrafraction motion can be observed, mainly related to breathing motion. Treatment margins are needed to compensate for these geometrical uncertainties, creating the planning target volume (PTV) out of the clinical target volume (CTV). Previous studies were able to define margins which provide sufficient target coverage for conventional treatment [5–7, 40]. It was found that large CTV-to-PTV margins are required to ensure adequate target coverage throughout the whole treatment period. This leads to irradiation of large volumes which includes healthy tissue around the CTV. The resulting excess radiation dose to the organs at risk could lead to complications [25, 36, 91–96]. It is therefore important to minimize the dose to healthy tissue by accurately defining the target volumes and potentially reducing treatment margins. Image-guided radiotherapy (IGRT) will increase accurate dose delivery and the current imaging standard for conventional treatment is (CB)CT. The primary tumor, involved nodes and the clinical target volume (CTV) consisting of the peri-esophageal fat often can hardly be discriminated on CBCT. Hence, set-up corrections are typically performed by online registration of the bony anatomy visible on CBCT, instead of direct matching on the tumor. The interfractional variation of the tumor position and shape in relation to the bony anatomy can be substantial and consequently large PTV margins are still required for adequate target coverage. Improved imaging quality is required for accurate target definition, online tumor matching and online treatment adaptation.

Magnetic Resonance Imaging (MRI) is an imaging modality with superior contrast compared to (CB)CT and has been suggested to be beneficial in radiotherapy treatments [21, 22]. In this thesis, we have investigated whether the use of MRI in radiotherapy for esophageal cancer could reduce geometrical uncertainties and lead to more accurate target definitions. We aimed at using MRI to accurately define the position and shape of esophageal cancer tumors throughout the period of treatment. Furthermore, we wanted to determine if the application of MRI in the treatment of esophageal cancer could be beneficial. On top of that the goal was to gain experience with MR imaging of esophageal cancer tumors and work towards a clinical implementation. The first part of this thesis is based on the results of the “**RE**peated magnetic resonance imaging in esophageal cancer for **A**daptive radiation treatment planning during neoadjuvant **C**hemoradio**T**herapy” (REACT) trial that we conducted in our clinic between December 2015 and April 2018. The main goal of this study was to work towards development of a patient-specific radiotherapy planning strategy using MRI. Geometric variations over the course of treatment were assessed by six weekly MRI scans during neoadjuvant chemoradiotherapy. In Chapters 2, 3, 4 and 5 we reported on the results of this study. The findings of the first part of this thesis were applied and clinically implemented in an online adaptive, MR-guided radiotherapy treatment workflow for patients with esophageal cancer. In the second part of this thesis we reported on our experiences with this workflow. The clinical implementation and feasibility of long-course fractionated MR-guided chemoradiotherapy for patients with esophageal cancer was described in Chapter 6. On top of that, the intrafraction motion patterns during online adaptive radiotherapy dose delivery were analyzed in Chapter 7.

Geometrical changes during neoadjuvant chemoradiotherapy of patients with esophageal cancer

Various anatomical changes can occur during 5 weeks of neoadjuvant chemoradiotherapy in the treatment of esophageal cancer. Previous studies have used CT images, often in combination with fiducial markers, to show these interfractional changes in position, shape and volume [5, 30, 31]. However, studies on weekly changes of the full anatomy of the tumor were lacking, whereas it has been shown that the full 3D changes of the anatomy could result in significant dosimetric changes in the targets and OARs [29]. The REACT study was designed to capture the full anatomy of the tumor with weekly MR images. Respiratory-triggered transversal and sagittal T2-weighted MRI scans were recorded to capture the anatomy of the tumor. Intrafraction motion was captured with two sagittal and

coronal cine-MRI series of each 45 seconds. With these images, a treatment simulation was performed to investigate the geometrical changes during neoadjuvant chemoradiotherapy of patients with esophageal cancer.

Volumetric response

We assessed the volumetric changes in the primary tumor during nCRT for esophageal cancer based on weekly MR images in **Chapter 2**. After five weeks of nCRT treatment we observed an average decrease in tumor volume of 28%. Furthermore, tumor regression already started after the first week of treatment, which implies that replanning can be beneficial after only one week of treatment. These findings are in line with previous studies which used follow-up scans after 10 or 20 fractions, respectively, to assess tumor regression [30,31]. An important finding of this study was that due to tumor regression, the heart could move into the high dose-regions as the treatment evolves. This was predominantly observed for large tumors (>50cc) dorsally situated from the heart. As an increase in heart dose has been related with complications and worse overall survival [25,36], adaptive strategies could be considered in this subpopulation of patients. A simple but effective strategy would be to standardly replan these patients after two weeks of treatment.

The impact of geometrical changes on target coverage

Geometric tumor changes between fractions account for the largest uncertainty in tumor position and have therefore the biggest impact on the inflation of treatment margins. Most studies reporting on motion patterns and treatment margins for esophageal cancer radiotherapy have used (4D)CT, often in combination with implemented markers as surrogate of the tumor position [5–7]. In these studies, treatment margins were calculated based on the van Herk recipe [14,15]. However, there are a few limitations when using the margin recipe to determine the treatment margins. First, the margin recipe assumes rigid movements of the entire CTV, whereas the CTV interfraction variation is often characterized by shape changes. Second, implemented markers are sampled over the tumor (GTV) and not over the CTV which may lead to different motion characteristics. Thirdly, the margin recipe assumes perfect conformity at every surface element of the PTV surface often in conjunction with steep dose gradients outside the PTV, which could lead to overestimation of the required margins. In **Chapter 3** we overcame these aforementioned limitations by performing a full dosimetric assessment of weekly replanning to calculate the smallest CTV-to-PTV margins that yield full target coverage over the course of a simulated treatment. By performing a

full dosimetric assessment, not only the dosimetric impact of day-to-day translations of the tumor itself was accounted for, but also the dosimetric effects of all morphologic changes (e.g. tumor regression) over the course of treatment were incorporated. The accumulated dose analysis revealed that CTV-to-PTV treatment margins of 8, 9 and 10 mm in posterior & right, anterior & cranial and left & caudal direction, respectively, were sufficient to account for interfraction tumor variations over the course of treatment when applying a daily online bone match set-up strategy. However, two patients with extreme esophageal interfraction motion were insufficiently covered with these margins and were identified as patients requiring replanning to achieve full target coverage, further highlighting the need for daily adaptive radiotherapy.

The impact of adaptive set-up strategies on target coverage

In current conventional IGRT for esophageal cancer, day-to-day shape and position changes of the tumor are typically uncorrected for and a match of the bony anatomy in close proximity of the tumor is used to ensure optimal alignment to the treatment plan [5, 7, 16–18, 25, 46, 77]. Therefore, not only geometric changes of the tumor itself, but also the variability in tumor position relative to the bony anatomy requires incorporation in treatment margins. Previous studies have investigated different set-up strategies, such as alignment to markers, implemented in and around the tumor, carina-based alignment, or a combination of soft-tissue and bony anatomy alignment [5, 18, 46]. It was concluded that currently no golden standard for patient set-up exists, but that patient set-up based on the bony anatomy provided sufficient accuracy for all tumor locations. Online MR guidance allows increased visualization of the tumor and evaluation of the entire 3D geometry of the GTV and CTV, allowing the use of adaptive set-up strategies. In **Chapter 4**, two set-up strategies were compared to account for positional tumor changes: a rigid alignment of the daily CTV to the planning CTV (i.e. adaptive MR-guided soft tissue set-up) was compared to rigid alignment to the bony anatomy (i.e. conventional CBCT set-up). It was found that direct CTV registration methods using in-room MRI only yielded a moderate increase in target coverage (94% and 90% of fractions were fully covered with a margin of 10 mm when using CTV and bone alignment, respectively) compared to the clinical (bone match) CBCT-IGRT protocols. Nevertheless, we were able to define the target coverage as a function of a preset isotropic margin for both set-up strategies. Furthermore, it was observed that distally located tumors often required larger margins to achieve geometrical target coverage, mostly caused by day-to-day changes in stomach filling. We concluded that an online adaptive workflow where a new plan is created based on the anatomy of the day is essential when pursuing highly conformal target irradiations for all treatment fractions. In

the next chapter we evaluated the potential dosimetric benefits of such an online adaptive workflow.

The dosimetric benefit of MRgRT

Radiation dose to organs at risk is inevitable in esophageal cancer radiotherapy. Various studies have analyzed toxicity effects of organs surrounding the esophagus, especially of concern is the radiation dose to heart and lungs [8–11, 118]. It has been shown that an increased dose to heart and lungs could lead to an increased incidence of complications and could even lead to an increased mortality rate. Various strategies to reduce organ at risk dose have been explored by multiple tumor sites and it has been hypothesized that a reduction of treatment margins will have a large impact in reducing toxicity of healthy tissue [51, 90, 119]. Following chapters 2, 3 and 4, it was concluded that daily plan adaptation is required for optimal target coverage. In **Chapter 5** we explored the potential benefit of full daily plan adaptation, allowing the use of small treatment margins only accounting for the intrafractional changes. A comparison between a simulated conventional IGRT strategy and an adaptive MRgRT strategy showed that smaller margins could lead to a large reduction in dose to organs at risk, especially in the high dose region ($>40\text{Gy}$), while target coverage was similar between both treatment strategies. Furthermore, it was shown that the gained dose reduction with online adaptive MRgRT could also be employed to increase the dose to the primary tumor while preserving the dose levels to the OARs from the conventional non-adaptive IGRT. This implies that high-precision online adaptive radiotherapy opens new perspectives for local boosting strategies to improve outcome of the local management of esophageal cancer.

A remark has to be made about the simplification of the two strategies, IGRT and MRgRT, used in Chapter 4. While the IGRT strategy represented the current conventional workflow with CBCT imaging in our clinic, recent innovations in cone-beam imaging driven by artificial intelligence could allow for adaptive radiotherapy [84, 85]. However, we believe that geometrical uncertainties of CBCT imaging could only yield a modest margin reduction in comparison to potential margin reduction as shown with the described MRgRT strategy, which makes use of the superior soft-tissue contrast of MRI. On top of that, future MRgRT for esophageal cancer could include respiratory gating and multi-leaf collimator tracking, which could compensate for intrafraction motion and should further allow margin reduction, especially in cranio-caudal direction [61, 66, 120]. Finally, it should be noted that for safety reasons a treatment margin of 2 to 3 mm may still be required, to compensate for mechanical, set-up, delineation and other

uncertainties [98,121].

Tissue sparing might also be achieved when using proton beam therapy instead of photon therapy, as the Bragg peak in proton therapy results in lower entry and exit doses. Planning studies have shown that treatment with proton beam therapy has the potential to significantly reduce dose to organs-at-risk in comparison to conventional photon therapy treatment for esophageal cancer [122–124]. However, proton beam therapy is associated with a range of uncertainties and whereas photons beams are relatively insensitive to density changes, these uncertainties become more complex and prominent in proton therapy, often resulting in the need for replanning [125–127]. Nevertheless, it is important for both proton therapy and MRgRT with reduced treatment margins to manage motion, especially during dose delivery, to provide sufficient target coverage and to prevent radiation toxicity to surrounding tissue. This becomes even more important when boosting strategies are employed. The use of adaptive MR-guided workflows reduces the geometric uncertainties, allowing for highly precise irradiations while reducing organ-at-risk dose. Furthermore, MRgRT could potentially be employed to compensate for intrafraction motion, which is a concern in proton beam therapy. In the future, model-based clinical evaluations might be used to determine which modality would provide the best treatment for each individual patient [128].

After analysis of the REACT study, it was found that various anatomical changes occurred during the treatment period. Volume changes were already observed after the first week of treatment. Furthermore, we observed position and shape changes throughout the treatment period, especially for tumors located around the gastroesophageal junction and into the stomach. A full dosimetric assessment revealed that treatment margins of 8-10mm would have been sufficient to provide sufficient target coverage in most patients when applying a daily online bone match. However, extreme interfraction motion was observed in two patients. Comparison of set-up strategies showed that a set-up strategy with CTV alignment only leads to a moderate increase of covered fractions (94% vs 90%) compared to a bone alignment set-up strategy, when similar margins are used. These findings emphasize the need for online adaptive treatment strategies. A simulation of an adaptive MRgRT strategy did show promising results. It was shown that smaller margins could lead to a large reduction in dose to organs at risk, especially in the high dose region ($>40\text{Gy}$), while target coverage was similar between both treatment strategies. It was concluded that MR-guided radiotherapy could be beneficial for patients with esophageal cancer and required further investigation.

First clinical experience with online MRgRT for esophageal cancer patients

After the findings discussed in earlier chapters, it was concluded that adaptive MR-guided radiotherapy could be beneficial for patients with esophageal cancer. In recent years, daily online plan adaptation has become available with the introduction of MR-Linacs to the clinic. Online adaptive workflows have been developed for the irradiation of various treatment sites, such as lymph nodes, pancreatic cancer, prostate cancer and rectal cancer [23, 24, 60, 61, 63, 129, 130]. Although there are many similarities between treatment sites, each tumor site is associated with specific technical complexities. In the past few years our group has worked towards the creation of a workflow for the adaptive treatment of patients with esophageal cancer. A feasibility study was performed in 2018, where the schedule consisted of five fraction with a dose of 4 Gy to the GTV (no CTV expansions). The experience gained with these short series of irradiations of confined target volumes allowed for improvement of the adaptive workflow. This resulted in the treatment with curative intent of nine esophageal cancer patients on a 1.5T MR-Linac with an adaptive workflow at our institute in 2019. In **Chapter 6**, the clinical implementation and feasibility of long-course fractionated MR-guided chemoradiotherapy for patients with esophageal cancer was reported. Our first experiences with MR-guided treatment of patients with esophageal cancer were associated with some technical and logistical complexities which are often unfamiliar to other treatment sites where online adaptive MR-guided workflows have been used. First, the online definition of the esophageal target volume involves recontouring of the GTV as well as a regeneration of the CTV which is more labor intensive and did require the onsite presence of a radiation oncologist. Second, the size of the target volume within the neoadjuvant treatment of esophageal cancers is large, which requires more extensive definitions of both the target volume and adjacent organs at risk, impacting the session time. Third, the total neoadjuvant treatment consisted of 23 fractions, which is at least uncommon if not unprecedented within the general framework of online adaptive MRgRT [60, 63, 130]. These elements made the online adaptive MR-guided workflow for esophageal cancer treatments not only more demanding for patients and staff, but also required extensive logistic planning. On top of that, the presented workflow resulted in longer treatment times; the average treatment time was 53 minutes of which a large part consisted of contour adaptation (20 minutes) to incorporate most changes of the daily anatomy in the dose plan. Comparison of the redefined target volumes of the first fractions with the final fractions revealed that the target volumes decreased over time, confirming our findings in Chapter 2. Some patients showed larger relative volume reductions than others. These pa-

tients would benefit the most from an adaptive treatment strategy, therefore identification of these patients should be investigated. For now, adaptive treatment is moderately feasible as two out of nine patients required treatment on a conventional linac for reasons of discomfort for more than 5% of fractions. On top of that, each treatment session requires the presence of specialized staff, which could negatively impact hospital logistics when the session time is extended. Therefore, a reduction of treatment time is desirable, to increase patient comfort and also ease the logistic planning surrounding the treatments. Nevertheless, it was shown that the adaptive treatment strategy resulted in a dose reduction to organs-at-risk compared to the conventional back-up plan. Further research is required to unlock the full potential of MR-guided radiotherapy for patients with esophageal cancer. Although daily plan adaptation removed the influence of interfraction motion, tumor motion throughout the treatment session could still be of concern. The medium intrafraction motion (drift) between the position verification MRI and post treatment MRI varied between patients. Further intrafraction motion analysis was performed in Chapter 7.

Intrafraction motion analysis

In the previous section, an adaptive MR-guided workflow was described and it was shown that some patients showed drift motion between MRI scans. In **Chapter 7** we analyzed intrafraction motion during dose delivery. Previous studies of intrafraction motion of esophageal tumors have mostly measured the motion of fiducial markers as a surrogate of intrafraction motion during treatment simulations [7,40]. Treatment of patients on the the MR-Linac allowed real-time imaging of the tumor during dose delivery. After analysis it was observed that two out of nine patients required a 5-mm margin in cranial-caudal direction to compensate for drifts and breathing motion, while a margin of $< 2\text{mm}$ sufficed for the remaining seven patients. These margins are significantly smaller than the margins applied in treatment of these patients as described in **Chapter 6**. However, the relatively small sample size of nine patients, with mostly distal tumors, could influence the results as distal tumors are more subject to large position variations. Furthermore, a larger sample size might have concluded that it could be possible to adjust treatment margins based on intrafraction motion patterns after the first week(s) of treatment, as the interfraction variability of intrafraction motion of individual patients appears to be low in this study. Secondly, the high-pass filter of 0.05 Hz was chosen to be low enough to contain all frequency components of the respiration motion, while allowing some variation in motion patterns. The breathing amplitude of patients who breathed at a very low rate could have been filtered out. This could have led to an underestimation of the respiratory amplitudes. We believe this would not have a large impact on our findings, as

we had long recordings of multiple fractions for each patient. Thirdly, the motion trajectories were determined from 2D cine-MR images, without adaptation of the GTV-mask. Deformations of the GTV-mask were not taken into account, which could have influenced the position of the center of mass. Furthermore, out-of-plane motion could have potentially resulted in inaccuracies in the determined motion patterns. Especially patients with a caudal tumor extension into the stomach might have been more vulnerable for out-of-plane motion. A solution could be to use deformable image registration to adapt the GTV contours to follow-up frames. However, this would have significantly increased the complexity and could have introduced an increase in sensitivity to registration errors, while the change in tumor shape was generally modest. Another possibility to capture out-of-plane motion could be to explore 3D cine imaging, which might decrease temporal resolution leading to an underestimation of the respiratory motion. We have shown that cine-MR images could be used to reconstruct the intrafraction motion. In general, the intrafraction motion was modest ($<5\text{mm}$), although a high inter-patient variability was observed. A potential next step would be to use the cine-MR images to reconstruct the delivered dose to assess the impact of intrafraction motion on the whole treatment [131].

Future perspectives

In this thesis, we have shown that an improved radiotherapy workflow is required to provide more accurate irradiations for patients with esophageal cancer. Improved visualization of the tumor combined with daily online replanning creates opportunities to improve the treatment of patients with esophageal cancer. MR guidance allows for a large reduction of treatment margins, which could lead to a significant decrease in dose to the organs-at-risk. Furthermore, we have described the workflow of online MR-guided adaptive radiotherapy for esophageal cancer. Optimization of the presented clinical workflow of adaptive MR-guided radiotherapy for patients with esophageal cancer is very much required in the near future. In the current state, the workflow is only moderately feasible as >45 minutes on-table time in 23 fractions is a challenge for patients in relatively poor condition. The lengthy process is not only a high burden for the patients, but also on hospital logistics. A few methods should be explored. First, technical improvements in automatic contouring should be used. Faster contour propagation between treatment sessions could be achieved by using better image registration methods. The propagated contours might already be used in the creation of an accurate treatment plan [132,133]. Another possibility would be the implementation of deep learning algorithms to provide automatic segmentation of heart, lungs,

other organs at risk and possibly the target contours [134,135]. Visual inspection of target delineations should reveal any remaining mis-adaptations. These are expected to be located around the gastroesophageal junction and into the stomach, as the tumor is most likely to be subject to displacements at these locations (as shown in Chapter 4). Another approach could be to investigate whether daily online adaptation of the full contour is required, or if contour adaptation of a few parts of the esophagus (i.e. those parts where displacements are clearly observed) could be sufficient to create an accurate treatment plan. On top of that, the used margin of 6mm is still generous, as suggested by our findings in Chapter 5. It can be argued that contouring errors are absorbed in this margin and that therefore a faster, potentially less precise than wished for, contouring procedure might lead to similar outcomes while the treatment burden will be reduced. Other parts of the workflow could also be optimized. Plan generation and plan evaluation currently take up 10% and 6% of total session time, respectively. Recent studies have investigated optimization of the planning algorithm by training convolutional neural networks which can accurately predict the dose distributions, these could be used to generate treatment plans but also assist in quality assurance [136–138]. Finally, training of radiation therapist to perform daily contour adaptation could be one of the possibilities to reduce the impact on hospital logistics and has proved to be accurate in other treatment sites [139,140].

On top of that, unlocking the full potential of MR guidance in esophageal cancer radiotherapy should be explored next to improvements in the current workflow. We have shown that an adaptive treatment plan with generous margins of 6mm provided sufficient target coverage. In Chapter 5 we have shown that treatment margins of 2mm were sufficient to cover motion in anterior-posterior and left-right directions, while a 5mm margin is required to compensate any breathing motion in the cranio-caudal plane. Gating and tracking strategies could potentially remove the impact of any intrafraction motion, often caused by breathing, for example by the addition of MLC-tracking during dose delivery [141,142]. This would allow a further decrease of treatment margins, especially in cranio-caudal direction. A recent study has shown that respiratory-gating already leads to a reduction of cardiac dose when using conventional margins [90]. However, these gating and tracking strategies will extend the treatment time, which is unwanted in the current workflow. Nevertheless, a patient assessment could be performed to investigate whether the benefits of very small margins and substantial organ-at-risk dose reduction outweigh the long treatment times. Finally, a minimum treatment margin of at least 2, and possibly 3 mm will still be required to compensate for any uncertainties in delineation, machine and other unexpected uncertainties [97,98,121]. Future developments should work towards a workflow with automatic delineations, without the in-room presence of a radiotherapist,

while using decreased margins of only 2 to 3 mm to bring this adaptive treatment to large cohorts. Using smaller treatment margins creates the opportunity to improve and reassess the standard treatment schedule. In the current CROSS schedule the total dose (of 41.4Gy) is spread out over multiple (23) fractions to reduce toxicity [32]. One can argue that with increased tumor visualization a more precise and possibly shorter treatment could achieve similar treatment outcomes or even improve local tumor control. This might be possible as MRgRT allows for optimal visualization and localization of the GTV, which could subsequently be targeted in (additional) treatment intensification protocols without the need of extensive treatment margins. If this can be done safely, hypofractionation becomes a possibility to improve efficiency of esophageal cancer treatments. Furthermore, real-time cine-MR imaging could be used to reconstruct the delivered dose and used as feedback in subsequent treatment fractions to optimize target coverage [143]. Similarly, additional functional imaging, such as DWI and DCE imaging, during a MRgRT treatment period could potentially predict the impact of the treatment (Figure 7.1) [87, 112, 144]. It could be decided that a treatment is prematurely abandoned, extended or intensified, based on this response guided adaptive treatment.

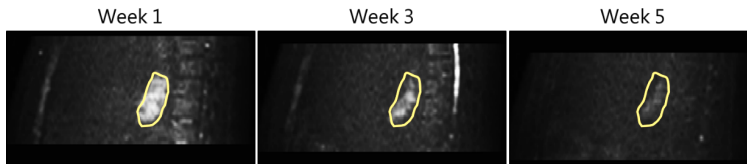


Figure 7.1: DWI imaging of the b500 signal within an esophageal tumor (yellow delineations) throughout the treatment period on the MR-Linac. The signal was clearly visible in week 1, reduced in week 3 and has almost disappeared in week 5 of MRgRT.

Therefore, MRgRT will allow for individualized treatments, as additional images could help decide on the next steps in each treatment, while reduced dose to organs-at-risk allows for treatment intensification strategies. However, it will be important to investigate which patients would benefit the most from these individualized treatments. Patients with squamous cell carcinoma are known to have better locoregional control and survival after chemoradiation compared to patients with adenocarcinoma that might lead to improved locoregional control [32, 145]. The benefits of additional treatment intensifications, after a normal treatment schedule has been completed, should be explored for these patients. Functional imaging could be used to delineate the residual tumor. On the contrary, if functional imaging during MRgRT indicates that tumors regression does not occur,

it could be decided to abandon the treatment and switch to other treatment options. Furthermore, analysis of interfraction and intrafraction tumor motion during MRgRT could be used to determine tailored margins.

We have seen improved tumor visualization when using MR-guided radiotherapy for esophageal cancer, allowing extensive analysis of the 3d mapping of the anatomy over time. Accurate target definitions allow for a treatment margin reduction, which potentially leads to a decrease in toxicity to heart, lungs and other organs at risk. This in turn opens up the possibility to improve the treatment protocols of esophageal cancer, possibly with the addition of treatment intensification to improve local tumor control. Following the results of this thesis, we hope to have contributed to the creation of improved treatment strategies with the aim of achieving the most optimal result for the patient.

References

- [1] GLOBOCAN Cancer Statistics 2020.
- [2] Shapiro, J., van Lanschot, J., Hulshof, M.C., et al. (2015). Neoadjuvant chemoradiotherapy plus surgery versus surgery alone for oesophageal or junctional cancer (CROSS): Long-term results of a randomised controlled trial. *The Lancet Oncology*, volume 16(9):1090–1098. ISSN 14745488.
- [3] Hulshoff, J.B., Faiz, Z., Karrenbeld, A., et al. (2015). Prognostic Value of the Circumferential Resection Margin in Esophageal Cancer Patients After Neoadjuvant Chemoradiotherapy. *Annals of Surgical Oncology*, volume 22(S3):1301–1309. ISSN 1068-9265.
- [4] Keall, P.J., Hsu, A., and Xing, L. Image-Guided Adaptive Radiotherapy.
- [5] Jin, P., van der Horst, A., de Jong, R., et al. (2015). Marker-based quantification of interfractional tumor position variation and the use of markers for setup verification in radiation therapy for esophageal cancer. *Radiotherapy and Oncology*, volume 117(3):412–418. ISSN 18790887.
- [6] Hoffmann, L., Poulsen, P.R., Ravkilde, T., et al. (2019). Setup strategies and uncertainties in esophageal radiotherapy based on detailed intra- and interfractional tumor motion mapping. *Radiotherapy and Oncology*, volume 136:161–168. ISSN 18790887.
- [7] Voncken, F.E., Nakhaee, S., Stam, B., et al. (2020). Quantification of Esophageal Tumor Motion and Investigation of Different Image-Guided Correction Strategies. *Practical Radiation Oncology*, volume 10(2):84–92. ISSN 18798500.
- [8] Gagliardi, G., Constine, L.S., Moiseenko, V., et al. (2010). Radiation Dose-Volume Effects in the Heart. *International Journal of Radiation Oncology Biology Physics*, volume 76(3 SUPPL.):77–85. ISSN 03603016.
- [9] Marks, L.B., Bentzen, S.M., Deasy, J.O., et al. (2010). Radiation Dose-Volume Effects in the Lung. *International Journal of Radiation Oncology*Biolog*Physics*, volume 76(3):S70–S76. ISSN 03603016.
- [10] Konski, A., Li, T., Christensen, M., et al. (2012). Symptomatic cardiac toxicity is predicted by dosimetric and patient factors rather than changes in 18F-FDG PET determination of myocardial activity after chemoradiotherapy for esophageal cancer. *Radiotherapy and Oncology*, volume 104(1):72–77. ISSN 01678140.
- [11] Thomas, M., Defraene, G., Lambrecht, M., et al. (2019). NTCP model for postoperative complications and one-year mortality after trimodality treatment in oesophageal cancer. *Radiotherapy and Oncology*, volume 141:33–40. ISSN 01678140.
- [12] Goense, L., van Rossum, P.S., Ruurda, J.P., et al. (2016). Radiation to the Gastric Fundus Increases the Risk of Anastomotic Leakage After Esophagectomy. *Annals of Thoracic Surgery*, volume 102(6):1798–1804. ISSN 15526259.
- [13] De Ruyscher, D., Niedermann, G., Burnet, N.G., et al. (2019). Radiotherapy toxicity. *Nature Reviews Disease Primers*, volume 5(1):13. ISSN 2056-676X.
- [14] Van Herk, M., Remeijer, P., Rasch, C., and Lebesque, J.V. (2000). The probability of correct target dosage: Dose-population histograms for deriving treatment margins in radiotherapy. *International Journal of Radiation Oncology Biology Physics*, volume 47(4):1121–1135. ISSN 03603016.

-
- [15] Van Herk, M. (2004). Errors and Margins in Radiotherapy. *Seminars in Radiation Oncology*, volume 14(1):52–64. ISSN 10534296.
- [16] Chen, Y.J., Han, C., Liu, A., et al. (2007). Setup Variations in Radiotherapy of Esophageal Cancer: Evaluation by Daily Megavoltage Computed Tomographic Localization. *International Journal of Radiation Oncology Biology Physics*, volume 68(5):1537–1545. ISSN 03603016.
- [17] Hawkins, M.A., Aitken, A., Hansen, V.N., McNair, H.A., and Tait, D.M. (2011). Set-up errors in radiotherapy for oesophageal cancers – Is electronic portal imaging or conebeam more accurate? *Radiotherapy and Oncology*, volume 98(2):249–254. ISSN 01678140.
- [18] van Nunen, A., van der Sangen, M., van Boxtel, M., and van Haaren, P. (2017). Cone-Beam CT-based position verification for oesophageal cancer: Evaluation of registration methods and anatomical changes during radiotherapy. *Technical Innovations & Patient Support in Radiation Oncology*, volume 3-4:30–36. ISSN 24056324.
- [19] Langen, K.M. and Jones, D.T.L. (2001). Organ motion and its management. *International Journal of Radiation Oncology Biology Physics*, volume 50(1):265–278. ISSN 03603016.
- [20] Jaffray, D.A., Siewerdsen, J.H., Wong, J.W., and Martinez, A.A. (2002). Flat-panel cone-beam computed tomography for image-guided radiation therapy. *International Journal of Radiation Oncology*Biolog*Physics*, volume 53(5):1337–1349. ISSN 03603016.
- [21] Lagendijk, J.J., Raaymakers, B.W., Raaijmakers, A.J.E., et al. (2008). MRI/linac integration. *Radiotherapy and Oncology*, volume 86(1):25–29. ISSN 01678140.
- [22] Lagendijk, J.J., Raaymakers, B.W., den Berg, C.A.T.V., et al. (2014). MR guidance in radiotherapy. *Physics in Medicine and Biology*, volume 59(21):R349. ISSN 0031-9155.
- [23] Lagendijk, J.J., Raaymakers, B.W., and van Vulpen, M. (2014). The Magnetic Resonance Imaging-Linac System. *Seminars in Radiation Oncology*, volume 24(3):207–209. ISSN 15329461.
- [24] Mutic, S. and Dempsey, J.F. (2014). The ViewRay System: Magnetic Resonance-Guided and Controlled Radiotherapy. *Seminars in Radiation Oncology*, volume 24(3):196–199. ISSN 15329461.
- [25] Johnson-Hart, C.N., Price, G.J., Faivre-Finn, C., Aznar, M.C., and van Herk, M. (2018). Residual Setup Errors Towards the Heart After Image Guidance Linked With Poorer Survival in Lung Cancer Patients: Do We Need Stricter IGRT Protocols? *International Journal of Radiation Oncology Biology Physics*, volume 102(2):434–442. ISSN 1879355X.
- [26] Yan, D., Vicini, F., Wong, J., and Martinez, A. (1997). Adaptive radiation therapy. *Physics in Medicine and Biology*, volume 42(1):123–132. ISSN 0031-9155.
- [27] Sonke, J.J., Aznar, M., and Rasch, C. (2019). Adaptive Radiotherapy for Anatomical Changes. *Seminars in Radiation Oncology*, volume 29(3):245–257. ISSN 10534296.
- [28] Ramella, S., Fiore, M., Silipigni, S., et al. (2017). Local Control and Toxicity of Adaptive Radiotherapy Using Weekly CT Imaging: Results from the LARTIA Trial in Stage III NSCLC. *Journal of Thoracic Oncology*, volume 12(7):1122–1130. ISSN 15560864.
- [29] Huang, H., Lu, H., Feng, G., et al. (2015). Determining appropriate timing of adaptive radiation therapy for nasopharyngeal carcinoma during intensity-modulated radiation therapy. *Radiation Oncology*, volume 10(1):192. ISSN 1748-717X.

- [30] Wang, J.Z., Li, J.B., Wang, W., et al. (2013). Detection of interfraction displacement and volume variance during radiotherapy of primary thoracic esophageal cancer based on repeated four-dimensional CT scans. *Radiation Oncology*, volume 8(1):1. ISSN 1748717X.
- [31] Wang, J.Z., Li, J.B., Wang, W., et al. (2015). Changes in tumour volume and motion during radiotherapy for thoracic oesophageal cancer. *Radiotherapy and Oncology*, volume 114(2):201–205. ISSN 18790887.
- [32] van Hagen, P., Hulshof, M.C., van Lanschot, J., et al. (2012). Preoperative Chemoradiotherapy for Esophageal or Junctional Cancer. *New England Journal of Medicine*, volume 366(22):2074–2084. ISSN 0028-4793.
- [33] Bol, G.H., Kotte, A.N.T.J., van der Heide, U.A., and Lagendijk, J.J. (2009). Simultaneous multi-modality ROI delineation in clinical practice. *Computer Methods and Programs in Biomedicine*, volume 96(2):133–140. ISSN 01692607.
- [34] R Core Team (2020). *R: A Language and Environment for Statistical Computing*. R Foundation for Statistical Computing, Vienna, Austria.
- [35] Rice, T.W., Blackstone, E.H., and Rusch, V.W. (2010). 7th Edition of the AJCC Cancer Staging Manual: Esophagus and Esophagogastric Junction. *Annals of Surgical Oncology*, volume 17(7):1721–1724. ISSN 1068-9265.
- [36] Beukema, J.C., Van Luijk, P., Widder, J., Langendijk, J.A., and Muijs, C.T. (2015). Is cardiac toxicity a relevant issue in the radiation treatment of esophageal cancer? *Radiotherapy and Oncology*, volume 114(1):80–85. ISSN 18790887.
- [37] Vollenbrock, S.E., Nowee, M.E., Voncken, F.E., et al. (2019). Gross Tumor Delineation in Esophageal Cancer on MRI Compared With 18F-FDG-PET/CT. *Advances in Radiation Oncology*, pp. 1–9. ISSN 24521094.
- [38] Ferlay, J., Steliarova-Foucher, E., Lortet-Tieulent, J., et al. (2013). Cancer incidence and mortality patterns in Europe: Estimates for 40 countries in 2012. *European Journal of Cancer*, volume 49(6):1374–1403. ISSN 09598049.
- [39] Gwynne, S., Hurt, C., Evans, M., et al. (2011). Definitive Chemoradiation for Oesophageal Cancer - a Standard of Care in Patients with Non-metastatic Oesophageal Cancer. *Clinical Oncology*, volume 23(3):182–188. ISSN 09366555.
- [40] Yamashita, H., Haga, A., Hayakawa, Y., et al. (2010). Patient setup error and day-to-day esophageal motion error analyzed by cone-beam computed tomography in radiation therapy. *Acta Oncologica*, volume 49(4):485–490. ISSN 0284186X.
- [41] Hawkins, M.A., Brooks, C., Hansen, V.N., Aitken, A., and Tait, D.M. (2010). Cone Beam Computed Tomography-Derived Adaptive Radiotherapy for Radical Treatment of Esophageal Cancer. *International Journal of Radiation Oncology Biology Physics*, volume 77(2):378–383. ISSN 03603016.
- [42] Fukada, J., Hanada, T., Kawaguchi, O., et al. (2013). Detection of esophageal fiducial marker displacement during radiation therapy with a 2-dimensional on-board imager: Analysis of internal margin for esophageal cancer. *International Journal of Radiation Oncology Biology Physics*, volume 85(4):991–998. ISSN 03603016.
- [43] Machiels, M., Van Hooft, J., Jin, P., et al. (2015). Endoscopy/EUS-guided fiducial marker placement in patients with esophageal cancer: A comparative analysis of 3 types of markers. *Gastrointestinal Endoscopy*, volume 82(4):641–649. ISSN 10976779.

-
- [44] Cohen, R.J., Paskalev, K., Litwin, S., et al. (2010). Original article: Esophageal motion during radiotherapy: quantification and margin implications. *Diseases of the Esophagus*, volume 23(6):473–479. ISSN 11208694.
- [45] Cardenas, M.L., Mazur, T.R., Tsien, C.I., and Green, O.L. (2018). A rapid, computational approach for assessing interfraction esophageal motion for use in stereotactic body radiation therapy planning. *Advances in Radiation Oncology*, volume 3(2):209–215. ISSN 24521094.
- [46] Machiels, M., Jin, P., van Gurp, C.H., et al. (2018). Comparison of carina-based versus bony anatomy-based registration for setup verification in esophageal cancer radiotherapy. *Radiation Oncology*, volume 13(1):1–9. ISSN 1748717X.
- [47] Boekhoff, M.R., Defize, I.L., Borggreve, A.S., et al. (2020). 3-Dimensional target coverage assessment for MRI guided esophageal cancer radiotherapy. *Radiotherapy and Oncology*, volume 147:1–7. ISSN 18790887.
- [48] Klein, S., Staring, M., Murphy, K., Viergever, M., and Pluim, J. (2010). elastix: A Toolbox for Intensity-Based Medical Image Registration. *IEEE Transactions on Medical Imaging*, volume 29(1):196–205. ISSN 0278-0062.
- [49] Heethuis, S.E., Borggreve, A.S., Goense, L., et al. (2018). Quantification of variations in intra-fraction motion of esophageal tumors over the course of neoadjuvant chemoradiotherapy based on cine-MRI. *Physics in Medicine and Biology*, volume 63(14). ISSN 13616560.
- [50] Nyeng, T.B., Nordmark, M., and Hoffmann, L. (2015). Dosimetric evaluation of anatomical changes during treatment to identify criteria for adaptive radiotherapy in oesophageal cancer patients. *Acta Oncologica*, volume 54(9):1467–1473. ISSN 1651226X.
- [51] Kontaxis, C., Bol, G.H., Kerkmeijer, L.G., Lagendijk, J.J., and Raaymakers, B.W. (2017). Fast online replanning for interfraction rotation correction in prostate radiotherapy. *Medical Physics*, volume 44(10):5034–5042. ISSN 00942405.
- [52] Corradini, S., Alongi, F., Andratschke, N., et al. (2019). MR-guidance in clinical reality: Current treatment challenges and future perspectives. *Radiation Oncology*, volume 14(1):1–12. ISSN 1748717X.
- [53] Dieleman, E.M.T., Senan, S., Vincent, A., et al. (2007). Four-dimensional computed tomographic analysis of esophageal mobility during normal respiration. *International Journal of Radiation Oncology Biology Physics*, volume 67(3):775–780. ISSN 03603016.
- [54] Keall, P.J., Barton, M., and Crozier, S. (2014). The Australian Magnetic Resonance Imaging-Linac Program. *Seminars in Radiation Oncology*, volume 24(3):203–206. ISSN 15329461.
- [55] Fallone, B.G. (2014). The Rotating Biplanar Linac-Magnetic Resonance Imaging System. *Seminars in Radiation Oncology*, volume 24(3):200–202. ISSN 15329461.
- [56] Winkel, D., Bol, G.H., Kroon, P.S., et al. (2019). Adaptive radiotherapy: The Elekta Unity MR-linac concept. *Clinical and Translational Radiation Oncology*, volume 18(xxxx):54–59. ISSN 24056308.
- [57] Bertelsen, A.S., Schytte, T., Møller, P.K., et al. (2019). First clinical experiences with a high field 1.5 T MR linac. *Acta Oncologica*, volume 0(0):1–6. ISSN 0284-186X.

- [58] Bol, G.H., Lagendijk, J.J.W., and Raaymakers, B.W. (2013). Virtual couch shift (VCS): Accounting for patient translation and rotation by online IMRT re-optimization. *Physics in Medicine and Biology*, volume 58(9):2989–3000. ISSN 00319155.
- [59] Hunt, A., Hansen, V.N., Oelfke, U., Nill, S., and Hafeez, S. (2018). Adaptive Radiotherapy Enabled by MRI Guidance. *Clinical Oncology*, volume 30(11):711–719. ISSN 14332981.
- [60] Werensteijn-Honingh, A.M., Kroon, P.S., Winkel, D., et al. (2019). Feasibility of stereotactic radiotherapy using a 1.5 T MR-linac: Multi-fraction treatment of pelvic lymph node oligometastases. *Radiotherapy and Oncology*, volume 134:50–54. ISSN 18790887.
- [61] Bohoudi, O., Bruynzeel, A.M., Senan, S., et al. (2017). Fast and robust online adaptive planning in stereotactic MR-guided adaptive radiation therapy (SMART) for pancreatic cancer. *Radiotherapy and Oncology*, volume 125(3):439–444. ISSN 18790887.
- [62] Acharya, S., Fischer-Valuck, B.W., Kashani, R., et al. (2016). Online Magnetic Resonance Image Guided Adaptive Radiation Therapy: First Clinical Applications. *International Journal of Radiation Oncology Biology Physics*, volume 94(2):394–403. ISSN 1879355X.
- [63] Henke, L.E., Olsen, J.R., Contreras, J.A., et al. (2019). Stereotactic MR-Guided Online Adaptive Radiation Therapy (SMART) for Ultracentral Thorax Malignancies: Results of a Phase 1 Trial. *Advances in Radiation Oncology*, volume 4(1):201–209. ISSN 24521094.
- [64] Wu, A.J., Bosch, W.R., Chang, D.T., et al. (2015). Expert Consensus Contouring Guidelines for Intensity Modulated Radiation Therapy in Esophageal and Gastroesophageal Junction Cancer. *International Journal of Radiation Oncology, Biology, Physics*, volume 92(4):911–920. ISSN 0360-3016.
- [65] Bol, G.H., Kotte, A.N., and Lagendijk, J.J. (2003). Volumetool: an image evaluation, registration, and delineation system for radiotherapy. *Phys Med*, volume 19(80).
- [66] Finazzi, T., Palacios, M.A., Spoelstra, F.O., et al. (2019). Role of On-Table Plan Adaptation in MR-Guided Ablative Radiation Therapy for Central Lung Tumors. *International Journal of Radiation Oncology Biology Physics*, volume 104(4):933–941. ISSN 1879355X.
- [67] Rudra, S., Jiang, N., Rosenberg, S.A., et al. (2019). Using adaptive magnetic resonance image-guided radiation therapy for treatment of inoperable pancreatic cancer. *Cancer Medicine*, volume 8(5):2123–2132. ISSN 20457634.
- [68] Doi, Y., Murakami, Y., Imano, N., et al. (2018). Quantifying esophageal motion during free-breathing and breath-hold using fiducial markers in patients with early-stage esophageal cancer. *PLoS ONE*, volume 13(6):1–12. ISSN 19326203.
- [69] Liu, F., Ng, S., Huguet, F., et al. (2016). Are fiducial markers useful surrogates when using respiratory gating to reduce motion of gastroesophageal junction tumors? *Acta Oncologica*, volume 55(8):1040–1046. ISSN 0284-186X.
- [70] Yamashita, H., Kida, S., Sakumi, A., et al. (2011). Four-Dimensional Measurement of the Displacement of Internal Fiducial Markers During 320-Multislice Computed Tomography Scanning of Thoracic Esophageal Cancer. *Int. J. Radiation Oncology Biol. Phys.*, volume 79(2):588–595.
- [71] Lever, F.M., Lips, I.M., Crijns, S.P.M., et al. (2013). Quantification of Esophageal Tumor Motion on Cine-Magnetic Resonance Imaging. *International journal of radiation oncology, biology, physics*. ISSN 1879-355X.

-
- [72] Jin, P., Hulshof, M.C., Jong, R.D., Hooft, J.E.V., and Bel, A. (2016). Quantification of respiration-induced esophageal tumor motion using fiducial markers and four-dimensional computed tomography. *Radiotherapy and Oncology*, volume 118(3):492–497. ISSN 0167-8140.
- [73] Heerkens, H.D., van Vulpen, M., Erickson, B., et al. (2018). MRI guided stereotactic radiotherapy for locally advanced pancreatic cancer. *The British Journal of Radiology*, volume 91(1091):20170563. ISSN 0007-1285.
- [74] Wolthaus, J.W., Sonke, J.J., van Herk, M., et al. (2008). Comparison of Different Strategies to Use Four-Dimensional Computed Tomography in Treatment Planning for Lung Cancer Patients. *International Journal of Radiation Oncology Biology Physics*, volume 70(4):1229–1238. ISSN 03603016.
- [75] Machiels, M., Jin, P., van Hooft, J.E., et al. (2019). Reduced inter-observer and intra-observer delineation variation in esophageal cancer radiotherapy by use of fiducial markers. *Acta Oncologica*, volume 58(6):943–950. ISSN 1651226X.
- [76] Jin, P., Hulshof, M.C., van Wieringen, N., Bel, A., and Alderliesten, T. (2017). Interfractional variability of respiration-induced esophageal tumor motion quantified using fiducial markers and four-dimensional cone-beam computed tomography. *Radiotherapy and Oncology*, volume 124(1):147–154. ISSN 18790887.
- [77] Roos, C.T., Faiz, Z., Visser, S., et al. (2021). A comprehensive motion analysis—consequences for high precision image-guided radiotherapy of esophageal cancer patients. *Acta Oncologica*, volume 60(3):277–284. ISSN 1651226X.
- [78] Boekhoff, M., Defize, I., Borggreve, A., et al. (2021). CTV-to-PTV margin assessment for esophageal cancer radiotherapy based on an accumulated dose analysis. *Radiotherapy and Oncology*, volume 161:16–22. ISSN 01678140.
- [79] Gao, H., Kelsey, C.R., Boyle, J., et al. (2019). Impact of Esophageal Motion on Dosimetry and Toxicity With Thoracic Radiation Therapy. *Technology in cancer research & treatment*, volume 18:1–10. ISSN 15330338.
- [80] Welsh, J., Settle, S.H., Amini, A., et al. (2012). Failure patterns in patients with esophageal cancer treated with definitive chemoradiation. *Cancer*, volume 118(10):2632–2640. ISSN 0008543X.
- [81] Versteijne, E., van Laarhoven, H.W., van Hooft, J.E., et al. (2015). Definitive chemoradiation for patients with inoperable and/or unresectable esophageal cancer: locoregional recurrence pattern. *Diseases of the Esophagus*, volume 28(5):453–459. ISSN 14422050.
- [82] Minsky, D., Pajak, T., Ginsberg, R., and al, E. (2014). III Trial of Combined-Modality Therapy for Esophageal Therapy. *J Clin Oncol*, volume 20(5):1167–1174.
- [83] Hulshof, M.C., Geijsen, D., Rozema, T., et al. (2020). A randomized controlled phase III multicenter study on dose escalation in definitive chemoradiation for patients with locally advanced esophageal cancer: ARTDECO study. *Journal of Clinical Oncology*, volume 38(4_suppl):281–281. ISSN 0732-183X.
- [84] Hu, Y., Byrne, M., Archibald-Heeren, B., et al. (2020). Validation of the preconfigured Varian Ethos Acuros XB Beam Model for treatment planning dose calculations: A dosimetric study. *Journal of Applied Clinical Medical Physics*, volume 21(12):27–42. ISSN 15269914.

- [85] Sibolt, P., Andersson, L.M., Calmels, L., et al. (2021). Clinical implementation of artificial intelligence-driven cone-beam computed tomography-guided online adaptive radiotherapy in the pelvic region. *Physics and Imaging in Radiation Oncology*, volume 17(December 2020):1–7. ISSN 24056316.
- [86] Van Sörnsen De Koste, J.R., Dahele, M., Mostafavi, H., et al. (2015). Markerless tracking of small lung tumors for stereotactic radiotherapy. *Medical Physics*, volume 42(4):1640–1652. ISSN 00942405.
- [87] Borggreve, A.S., Heethuis, S.E., Boekhoff, M.R., et al. (2020). Optimal timing for prediction of pathologic complete response to neoadjuvant chemoradiotherapy with diffusion-weighted MRI in patients with esophageal cancer. *European Radiology*, volume 30(4):1896–1907. ISSN 14321084.
- [88] Zachiu, C., Denis De Senneville, B., Moonen, C., and Ries, M. (2015). A framework for the correction of slow physiological drifts during MR-guided HIFU therapies: Proof of concept. *Medical Physics*, volume 42(7):4137–4148. ISSN 00942405.
- [89] Zachiu, C., Papadakis, N., Ries, M., Moonen, C., and Denis De Senneville, B. (2015). An improved optical flow tracking technique for real-time MR-guided beam therapies in moving organs. *Physics in Medicine and Biology*, volume 60(23):9003–9029. ISSN 13616560.
- [90] Lee, S.L., Mahler, P., Olson, S., et al. (2021). Reduction of cardiac dose using respiratory-gated MR-linac plans for gastro-esophageal junction cancer. *Medical Dosimetry*, volume 46(2):152–156. ISSN 09583947.
- [91] van Rossum, P.S., Deng, W., Routman, D.M., et al. (2020). Prediction of Severe Lymphopenia During Chemoradiation Therapy for Esophageal Cancer: Development and Validation of a Pretreatment Nomogram. *Practical Radiation Oncology*, volume 10(1):e16–e26. ISSN 18798500.
- [92] Pao, T.H., Chang, W.L., Chiang, N.J., et al. (2020). Cardiac radiation dose predicts survival in esophageal squamous cell carcinoma treated by definitive concurrent chemotherapy and intensity modulated radiotherapy. *Radiation Oncology*, volume 15(1):1–10. ISSN 1748717X.
- [93] Wang, J., Wei, C., Tucker, S.L., et al. (2013). Predictors of postoperative complications after trimodality therapy for esophageal cancer. *International Journal of Radiation Oncology Biology Physics*, volume 86(5):885–891. ISSN 03603016.
- [94] Cella, L., Palma, G., Deasy, J.O., et al. (2014). Complication probability models for radiation-induced heart valvular dysfunction: Do heart-lung interactions play a role? *PLoS ONE*, volume 9(10):1–11. ISSN 19326203.
- [95] Nicholas, O., Bowden, C., Selby, A., et al. (2020). Comparative Dosimetric Analysis and Normal Tissue Complication Probability Modelling of Four-Dimensional Computed Tomography Planning Scans Within the UK NeoSCOPE Trial. *Clinical Oncology*, volume 32(12):828–834. ISSN 14332981.
- [96] Münch, S., Oechsner, M., Combs, S., and Habermehl, D. (2017). DVH- and NTCP-based dosimetric comparison of different longitudinal margins for VMAT-IMRT of esophageal cancer. *Radiation Oncology*, volume 12(1):128. ISSN 1748-717X.

-
- [97] Tijssen, R.H., Philippens, M.E., Paulson, E.S., et al. (2019). MRI commissioning of 1.5T MR-linac systems – a multi-institutional study. *Radiotherapy and Oncology*, volume 132:114–120. ISSN 18790887.
- [98] Raaymakers, B.W., Jürgenliemk-Schulz, I.M., Bol, G.H., et al. (2017). First patients treated with a 1.5 T MRI-Linac: Clinical proof of concept of a high-precision, high-field MRI guided radiotherapy treatment. *Physics in Medicine and Biology*, volume 62(23):L41–L50. ISSN 13616560.
- [99] Raaijmakers, A.J.E., Hårdemark, B., Raaymakers, B.W., Raaijmakers, C.P.J., and Lagendijk, J.J.W. (2007). Dose optimization for the MRI-accelerator: IMRT in the presence of a magnetic field. *Physics in Medicine and Biology*, volume 52(23):7045–7054. ISSN 0031-9155.
- [100] Yang, Y.M., Geurts, M., Smilowitz, J.B., Sterpin, E., and Bednarz, B.P. (2015). Monte Carlo simulations of patient dose perturbations in rotational-type radiotherapy due to a transverse magnetic field: A tomotherapy investigation. *Medical Physics*, volume 42(2):715–725. ISSN 00942405.
- [101] Nachbar, M., Mönnich, D., Kalwa, P., et al. (2019). Comparison of treatment plans for a high-field MRI-linac and a conventional linac for esophageal cancer. *Strahlentherapie und Onkologie*, volume 195(4):327–334. ISSN 1439099X.
- [102] Finazzi, T., Palacios, M.A., Haasbeek, C.J., et al. (2020). Stereotactic MR-guided adaptive radiation therapy for peripheral lung tumors. *Radiotherapy and Oncology*, volume 144:46–52. ISSN 18790887.
- [103] Boekhoff, M., Defize, I., Borggreve, A., et al. (2021). An in-silico assessment of the dosimetric benefits of MR-guided radiotherapy for esophageal cancer patients. *Radiotherapy and Oncology*, volume 162:76–84. ISSN 0167-8140.
- [104] Winkel, D., Bol, G.H., Werensteijn-Honingh, A.M., et al. (2020). Target coverage and dose criteria based evaluation of the first clinical 1.5T MR-linac SBRT treatments of lymph node oligometastases compared with conventional CBCT-linac treatment. *Radiotherapy and Oncology*, volume 146:118–125. ISSN 18790887.
- [105] van Rossum, P.S., van Lier, A.L., van Vulpen, M., et al. (2015). Diffusion-weighted magnetic resonance imaging for the prediction of pathologic response to neoadjuvant chemoradiotherapy in esophageal cancer. *Radiotherapy and Oncology*, volume 115(2):163–170. ISSN 01678140.
- [106] Fang, P., Musall, B.C., Son, J.B., et al. (2018). Multimodal Imaging of Pathologic Response to Chemoradiation in Esophageal Cancer. *International Journal of Radiation Oncology*Biography*Physics*, volume 102(4):996–1001. ISSN 03603016.
- [107] Verkooijen, H.M., Kerkmeijer, L.G.W., Fuller, C.D., et al. (2017). R-IDEAL: A Framework for Systematic Clinical Evaluation of Technical Innovations in Radiation Oncology. *Frontiers in Oncology*, volume 7. ISSN 2234-943X.
- [108] de Mol van Otterloo, S.R., Christodouleas, J.P., Blezer, E.L., et al. (2020). The MOMENTUM Study: An International Registry for the Evidence-Based Introduction of MR-Guided Adaptive Therapy. *Frontiers in Oncology*, volume 10(September). ISSN 2234943X.
- [109] Stemkens, B., Paulson, E.S., and Tijssen, R.H.N. (2018). Nuts and bolts of 4D-MRI for radiotherapy. *Physics in Medicine & Biology*, volume 63(21):21TR01. ISSN 1361-6560.

- [110] Hackett, S., van Asselen, B., Feist, G., et al. (2016). SU-F-J-148: A Collapsed Cone Algorithm Can Be Used for Quality Assurance for Monaco Treatment Plans for the MR-Linac. *Medical Physics*, volume 43(6Part11):3441–3441. ISSN 00942405.
- [111] Defize, I.L., Boekhoff, M.R., Borggreve, A.S., et al. (2020). Tumor volume regression during neoadjuvant chemoradiotherapy for esophageal cancer: a prospective study with weekly MRI. *Acta Oncologica*, volume 59(7):753–759. ISSN 1651226X.
- [112] Heethuis, S.E., Goense, L., van Rossum, P.S.N., et al. (2018). DW-MRI and DCE-MRI are of complementary value in predicting pathologic response to neoadjuvant chemoradiotherapy for esophageal cancer. *Acta Oncologica*, volume 0(0):1–8. ISSN 0284-186X.
- [113] Boekhoff, M., Bouwmans, R., Doornaert, P., et al. (2022). Clinical implementation and feasibility of long-course fractionated MR-guided chemoradiotherapy for patients with esophageal cancer: An R-IDEAL stage 1b/2a evaluation of technical innovation. *Clinical and Translational Radiation Oncology*, volume 34:82–89. ISSN 24056308.
- [114] Denis de Senneville, B., Zachiu, C., Ries, M., and Moonen, C. (2016). EVolution: an edge-based variational method for non-rigid multi-modal image registration. *Physics in Medicine and Biology*, volume 61(20):7377–7396. ISSN 0031-9155.
- [115] Alam, S., Thor, M., Rimner, A., et al. (2020). Quantification of accumulated dose and associated anatomical changes of esophagus using weekly Magnetic Resonance Imaging acquired during radiotherapy of locally advanced lung cancer. *Physics and Imaging in Radiation Oncology*, volume 13:36–43. ISSN 24056316.
- [116] Delombaerde, L., Petillion, S., Weltens, C., and Depuydt, T. (2021). Intra-fraction motion monitoring during fast modulated radiotherapy delivery in a closed-bore gantry linac. *Physics and Imaging in Radiation Oncology*, volume 20:51–55. ISSN 24056316.
- [117] Kontaxis, C., Bol, G.H., Stemkens, B., et al. (2017). Towards fast online intrafraction replanning for free-breathing stereotactic body radiation therapy with the MR-linac. *Physics in Medicine & Biology*, volume 62(18):7233–7248. ISSN 1361-6560.
- [118] Xu, C., Guo, L., Liao, Z., et al. (2019). Heart and lung doses are independent predictors of overall survival in esophageal cancer after chemoradiotherapy. *Clinical and Translational Radiation Oncology*, volume 17:17–23. ISSN 24056308.
- [119] Bohoudi, O., Bruynzeel, A.M., Meijerink, M.R., et al. (2019). Identification of patients with locally advanced pancreatic cancer benefitting from plan adaptation in MR-guided radiation therapy. *Radiotherapy and Oncology*, volume 132:16–22. ISSN 18790887.
- [120] Lee, S.L., Bassetti, M., Meijer, G.J., and Mook, S. (2021). Review of MR-Guided Radiotherapy for Esophageal Cancer. *Frontiers in Oncology*, volume 11(March):1–8. ISSN 2234943X.
- [121] Winkel, D., Werensteijn-Honingh, A.M., Kroon, P.S., et al. (2019). Individual lymph nodes: “See it and Zap it”. *Clinical and Translational Radiation Oncology*, volume 18:46–53. ISSN 24056308.
- [122] Liu, C., Bhangoo, R.S., Sio, T.T., et al. (2019). Dosimetric comparison of distal esophageal carcinoma plans for patients treated with small-spot intensity-modulated proton versus volumetric-modulated arc therapies. *Journal of Applied Clinical Medical Physics*, volume 20(7):15–27. ISSN 1526-9914.

-
- [123] Wang, X., Hobbs, B., Gandhi, S.J., et al. (2021). Current status and application of proton therapy for esophageal cancer. *Radiotherapy and Oncology*, volume 164:27–36. ISSN 01678140.
- [124] Hoffmann, L., Mortensen, H., Shamshad, M., et al. (2022). Treatment planning comparison in the PROTECT-trial randomising proton versus photon beam therapy in oesophageal cancer: Results from eight European centres. *Radiotherapy and Oncology*, volume 172:32–41. ISSN 01678140.
- [125] Paganetti, H., Beltran, C., Both, S., et al. (2021). Roadmap: proton therapy physics and biology. *Physics in Medicine & Biology*, volume 66(5):05RM01. ISSN 0031-9155.
- [126] Shamshad, M., Møller, D.S., Mortensen, H.R., et al. (2022). Bone versus soft-tissue setup in proton therapy for patients with oesophageal cancer. *Acta Oncologica*, volume 61(8):994–1003. ISSN 0284-186X.
- [127] Pham, T.T., Whelan, B., Oborn, B.M., et al. (2022). Magnetic resonance imaging (MRI) guided proton therapy: A review of the clinical challenges, potential benefits and pathway to implementation. *Radiotherapy and Oncology*, volume 170:37–47. ISSN 01678140.
- [128] Langendijk, J.A., Boersma, L.J., Rasch, C.R., et al. (2018). Clinical Trial Strategies to Compare Protons With Photons. *Seminars in Radiation Oncology*, volume 28(2):79–87. ISSN 10534296.
- [129] Fischer-Valuck, B.W., Henke, L., Green, O., et al. (2017). Two-and-a-half-year clinical experience with the world’s first magnetic resonance image guided radiation therapy system. *Advances in Radiation Oncology*, volume 2(3):485–493. ISSN 24521094.
- [130] Intven, M.P.W., Otterloo, S.R.D.M.V., Mook, S., et al. (2021). Online adaptive MR-guided radiotherapy for rectal cancer ; feasibility of the workflow on a 1 . 5T MR-linac : clinical implementation and initial experience. *Radiotherapy and Oncology*, volume 154:172–178. ISSN 0167-8140.
- [131] Kontaxis, C., de Muinck Keizer, D.M., Kerkmeijer, L.G., et al. (2020). Delivered dose quantification in prostate radiotherapy using online 3D cine imaging and treatment log files on a combined 1.5T magnetic resonance imaging and linear accelerator system. *Physics and Imaging in Radiation Oncology*, volume 15:23–29. ISSN 24056316.
- [132] Christiansen, R.L., Johansen, J., Zukauskaitė, R., et al. (2021). Accuracy of automatic structure propagation for daily magnetic resonance image-guided head and neck radiotherapy. *Acta Oncologica*, volume 60(5):589–597. ISSN 0284-186X.
- [133] Sritharan, K., Dunlop, A., Mohajer, J., et al. (2022). Dosimetric comparison of automatically propagated prostate contours with manually drawn contours in MRI-guided radiotherapy: A step towards a contouring free workflow? *Clinical and Translational Radiation Oncology*, volume 37:25–32. ISSN 24056308.
- [134] Eppenhof, K., Maspero, M., Savenije, M., et al. (2020). Fast contour propagation for MR-guided prostate radiotherapy using convolutional neural networks. *Medical Physics*, volume 47(3):1238–1248. ISSN 0094-2405.
- [135] Fransson, S., Tilly, D., and Strand, R. (2022). Patient specific deep learning based segmentation for magnetic resonance guided prostate radiotherapy. *Physics and Imaging in Radiation Oncology*, volume 23:38–42. ISSN 24056316.

- [136] Freedman, J.N., Gurney-Champion, O.J., Nill, S., et al. (2021). Rapid 4D-MRI reconstruction using a deep radial convolutional neural network: Dracula. *Radiotherapy and Oncology*, volume 159:209–217. ISSN 01678140.
- [137] Guerreiro, F., Seravalli, E., Janssens, G., et al. (2021). Deep learning prediction of proton and photon dose distributions for paediatric abdominal tumours. *Radiotherapy and Oncology*, volume 156:36–42. ISSN 01678140.
- [138] Tsekas, G., Bol, G.H., Raaymakers, B.W., and Kontaxis, C. (2021). DeepDose: a robust deep learning-based dose engine for abdominal tumours in a 1.5 T MRI radiotherapy system. *Physics in Medicine & Biology*, volume 66(6):065017. ISSN 0031-9155.
- [139] Willigenburg, T., de Muinck Keizer, D.M., Peters, M., et al. (2021). Evaluation of daily online contour adaptation by radiation therapists for prostate cancer treatment on an MRI-guided linear accelerator. *Clinical and Translational Radiation Oncology*, volume 27:50–56. ISSN 24056308.
- [140] Rasing, M.J., Sikkens, G.G., Vissers, N.G., et al. (2022). Online adaptive MR-guided radiotherapy: Conformity of contour adaptation for prostate cancer, rectal cancer and lymph node oligometastases among radiation therapists and radiation oncologists. *Technical Innovations & Patient Support in Radiation Oncology*, volume 23:33–40. ISSN 24056324.
- [141] Keiper, T.D., Tai, A., Chen, X., et al. (2020). Feasibility of real-time motion tracking using cine MRI during MR-guided radiation therapy for abdominal targets. *Medical Physics*, volume 47(8):3554–3566. ISSN 0094-2405.
- [142] Uijtewaal, P., Borman, P.T., Woodhead, P.L., et al. (2022). First experimental demonstration of VMAT combined with MLC tracking for single and multi fraction lung SBRT on an MR-linac. *Radiotherapy and Oncology*, volume 174:149–157. ISSN 01678140.
- [143] McDonald, B.A., Zachiu, C., Christodouleas, J., et al. (2023). Dose accumulation for MR-guided adaptive radiotherapy: From practical considerations to state-of-the-art clinical implementation. *Frontiers in Oncology*, volume 12. ISSN 2234-943X.
- [144] Borggreve, A.S., Goense, L., van Rossum, P.S., et al. (2020). Preoperative Prediction of Pathologic Response to Neoadjuvant Chemoradiotherapy in Patients With Esophageal Cancer Using 18F-FDG PET/CT and DW-MRI: A Prospective Multicenter Study. *International Journal of Radiation Oncology*Biography*Physics*, volume 106(5):998–1009. ISSN 03603016.
- [145] Hulshof, M.C.C.M., Geijssen, E.D., Rozema, T., et al. (2021). Randomized Study on Dose Escalation in Definitive Chemoradiation for Patients With Locally Advanced Esophageal Cancer (ARTDECO Study). *Journal of Clinical Oncology*, volume 39(25):2816–2824. ISSN 0732-183X.

Appendices

Summary in Dutch (Nederlandse Samenvatting)

Slokdarmkanker is een ziekte met een doorgaans slechte overlevingskans. In Nederland is de standaardbehandeling voor patiënten met slokdarmkanker zonder metastasen neoadjuvante chemoradiotherapie (nCRT) volgens het CROSS schema, gevolgd door een slokdarmresectie. Het primaire doel van chemoradiotherapie is het verkleinen van de primaire tumor, zodat de kans op een radicale resectie toeneemt. In deze thesis stond onderzoek naar de radiotherapiebehandeling van patiënten met slokdarmkanker centraal. Voor iedere patiënt wordt een radiotherapieplan gecreëerd met als doel om het tumorgebied zo nauwkeurig mogelijk te bestralen. De berekende dosis uit dit plan wordt vervolgens verdeeld afgeleverd over meerdere losse fracties over een periode van 5 weken, om de nadelige effecten van radiotherapie zo veel mogelijk te beperken. Echter kunnen er tussen deze behandelsessies verschillende anatomische veranderingen plaatsvinden in de thorax, waardoor de vorm of positie van de tumor niet meer overeenkomt met het plan. Door deze veranderingen kan het radiotherapieplan onnauwkeurig worden, waardoor de dosis niet meer precies terecht komt op de gewenste locatie. Dit kan leiden tot een onderdosering van de tumor en een overdosering van gezond weefsel. Het is dus van belang om een hoge nauwkeurigheid van het radiotherapie plan na te streven. Beeldvorming is een belangrijk hulpmiddel bij radiotherapie behandelingen. De planning voorafgaand aan een behandeling maakt gebruik van een *Computed Tomography* (CT) scan. Op basis van deze CT scan wordt de tumor gelokaliseerd waardoor het dosisplan kan berekend. De toepassing van beeldvorming in de radiotherapie wordt beeldgestuurde radiotherapie (*image guided radiotherapy*, IGRT) genoemd. Tijdens de losse fracties wordt gebruik gemaakt van beeldvorming met *Cone Beam Computed Tomography* (CB)CT, waarbij de tumor meestal slecht te onderscheiden is van omliggend weefsel. Echter zijn slokdarmtumoren onderhevig aan inter- en intrafractie bewegingen, waardoor de vorm en positie van de tumor kan veranderen. Om hiervoor te compenseren worden vaak grote marges tussen het *clinical target volume* (CTV) en *planning target volume* (PTV) gebruikt, zodat er een grote zekerheid is dat het doelgebied voldoende dosis ontvangt gedurende de gehele behandelperiode. Het uiteindelijke doelgebied

overlapt dan ook vaak met omliggend gezond weefsel. Een verhoogde dosis op het omliggende gezonde weefsel leidt echter tot een vergrote kans op complicaties. Het is daarom zeer belangrijk om de dosis op het gezonde weefsel te minimaliseren door het tumor doelgebied accuraat te definiëren en mogelijk kleinere marges te gebruiken. De afgelopen jaren is er veel vooruitgang in beeldvorming in de radiotherapie geboekt. Met name het gebruik van *Magnetic Resonance Imaging* (MRI) is enorm toegenomen. Met MRI kan zacht weefsel, zoals de slokdarm, beter afgegrensd worden dan op CT beelden. Dit heeft geleid tot de ontwikkeling van de *MR-Linac*, een versneller gecombineerd met MRI beeldvorming. Hiermee kunnen zeer duidelijke beelden tijdens een behandeling worden gemaakt. Door het gebruik van MRI in radiotherapie kunnen veranderingen in de anatomie sneller worden geobserveerd en zou men het plan zo kunnen aanpassen dat het doelgebied voldoende dosis ontvangt terwijl de dosis op het omliggend gezonde weefsel kan worden geminimaliseerd. Bovendien zou de verbeterde nauwkeurigheid kunnen zorgen voor het gebruik van kleinere marges. Het toepassen van een MR-Linac op een tumorgebied, zoals dat van de slokdarmtumor, dat onderhevig is aan verschillende anatomische veranderingen biedt dus mogelijk voordelen. Het doel van dit proefschrift was om te onderzoeken wat de voordelen van MR-gestuurde radiotherapie zijn bij de behandeling van patiënten met slokdarmkanker en dit te koppelen aan een klinisch implementatietraject.

Dit is in twee delen onderzocht. In het eerste deel van dit proefschrift (hoofdstukken 2 t/m 5) zijn de resultaten van de “**RE**peated magnetic resonance imaging in esophageal cancer for **Ad**aptive radiation treatment planning during neoadjuvant **ChemoradioTherapy**” (REACT) studie beschreven. In deze studie werden zes wekelijkse MRI scans opgenomen bij 32 patiënten tussen december 2015 en april 2018 tijdens hun reguliere behandelingen. Het hoofddoel van deze studie was om anatomische veranderingen tijdens de behandeling op basis van MR beeldvorming in kaart te brengen en in silico de rol van *MR-geleide Radiotherapie* (MRgRT) te evalueren. De bevindingen van het eerste deel van dit proefschrift werden vervolgens toegepast en klinisch geïmplementeerd in een workflow voor een online adaptieve, MR-geleide radiotherapiebehandeling voor patiënten met slokdarmkanker. Tussen juli 2019 en maart 2021 zijn de eerste negen slokdarmkankerpatiënten behandeld op een 1,5T MR-Linac in het UMC Utrecht. In het tweede deel (hoofdstuk 6 & 7) van dit proefschrift is deze workflow beschreven en geëvalueerd.

In **hoofdstuk 2** zijn de veranderingen in tumorvolume die plaatsvonden tijdens een nCRT behandeling geanalyseerd op basis van wekelijkse MR-beelden. Na vijf weken werd een gemiddelde afname van het tumorvolume van 28% geconstateerd. Bovendien begon de tumorregressie al na de eerste week van de behandeling, wat

betekent dat optimalisatie van het doseringsplan al na één week van de behandeling nodig kan zijn voor het behalen van een optimale dosis aan het doelgebied en het sparen van gezond weefsel. Een belangrijke bevinding van deze studie was dat door tumorregressie het hart naar de hoge dosis-regio's kon verschuiven naar mate de behandeling vorderde. Dit werd voornamelijk waargenomen voor grote tumoren (>50cc) die zich dorsaal van het hart bevonden. Aangezien een verhoging van de hartsdosis in verband is gebracht met complicaties en een slechtere algehele overleving zouden bij deze subpopulatie patiënten adaptieve strategieën kunnen worden overwogen. Een eenvoudige maar doeltreffende strategie zou zijn om deze patiënten standaard na twee weken behandeling opnieuw te plannen. In **hoofdstuk 3** hebben we een volledige dosimetrische analyse uitgevoerd om de kleinste CTV-to-PTV marges te berekenen die een volledige dekking van het doelgebied opleverden tijdens een gehele gesimuleerde behandeling. Door een volledige dosimetrische analyse uit te voeren, werd niet alleen rekening gehouden met het dosimetrische effect van de dagelijkse translatie van de tumor zelf, maar werden ook de dosimetrische effecten van alle morfologische veranderingen (zoals tumorregressie) in de loop van de behandeling meegenomen. Uit de geaccumuleerde dosisanalyse bleek dat CTV-to-PTV-marges van 8, 9 en 10 mm in respectievelijk posterieur & rechts, anterieur & craniaal en links & caudale richtingen, voldoende waren om rekening te houden met interfractionele veranderingen in tumor volume, vorm en positie in de loop van de behandeling bij toepassing van een dagelijkse online bot match set-up strategie. Opgemerkt moet worden dat deze marges voor twee patiënten niet afdoende was, wat de noodzaak van dagelijkse adaptieve radiotherapie verder benadrukt. In de conventionele IGRT voor slokdarmkanker wordt doorgaans niet gecorrigeerd voor dagelijkse vorm- en positieveranderingen van de tumor en wordt een match van de botstructuur in de nabijheid van de tumor gebruikt om een optimale afstemming op het behandelplan te waarborgen. Hierdoor moeten niet alleen geometrische veranderingen van de tumor zelf, maar ook de variabiliteit in tumorpositie ten opzichte van de botanatomie worden meegenomen in de behandelingsmarges. In eerdere studies zijn verschillende positioneringsstrategieën onderzocht, zoals uitlijning op markers, geïmplementeerd in en rond de tumor, een strategie gebaseerd op opstelling op de positie van de carina, of opstelling op basis van een combinatie van de positie van zacht weefsel en botanatomie. Geconcludeerd werd dat er momenteel geen gouden standaard bestaat voor de instelling van de patiënt, maar dat de patiëntpositionering op basis van de botanatomie veelal de beste nauwkeurigheid biedt voor de meeste tumorlocaties. Online MR-geleiding maakt een betere visualisatie van de tumor en evaluatie van de gehele 3D-geometrie van het *gross tumor volume* (GTV) en CTV mogelijk, waardoor adaptieve behandelstrategieën kunnen worden toegepast. In **hoofdstuk 4** werden twee strategieën vergeleken die compenseren voor positionele

tumorveranderingen: een rigide positionering van de dagelijkse positie van het CTV op de planning-CTV (adaptieve MR-geleide strategie) werd vergeleken met een rigide positionering op basis van de botstructuur (conventionele CBCT strategie). Het bleek dat directe CTV-registratiemethoden met behulp van MRI slechts een matige toename van de dekking van het doelgebied opleverden (94% en 90% van de fracties werden volledig bedekt met een marge van 10 mm bij gebruik van respectievelijk CTV-match en bot-match strategieën) in vergelijking met de klinische CBCT-IGRT-protocollen (botuitlijning). Voor beide strategieën werd de dekking van het doelgebied bepaald als functie van een vooraf ingestelde isotrope marge. Verder bleek, als gevolg van dagelijkse veranderingen in de maagvulling, dat distaal gelegen tumoren vaak grotere marges nodig hadden om geometrisch volledig gedekt te worden. Hieruit werd geconcludeerd dat een online adaptieve workflow waarbij een nieuw plan wordt gemaakt op basis van de anatomie van de dag, essentieel is bij het nastreven van zeer conforme doelbestralingen voor alle behandelingsfracties. Stralingsdosis op nabijgelegen gezonde organen is onvermijdelijk bij radiotherapie voor slokdarmkanker. Verschillende studies hebben aangetoond dat een verhoogde hartsdosis en longdosis kan leiden tot een verhoogde kans op complicaties en zelfs tot een verhoogd sterftecijfer. Naar aanleiding van de hoofdstukken 2, 3 en 4 werd geconcludeerd dat dagelijkse aanpassing van het plan op basis van de anatomie nodig is voor een optimale doelbedekking. In **hoofdstuk 5** onderzochten we hoe de margereductie die we met een MR-gestuurde behandeling zou kunnen realiseren zich zou vertalen naar dosimetrisch voordeel voor de patiënt. Een vergelijking tussen een gesimuleerde conventionele IGRT-strategie en een adaptieve MRgRT-strategie toonde aan dat verkleinde marges kunnen leiden tot een grote dosisvermindering op risico-organen, vooral in het hoge-dosisgebied ($>40\text{Gy}$), terwijl de dekking van het doelgebied tussen beide behandelingsstrategieën vergelijkbaar was. Daarbij werd aangetoond dat de gewonen dosisvermindering met online adaptieve MRgRT ook kan worden gebruikt om de dosis voor de primaire tumor te verhogen, terwijl de dosisniveaus van risico-organen niet groter is dan de dosisniveaus wanneer conventionele niet-adaptieve IGRT wordt gebruikt. Dit betekent dat online adaptieve radiotherapie nieuwe perspectieven biedt voor lokale boosting-strategieën om mogelijk het resultaat van de slokdarmkankerbehandeling te verbeteren.

In **hoofdstuk 6** werd verslag gedaan van de klinische implementatie en haalbaarheid van gefractioneerde MR-geleide chemoradiotherapie voor patiënten met slokdarmkanker. Onze eerste ervaringen met adaptieve MR-geleide behandeling van patiënten met slokdarmkanker gingen gepaard met enkele technische en logistieke complexiteiten die vaak onbekend zijn bij andere behandelingslocaties waar online adaptieve MR-geleide workflows zijn gebruikt. De online definitie

van het doelgebied van slokdarmtumoren vereist een accurate hercontouring van zowel het doelgebied als de omliggende risico-organen. Gezien de ruime omvang van het doelgebied is dit proces arbeidsintensief gebleken wat gevolgen heeft voor de sessietijd. Ook bestaat de totale neoadjuvante behandeling uit 23 fracties, wat op zijn minst ongebruikelijk is binnen het algemene kader van online adaptieve MRgRT. Deze elementen maakten de online adaptieve MR-geleide workflow voor slokdarmkankerbehandelingen niet alleen veeleisender voor patiënten en personeel, maar vereisten ook een uitgebreide logistieke planning. Bovendien resulteerde de huidige workflow in langere behandel tijden; de gemiddelde behandel tijd bedroeg 53 minuten, waarvan een groot deel bestond uit contouraanpassing (20 minuten) om de meeste veranderingen van de dagelijkse anatomie in het doseringsplan op te nemen. Bij vergelijking van de opnieuw gedefinieerde doelgebieden van de eerste fracties met de laatste fracties bleek dat de volumes van de doelgebieden in de loop van de tijd afnamen, hetgeen onze bevindingen in hoofdstuk 2 bevestigt. Sommige patiënten vertoonden grotere tumorreducties dan andere. Deze patiënten zouden het meeste baat hebben bij een adaptieve behandelingsstrategie; daarom moet worden onderzocht of deze patiënten vooraf te identificeren zijn. Voorlopig is adaptieve behandeling matig uitvoerbaar, ook aangezien twee van de negen patiënten wegens ongemak gedurende meer dan 5% van de fracties op een conventionele versneller behandeld moesten worden. Daarom is een verkorting van de behandelings tijd wenselijk, om het comfort van de patiënt te verhogen en ook de logistieke planning rond de behandelingen te vergemakkelijken. Niettemin werd aangetoond dat de adaptieve behandelingsstrategie resulteerde in een dosisvermindering voor risico-organen in vergelijking met het conventionele back-up plan. Verder onderzoek is nodig om het volledige potentieel van MR-geleide radiotherapie voor patiënten met slokdarmkanker te ontsluiten. Hoewel dagelijkse planaanpassing de invloed van interfractiebeweging heeft weggenomen, kan de tumorbeweging tijdens de behandelingssessie nog steeds een punt van zorg zijn. De gemiddelde intrafractiebeweging (drift) tussen de positieverificatie-MRI en de MRI na de behandeling varieerde tussen patiënten. Verdere analyse van de intrafractiebeweging werd uitgevoerd in **hoofdstuk 7**. Na analyse werd vastgesteld dat twee van de negen patiënten een marge van 5 mm in craniaal-caudale richting nodig hadden ter compensatie van drifts en ademhalingsbeweging, terwijl bij zeven patiënten een marge van slechts 3 mm noodzakelijk was. Deze marges zijn aanzienlijk kleiner dan de marge van 6 mm die is gebruikt bij de behandeling van deze patiënten zoals beschreven in **hoofdstuk 6**.

Door de toepassing van MRI in radiotherapiebehandelingen voor slokdarmkanker is de visualisatie van de tumor verbeterd. Hierdoor is het mogelijk om nauwkeuriger de doelgebieden te definiëren, waardoor de marges verkleind kunnen worden. Dit

leidt tot een vermindering van de toxiciteit voor hart, longen en andere organen waarbij een verlaagde dosis wenselijk is. Vervolgens opent dit de mogelijkheid om de behandelingsprotocollen van slokdarmkanker te verbeteren, bijvoorbeeld door mogelijke toevoeging van boosting-strategieën om de lokale tumorcontrole te verbeteren. Naar aanleiding van de resultaten van dit proefschrift hoop ik te hebben bijgedragen aan de totstandkoming van verbeterde behandelstrategieën met als doel om het meest optimale resultaat voor de patiënt te bereiken.

List of publications

Published papers

Mick R. Boekhoff, Ingmar L. Defize, Alicia S. Borggreve, Noriyoshi Takahashi, Astrid L.H.M.W. van Lier, Jelle P. Ruurda, Richard van Hillegersberg, Jan J.W. Lagendijk, Stella Mook and Gert J. Meijer. (2020) 3-Dimensional target coverage assessment for MRI guided esophageal cancer radiotherapy. *Radiother Oncol.* 147:1-7. doi: 10.1016/j.radonc.2020.03.007

Ingmar L. Defize, **Mick R. Boekhoff**, Alicia S. Borggreve, Astrid L.H.M.W. van Lier, Noriyoshi Takahashi, Nadia Haj Mohammad, Jelle P. Ruurda, Richard van Hillegersberg, Stella Mook and Gert J. Meijer. (2020) Tumor volume regression during neoadjuvant chemoradiotherapy for esophageal cancer: a prospective study with weekly MRI. *Acta Oncol.* 59(7):753-759. doi: 10.1080/0284186X.2020.1759819

Mick R. Boekhoff, Ingmar L. Defize, Alicia S. Borggreve, Richard van Hillegersberg, Alexis N.T.J. Kotte, Jan J.W. Lagendijk, Astrid L.H.M.W. van Lier, Jelle P. Ruurda, Noriyoshi Takahashi, Stella Mook and Gert J. Meijer. (2021) CTV-to-PTV margin assessment for esophageal cancer radiotherapy based on an accumulated dose analysis. *Radiother Oncol.* 161:16-22. doi: 10.1016/j.radonc.2021.05.005

Mick R. Boekhoff, Ingmar L. Defize, Alicia S. Borggreve, Richard van Hillegersberg, Alexis N.T.J. Kotte, Jan J.W. Lagendijk, Astrid L.H.M.W. van Lier, Jelle P. Ruurda, Noriyoshi Takahashi, Stella Mook and Gert J. Meijer. (2021) An in-silico assessment of the dosimetric benefits of MR-guided radiotherapy for esophageal cancer patients. *Radiother Oncol.* 162:76-84. doi: 10.1016/j.radonc.2021.06.038

Mick R. Boekhoff, Roel Bouwmans, Patricia A.H. Doornaert, Martijn P.W. Intven, Jan J.W. Lagendijk, Astrid L.H.M.W. van Lier, Marnix J.A. Rasing, Saskia van de Ven, Gert J. Meijer and Stella Mook. (2022) Clinical implementation and feasibility of long-course fractionated MR-guided chemoradiotherapy for

patients with esophageal cancer: an R-IDEAL stage 1b/2a evaluation of technical innovation. *Clin. Transl. Radiat. Oncol.* 34:82-89. doi: 10.1016/j.ctro.2022.03.008

Mick R. Boekhoff, Jan J.W. Lagendijk, Astrid L.H.M.W. van Lier, Stella Mook, Gert J. Meijer. (2023) Intrafraction motion analysis in online adaptive radiotherapy for esophageal cancer. *Physics and Imaging in Radiation Oncology* (2023) 26, 100432. doi: 10.1016/j.phro.2023.100432

Additional papers

Alicia S. Borggreve, Sophie E. Heethuis, **Mick R. Boekhoff**, Lucas Goense, Peter S.N. van Rossum, Lodewijk A.A. Brosens, Astrid L.H.M.W. van Lier, Richard van Hillegersberg, Jan J.W. Lagendijk, Stella Mook, Jelle P. Ruurda. and Gert J. Meijer. (2020) Optimal timing for prediction of pathologic complete response to neoadjuvant chemoradiotherapy with diffusion-weighted MRI in patients with esophageal cancer. *Eur Radiol.* 30(4):1896-1907. doi: 10.1007/s00330-019-06513-0

Hidde Eijkelenkamp, **Mick R. Boekhoff**, Maaïke E. Verweij, Femke P. Peters, Gert J. Meijer and Martijn P.W. Intven. (2021) Planning target volume margin assessment for online adaptive MR-guided dose-escalation in rectal cancer on a 1.5 T MR-Linac. *Radiother Oncol.* 162:150-155. doi: 10.1016/j.radonc.2021.07.011

Abstracts and conference proceedings

Mick R. Boekhoff, Alicia S. Borggreve, Alexis N.T.J. Kotte, Astrid L.H.M.W. van Lier, Jan J.W. Lagendijk, Noriyoshi Takahashi, Stella Mook and Gert J. Meijer. Dosimetric evaluation of in-silico simulated MR-guided esophageal cancer radiotherapy. *Oral presentation at 8th MRinRT, 2021*

Mick R. Boekhoff, Ingmar L. Defize, Alexis N.T.J. Kotte, Noriyoshi Takahashi, Alicia S. Borggreve, Astrid L.H.M.W. van Lier, Jan J.W. Lagendijk, Stella Mook and Gert J. Meijer. CTV-to-PTV margin assessment for esophageal cancer radiotherapy based on an accumulated dose analysis *Poster Discussion at ESTRO 39, 2020*

Mick R. Boekhoff, Stella Mook, Alicia S. Borggreve, Lucas Goense, Peter S.N. van Rossum, Noriyoshi Takahashi, Astrid L.H.M.W. van Lier, Alexis N.T.J. Kotte, Jan J.W. Lagendijk and Gert J. Meijer. MRI guided set-up corrections for esophageal cancer: what margin do we need? *Oral presentation at ESTRO 38, 2019*

Mick R. Boekhoff, Alexis N.T.J. Kotte, Stella Mook, Alicia S. Borggreve, Lucas Goense, Sophie E. Heethuis, Peter S.N. van Rossum, Astrid L.H.M.W. van Lier, Jan J.W. Lagendijk and Gert J. Meijer. What CTV-to-PTV margins are required for esophageal cancer radiotherapy? *Poster at ESTRO 37, 2018*

Authors and affiliations

University Medical Center Utrecht, Utrecht, The Netherlands

Department of Radiation Oncology

Roel Bouwmans

Patricia A.H. Doornaert, MD, PhD

Sophie E. Heethuis, PhD

Martijn P.W. Intven, MD, PhD

Alexis N.T.J. Kotte, PhD

Jan J.W. Lagendijk, PhD

Astrid L.H.M.W. van Lier, PhD

Gert J. Meijer, PhD

Stella Mook, MD, PhD

Marnix J.A. Rasing, MD

Peter S.N. van Rossum, MD, PhD

Saskia van de Ven, MD

Department of Surgery

Alicia S. Borggreve, MD, PhD

Ingmar L. Defize, MD

Lucas Goense, MD, PhD

Richard van Hillegersberg, MD, PhD

Jelle P. Ruurda, MD, PhD

Tohoku University Graduate School of Medicine, Japan

Department of Radiation Oncology

Noriyoshi Takahasi, MD, PhD

Dankwoord

Dit proefschrift is dankzij de bijdrage van velen tot stand gekomen en graag zou ik iedereen die in welke vorm dan ook heeft bijgedragen willen bedanken.

Mijn dank is groot aan alle patiënten die hebben deelgenomen aan de studies waarop dit proefschrift is gebaseerd. Terwijl zij een intensief behandeltraject doorliepen, ondergingen zij extra MRI scans om bij te dragen aan toekomstige verbeteringen in de behandeling van slokdarmtumoren.

Mijn promotor, prof. Lagendijk, Jan, dank voor de kans om mijzelf te ontwikkelen in het promotietraject op de afdeling radiotherapie. Ik heb mijzelf hier kunnen ontwikkelen en bovendien heb ik genoten van de fijne werkomgeving. Jouw anekdotes, bijvoorbeeld over het bestralen van een prijswinnende stier, zal ik niet snel vergeten.

Gert, heel erg bedankt voor de begeleiding de afgelopen jaren. Je hebt vele ideeën over mogelijke verbeteringen in de behandeling van slokdarmtumoren en ik ben trots dat ik hieraan heb kunnen bijdragen met dit proefschrift. Ik vond het erg fijn dat jouw deur altijd open stond om te sparren. Ook heb ik veel bewondering hoe jij om bent gegaan met zware persoonlijke tegenslag. Ik heb veel van jou kunnen leren, zowel op wetenschappelijk als persoonlijk vlak, en had dan ook geen betere dagelijks begeleider kunnen wensen.

Stella, zonder jouw klinische kennis en bijdrages was dit onderzoek niet tot stand gekomen. Ik waardeer het dat je altijd bereid was om mee te kijken naar in-tekeningen, figuren en manuscripts of om aan te sluiten bij een overleg. Daarnaast verwacht ik nu altijd met klinische kennis overladen te worden wanneer ik iemand met hakken op de gang hoor lopen.

Beste leden van de beoordelingscommissie, Prof. dr. B.L.A.M. Weusten, Prof. dr. B.W. Raaymakers, Prof. dr. R. van Hillegersberg, Dr. P.S.N. van Rossum en Prof. U.A. van der Heide, bedankt voor uw tijd en moeite om dit proefschrift te lezen en beoordelen.

Mijn kamergenoten van Q.0S.4.37, Daan, Steven, Soraya, Jorine, Dennis, Jorine, Prescilla, Hans, Sophie, Joris, Sanam, Robin en Filipa, dank voor de leuke tijd

in de gezelligste kamer van het UMCU. Ik heb genoten van de vele ontspannen momentjes, lunches, Nederlandse lessen en pouletjes. Daan, als achterbuurman heb je me kunnen helpen wanneer een script net niet lekker liep, ook waardeer ik jouw zeer strakke planning en werkwijze. Ik heb genoten van de trip naar de ESTRO in Milaan. Steven, dank voor het beantwoorden van al mijn vragen over statistiek. Daarnaast waardeer ik je inbreng van kunst in de kamer. Thomas, dank voor de gastvrijheid bij het kameruitje bij jou thuis. Helaas hebben we die trend door corona niet voort kunnen zetten. Soraya, ik ben heel trots op jouw progressie in het leren van Nederlands. Het was altijd leuk om jou weer nieuwe spreekwoorden te leren.

Collega's van de Oes groep: Gert, Stella, Astrid, Peter, Lucas, Sophie, Alicia, Ingmar, Sophie, Noriyoshi, Charlotte en Robin. Bedankt voor de overleggen en kennisoverdracht. Astrid, bedankt voor de waardevolle feedback op mijn manuscripts. Noriyoshi, thank you for helping with the delineations of the REACT scans. Alicia, heel erg bedank voor jouw inzet rondom de REACT studie.

Tevens wil ik al mijn co-auteurs bedanken voor hun bijdragen aan de publicaties.

Alle andere PhD studenten op de afdeling, waaronder Stefan, Maureen, Ellis, Tom, Veerle, Jeanine, Freek en allen die ik vergeet te benoemen, dank voor alle gezellige lunches, congressen en andere RT-uitjes.

Ook dank aan het personeel op de afdeling radiotherapie, waaronder het secretariaat, Gijs & Alexis voor de support rondom volumetool en Cornel voor het helpen met de registraties.

Mijn vrienden: Tim, Roan, Nik, Mark, Thomas, Tim, Taco, al jaren samen aan het (zaal)voetballen en sinds een aantal jaar ook op pad in het jaarlijkse fietsweekend. Ik ben dankbaar voor jullie vriendschap.

Gerard, Ghislaine & Demi, dank voor jullie onvoorwaardelijke support.

Lieve Emma, ik ben blij dat jij in mijn leven bent gekomen. Samen hebben wij al veel mooie momenten gedeeld en daar zullen er nog minstens zo veel van bij komen. Ik hou van jou.

Curriculum Vitae



Mick Remo Boekhoff was born in Amsterdam, the Netherlands, on the 25th of September 1992. He grew up in Bussum, where he obtained his high school diploma (gymnasium) at Goois Lyceum in 2010.

Afterwards he studied physics at the University of Amsterdam, where he received his bachelor's degree in 2014 followed by his master's degree in 2016. His bachelor's internship was carried out at the Biomedical Engineering and Physics department of the Academic Medical Center and his master's internship was carried out in the Biological Soft Matter group at AMOLF.

In March 2017 he started as a PhD student at the department of Radiotherapy at the University Medical Center Utrecht under supervision of prof. dr. ir. J.J.W. Lagendijk, dr. G.J. Meijer and dr. S. Mook. His research, of which the results are described in this thesis, focused on the clinical introduction of MR-guided radiotherapy for esophageal cancer.

After his PhD research he started working as a Data Engineer at Medical Research Data Management.